Ministry of Environment and Energy
National Environmental Research Institute

The Aquatic Environment

Phthalates and Nonylphenols in Roskilde Fjord

A Field Study and Mathematical Modelling of Transport and Fate in Water and Sediment

NERI Technical Report No. 339

Ministry of Environment and Energy
National Environmental Research Institute

The Aquatic Environment

Phthalates and Nonylphenols in Roskilde Fjord

A Field Study and Mathematical Modelling of Transport and Fate in Water and Sediment

NERI Technical Report No. 339
February 2001

Jørgen Vikelsøe
Patrik Fauser
Peter B. Sørensen
Lars Carlsen
Department of Environmental Chemistry

Data sheet

Title:	Phthalates and Nonylphenols in Roskilde Fjord
Subtitle:	A Field Study and Mathematical Modelling of Transport and Fate in Water and Sediment. The Aquatic Environment
Authors	Jørgen Vikelsøe, Patrik Fauser, Peter B. Sørensen & Lars Carlsen
Analytical laboratory:	Elsebeth Johansen
Department:	Department of Environmental Chemistry
Sediment samples:	Rikke Hansen
Serial title and no.:	NERI Technical Report No. 339
Publisher:	Ministry of Environment and Energy National Environmental Research Institute ©
URL:	http://www.dmu.dk
Date of publication:	February 2001
Referee:	Henrik Søren Larsen, Danish Environmental Protection Agency
Layout:	Jørgen Vikelsøe, Patrik Fauser & Majbritt Pedersen-Ulrich
Please cite as:	Vikelsøe, J., Fauser, P., Sørensen, P.B. & Carlsen, L. (2001): Phthalates and Nonylphenols in Roskilde Fjord. A Field Study and Mathematical Modelling of Transport and Fate in Water and Sediment. The Aquatic Environment. National Environmental Research Institute, Roskilde. 106pp. NERI Technical Report. No. 339

Abstract: The aim of the study has been to investigate the occurrence, sources, transport and fate of nonylphenols and phthalates in the aquatic environment of Roskilde Fjord. It was further intended to find the temporal as well as the spatial variation of these xenobiotics in the fjord and stream water. Further, to investigate nonylphenols and phthalates in sediment in the fjord including a sediment core in the southern part, expected to yield clues regarding the historical variation of the concentration of xenobiotics, as well as some streams and lakes. Finally, an important aim was to make a mass balance for the fjord system, including sources, transport and the mechanisms of elimination, and to make a mathematical model describing the fate of the substances in the fjord system.

Keywords:	Phthalates, PAE, Nonylphenols, NPE, DEHP, analysis, estuary, fjord, water, sediment, mathematical model, mass balance.
ISBN:	87-7772-585-9
ISSN (print):	0905-815X
ISSN (electronic):	1600-0048
Paper quality and print:	Cyclus Office, 100 % recycled paper. Grønager's Grafisk Produktion AS. This publication has been marked with the Nordic environmental logo "Svanen".
Number of pages:	106
Circulation:	200
Price:	DKK 75,- (incl. 25% VAT, excl. freight)
Internet-version:	The report is also available as a PDF-file from NERI's homepage
For sale at:	National Environmental Research Institute Postboks 358 Frederiksborgvej 399 DK-4000 Roskilde Tel.: +45 46 30 12 00 Fax: +45 46 30 11 14
	Miljøbutikken Information and Books Læderstræde 1 DK-1201 Copenhagen K Denmark Tel.: +45 33 95 40 00 Fax: +45 33 92 76 90 e-mail: butik@mem.dk www.mem.dk/butik

Contents

Summary

The occurrence sources, transport and fate of nonylphenols and phthalates in the aquatic environment of a fjord was investigated. The substances analysed were: NP, NPDE, DBP, DPP, BBP, DEHP, DnOP and DnNP. The analytical methods were specifically developed for the investigation, using high resolution GC/MS. The investigation comprised measurements of water and sediment in the fjord as well as in sources.

The level and the temporal and spatial variation of the xenobiotics in the water of the fjord were studied during three seasonal campaigns, involving widespread different locations. Very low concentrations were found. DEHP was the most abundant substance, followed by much lower concentrations of DBP, BBP, DPP and NP. NPDE was not found. The concentrations of the higher phthalates were highly significantly intercorrelated. On a large geographical scale the spatial variation was insignificant, but a significant seasonal variation was present, indicated by a maximum for June and a minimum for December, confirmed by analysis of variance. The largest seasonal variation and a significant short-term variation were present at the narrow middle location, where the current velocity is high. The broad innermost part, near Roskilde, was most constant.

Sediment was investigated in the innermost part of the fjord (Roskilde Vig). Much higher concentrations were found than in the water, DEHP, DBP NP and NPDE being most abundant. A decreasing gradient from the WWTP outlet to a location 6 km away was observed, approaching the concentrations found in the other less polluted fjord, Isefjord. Thus, horizontal transport through the water is limited to some kilometres, and the main transport process seems to be sedimentation, or binding to sediment in the fjord bottom.

The sediment investigation including a core 22 cm deep (~80 y old) from Roskilde Vig. A decreasing tendency with depth/age was observed for DEHP and BBP, reflection the historical development in consumption of phthalates. For NP and NPDE, a more complicate pattern was found, characterised by low concentrations in the upper/youngest part and two deeper maxima, probably caused by variation in the use of NPEs .

The seasonal sampling further comprised three streams and a lake, including water and sediment. In the water of the streams, the DEHP concentrations ranged up to the triple of the fjord. The spatial and temporal variations were more pronounced and random, certainly because the streams - unlike the fjord - are hydraulic and geographic separate entities having different sources and flows. The lake sediment indicated a significant sedimentation of all substances – in particular NP and NPDE – in the deepest part of the lake.

Numerical models were set up in order to describe the fate of the substances in the water and sediment compartments of the fjord. Only DEHP data was used since DEHP was the most abundant substance and the only one to occur in concentrations that are of environmental significance.

The physico-chemical processes in the fjord that were considered to influence the fate of DEHP, were: 1st order degradation of dissolved DEHP, adsorption to particulate matter, sedimentation of particulate matter, vertical diffusion in the sediment and dispersive mixing in the water. DEHP sources to the fjord were streams, wastewater treatment plant discharges and atmospheric deposition. Water exchange with the surrounding sea removes DEHP, since the DEHP concentrations is negligible in the sea.

In order to establish a simple robust model, the seasonal variations were not considered. More data concerning the growth and wilting cycle of the vegetation and the influence of changing emission patterns from consumers and wastewater treatment plants were needed and therefore mean annual conditions were simulated based on constant flows and concentrations.

The numerical models were validated with analytical expressions. The experimental sediment core data was used to calibrate the sediment model yielding a sedimentation rate of 2.5 mm pr. year, corresponding well to a rate previously found for the fjord. Furthermore a distribution coefficient equal to 10000 litre pr. kg dm and a 1st order degradation rate of $2 \cdot 10^{-5}$ sec^{-1} were found.

The sediment simulations showed that it is the sedimentation process that governs the vertical transport of substance in the sediment. Diffusion is only significant in the theoretical upstart of the system, where the concentration gradient is large at the surface. This fact has further been investigated in *Sørensen et al. (2000),* in relation to evaluating the generic compartment model, SimpleBox, comprised in the European Union System for the Evaluation of Substances, EUSES.

The water model was made by dividing the fjord into two sections of total mixing along the horizontal axis, where the surface areas were large and into a narrow dispersive section where the horizontal flow was high. The shallow water was considered to be totally mixed along the vertical axis in the whole fjord. The experimental water concentrations were approximately constant only displaying minor spatial variations that could not be modelled, probably because of short-term effects such as tidal flow. The mean experimental concentration was a factor of 5 higher than the mean calculated concentration.

Freshwater from streams were the predominant DEHP source to the fjord, followed by atmospheric deposition and wastewater treatment plants. Sedimentation was the predominant removal mechanism followed by water exchange with the sea and degradation.

In spite of the deviation between the experimental and calculated DEHP concentrations in the water, the used modelling approach is considered to simulate the complex interactions that take place in a system such as Roskilde Fjord, satisfactorily. However, in order to employ the model as a risk assessment tool it is necessary to further investigate analytical detection limits, source contributions and temporal variations of the system.

Resumé

Forekomst, kilder, transport og skæbne af nonylphenoler og phthalater i det akvatiske miljø af Roskilde Fjord blev undersøgt.

Der blev analyseret for stofferne NP, NPDE, DBP, DPP, BBP, DEHP, DnOP og NP. De analytiske metoder var udviklet specielt for undersøgelsen, og anvendte højtopløsende GC/MS. Undersøgelsen omfattede målinger af vand og sediment i fjorden samt kilder.

Forekomst og variation i tid og rum af de miljøfremmede stoffer blev undersøgt i tre årstid prøvetagninger, der omfattede lokaliteter vidtstrakt langs fjorden. Der blev fundet meget lave koncentrationer i fjordvandet. DEHP forekom i højest koncentration, fulgt af DBP i meget lavere koncentration, og minimale mængder af BBP, DPP og NP. NPDE kunne ikke påvises. Der var en højsignifikant korrelation mellem de højere phthalater. I geografisk stor skala var de rumlige variationer ikke signifikante, men der var en signifikant årstidsvariation tilstede, kendetegnet ved et maksimum i juli og et minimum i december, bekræftet ved variansanalyse. Den største variation og en betydelig korttidsvariation fandtes i den snævre midterste sted, hvor strømningshastigheden er høj. Den inderste del, nær Roskilde, var mere konstant.

Der blev undersøgt sediment i den inderste del af fjorden (Roskilde Vig). Her fandtes meget højere koncentrationer end i vandet, idet DEHP, DBP, NP og NPDE var mest forekommende. En aftagende gradient fandtes fra udløbet af rensningsanlægget til en position i 6 km afstand, hvor koncentrationen nærmede sig koncentrationen i Isefjorden, der anses for mindre forurenet. Horisontal transport gennem vandet er således begrænset til nogle få kilometer, og hovedtransportprocessen synes at være sedimentation, eller binding til sediment på fjordbunden.

I sedimentundersøgelsen indgik en kærne 22 cm dyb (ca. 80 år gammel) fra Roskilde Vig. I denne sås en aftagende koncentration med dybde/alder af DEHP og BBP, hvilket afspejler den historiske udvikling i forbruget af phthalater. For NP og NPDE blev fundet et mere kompliceret mønster, kendetegnet ved to dybere maxima, som formentlig er forårsaget af ændringer i forbruget af NPE.

Årstids prøvetagningen omfattede tillige vand og sediment i tre åer og en sø. I åvandet gik DEHP koncentrationen op til det tredobbelte af fjordvandet. Variationerne i tid og sted var mere udtalte og tilfældige, hvilket kunne forventes fordi åerne i modsætning til fjorden er hydraulisk og geografisk adskilte enheder med forskellige kilder og strømning. Søsedimentet antydede en betydelig sedimentation af alle stoffer – særlig NP og NPDE – i den dybeste del af søen.

Numeriske modeller blev lavet med det formål, at beskrive skæbnen af stofferne i henholdsvis fjordens vand og sediment. Det var kun DEHP koncentrationerne der var tilstrækkeligt høje til at have miljømæssig betydning og derfor blev disse kun anvendt.

De fysisk-kemiske processer i fjorden, der ansås at være af betydning for DEHP's skæbne, var: 1^{ste} ordens nedbrydning af opløst DEHP, adsorption til partikulært materiale, sedimentation af partikler, vertikal diffusion i sediment og dispersiv opblanding i vandfasen. DEHP kilder til fjorden var åer og vandløb, rensningsanlæg og atmosfærisk deposition. Vandudveksling med havet (Kattegat) fjernede DEHP, da koncentrationerne var ubetydelige i havet.

For at kunne fastlægge en simpel og robust model blev der ikke taget højde for de tidslige variationer i systemet. En større mængde data omkring planters og dyrs vækstcyklus og betydningen af skiftende emissioner fra såvel forbrugere som rensningsanlæg ville være nødvendigt i den henseende. Derfor blev årsmiddelværdier med konstante vandmængder og koncentrationer anvendt.

De numeriske modeller blev valideret med analytiske udtryk. De eksperimentelle data for sedimentkernen blev brugt til at kalibrere sediment modellen, hvilket gav en sedimentationsrate på 2.5 mm pr. år, som svarede godt til tidligere undersøgelser for fjorden. Derudover blev der fundet en fordelingskoefficient på 10000 liter pr. kg tørstof og en 1^{ste} ordens nedbrydningsrate på $2 \cdot 10^{-5}$ sek^{-1}.

Sediment beregningerne viste, at sedimentationsprocessen er bestemmende for den vertikale transport af stof i sedimentet. Diffusion er kun betydende i den teoretiske opstartsfase af systemet, hvor koncentrationsgradienten ved sedimentoverfladen er meget stor. Dette er undersøgt yderligere i *Sørensen et al. (2000)*, i forbindelse med en evaluering af den generiske compartmenmodel, SimpleBox, som indgår i "European Union System for the Evaluation of Substances, EUSES".

Vandmodellen blev lavet ved at inddele fjorden i to dele med fuldstændig opblanding, hvor overfladearealet var stort og i en smal passage med dispersion, hvor den horisontale vandstrømning var høj. Den lavvandede fjord ansås at være fuldstændigt opblandet i dybden. De eksperimentelle vandkoncentrationer var tilnærmelsesvist konstante og udviste kun mindre variationer som funktion af stedet. Disse blev ikke modelleret, da de sandsynligvis skyldtes korttids effekter såsom tidsvandsstrømninger. Den gennemsnitlige eksperimentelle koncentration var en faktor 5 højere end den gennemsnitlige beregnede koncentration.

Ferskvand fra vandløb og åer var den dominerende DEHP kilde, efterfulgt af atmosfærisk deposition og rensningsanlæg. Sedimentation var den dominerende fjernelsesmekanisme, efterfulgt af vandskifte med havet og nedbrydning.

På trods af afvigelsen mellem de eksperimentelle og beregnede DEHP koncentrationer i vandet, må den opstillede model anses for at simulere de komplekse interaktioner i Roskilde Fjord tilfredsstillende. For at anvende modellen som et risikovurderingsværktøj vil det imidlertid være nødvendigt at undersøge forhold omkring detektionsgrænser for de betragtede stoffer samt kildetilførsler og tidslige variationer mere indgående.

1 Introduction

The finding of octyl-phthalates in wastewater at high concentrations several years ago *(Miljøstyrelsen 1994)* caused considerable concern, because some phthalates just by then had been recognised as possibly oestrogen-like or carcinogenic, making them harmful to human health. Since then, many investigations of Danish waste water and sewage sludge have confirmed the presence of phthalates, (PAE) as well as nonylphenol-ethoxylates (NPEs), PAHs and an array of other pollutants. The emission of chemicals into the environment leads to the risk of human exposure.

The most severe effects ascribed to oestrogen-like substances seem on the human reproductive health, causing reduced sperm quality and testicular cancer in men, and breast cancer in as well men as women (and other forms of cancer). Although the oestrogen-like effects for the nonylphenols and phthalates are weak compared to many other substances and to oestrogen itself, the concentrations of these compounds in wastewater are high compared to other xenobiotics *(Toppary et al. 1995)*. Hence, nonylphenols and phthalates presumably play a significant role for the total oestrogen-like effect of sludge and wastewater.

This line of thought initiated a series of investigations of the sources, transport and fate of xenobiotics, sponsored by the Danish Environmental Protection Agency (DEPA), carried out by NERI. These investigation were limited to the local community of Roskilde city and surroundings. The present investigation is a part of the series.

In the previous investigations of the project, the emissions to wastewater from an array of pre-selected industries and institutions pre-selected sources were studied. The deposition of nonylphenols and phthalates was measured in a nearby ground station, assumed to represent the fjord surface reasonably well. Also, nonylphenols and phthalates in some streams were investigated *(Vikelsøe et al. 1998)*. However, in that study only about one tenth of the total sources for wastewater was found. The substances are to a large extent removed from wastewater by wastewater treatment plants (WWTPs), but nevertheless some residual substances remain in the outlet. This has been measured in connection with the source project, and again in the WWTP modelling project *(Fauser et al. 2000)*.

The present investigation sets the focus on Roskilde Fjord as a recipient of NPE and PAE, involving sources, transport and fate. It continues the above mentioned source study, and includes measurements of the fjord water itself. The sources of relevance for the fjord are the wastewater treatment plan outlet, the deposition, and some small streams running into the fjord. Furthermore, sediment from the fjord is investigated, since sediments play an important role in the transport and fate of xenobiotics in the aquatic environment of the fjord.

2 Purpose

The aim of the study has been to investigate the occurrence, sources, transport and fate of nonylphenols and phthalates in the aquatic environment of Roskilde Fjord. It was further intended to find the temporal as well as the spatial variation of these xenobiotics in the fjord and stream water. Further, to investigate nonylphenols and phthalates in sediment in the fjord including a sediment core in the southern part, expected to yield clues regarding the historical variation of the concentration of xenobiotics, as well as some streams and lakes. Finally, an important aim was to make a mass balance for the fjord system, including sources, transport and the mechanisms of elimination, and to make a mathematical model describing the fate of the substances in the fjord system.

3 Experimental

3.1 Monthly samples of fjord water

Monthly water samples were taken at two locations, one in the Southern part (Roskilde Vig) near the city of Roskilde, and one further North (Roskilde Bredning). County of Roskilde Authority took these samples from a boat, as an extension of the routine fjord-monitoring program, Table 1.

Table 1 Monthly water samples taken in the southern part of Roskilde Fjord 1998

Location (station)	**Dir** km	**Sampling dates** 24 Mar	 21 Apr	 19 May	 23 Jun	 16 Jul	 18 Aug	 6 Oct	 19 Oct	 20 Nov	 21 Dec
Roskilde Vig (St. 2)	N 2		W	W	W	W	W	W	W	W	W
Roskilde Bredning (St. 60)	N 7	W	W	W	W	W	W	W	W	W	W

Dir = direction and distance from Roskilde Harbour W = water sample

3.2 Seasonal sampling plan

Furthermore, the experimental plan involved three seasonal sampling campaigns, shown in overview in Table 2. Each campaign comprised sampling of fjord water at the mouth of the fjord and at a narrow and a broader place at the middle. These samples were taken from the beach, a bank or a bridge. In the June sampling session, some samples were taken the same day with a time interval of 6 hours, corresponding to different tide, and hence current direction in the narrowest part of the fjord. In each seasonal campaign, water samples were further taken in a brook (Helligrenden), two streams (Maglemose Å and Hove Å) and a lake (Gundsømagle Sø), which Hove Å flows through. In Hove Å and Gundsømagle Lake, some sediment samples were also taken. The lake is involved in the Danish national monitoring program, NOVA.

Table 2 Seasonal sampling, overview

Location	**Type**	**Dir** km	**Sampling dates** Mar 98	 Jun 98	 Sep 98	 Dec 98	 Nov 99
Skuldelev	Fjord	N 16		W	W	W	
Frederiksund	Fjord	N 21		W *	W	W	
Kulhuse (mouth of fjord)	Fjord	N 37		W *	W	W	
Helligrenden mouth	Brook	E 12	W	W	W	W	
Maglemose Å mouth	Stream	N 7	W	W			
Hove Å upstream lake	Stream			W S	W	W	W S
Lake Gundsømagle	Lake		W	W S	W	W S	W S
Hove Å mouth	Stream	N 8	W	W S	W	W S	

W = water S = sediment * Sampled twice with 6 hours interval

In Table 3 the flow in the streams 1998 on the sampling dates as well as the monthly means are given according to hydrometric information from *Roskilde County (1999)*.

Table 3 Flow in streams 1998

Flow l/s		**Jan**	**Feb**	**Mar**	**Apr**	**May**	**Jun**	**Jul**	**Aug**	**Sep**	**Oct**	**Nov**	**Dec**
Hove Å ups	S						52.7			41.0			313
	M	243	368	438	464	135	48.3	64.0	57.5	45.1	138	363	373
Hove Å dns	S			510			54.2			41.0			774
	M	239	389	621	585	141	42.6	69.6	59.0	36.3	83.0	577	552
Maglemose Å	S			117			34.2						
	M	86.6	149	212	230	36.7	16.4	35.1	29.0	13.3	70.1	124	148
Helligrenden	S			71.4			11.0			4.0			48.8
	M	62.0	82.4	93.6	99.8	25.9	11.1	9.2	5.8	4.0	29.9	45.9	66.9

S = Sampling day M = Month mean ups = upstream the Lake dns = downstream

The sampling locations are shown on the overview map in Figure 1.

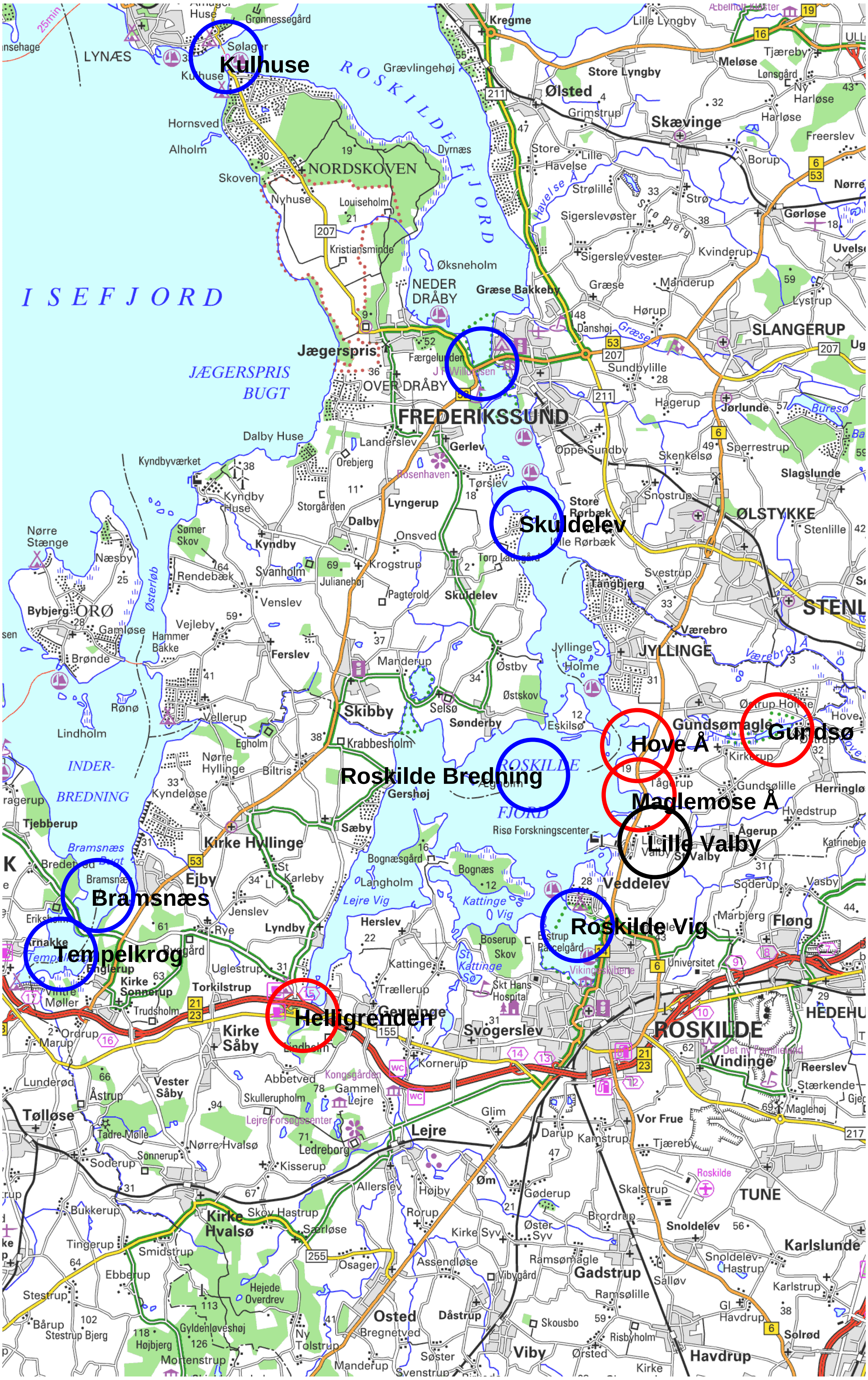

).

Figure 1 Map in scale 1/200,000 showing the sampling locations.
(Colour of circles: Fjord blue, streams and lake red, deposition black

3.3 Samples of fjord sediment

Finally, sediment samples in the fjord was taken during 1996, most of them in Roskilde Vig in a fan-shaped geometry near the outlet from Roskilde WWTP (map Figure 2).

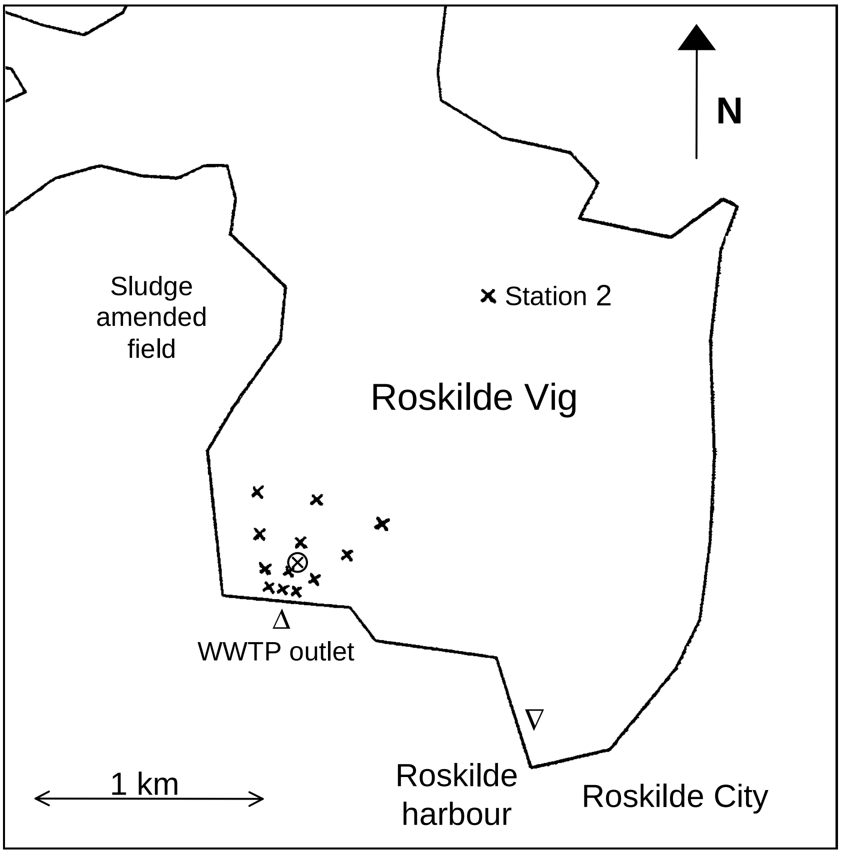

Figure 2 Local map of Roskilde Vig, 1:25000, showing locations of sediment sampling sites and sources.

x	Sampling sites	⊗	Sediment core
Δ	WWTP outlet	∇	Sludge dumping site

The sampling design is based on investigations carried out 1994-95 for Roskilde County Authority and Roskilde Municipality by Danish Hydraulic Institute and Water Consult. According to these reports the current is circulating in the Vig mainly driven by the wind, the tide playing a minor role. The wind is predominantly in the West direction, leading to an South-East water current in the area having a velocity of 2-6 cm/sec.

The WWTP average outlet of waste water is 19000 m^3/day.

Some samples were taken further North in Roskilde Vig and in Roskilde Bredning, on the same locations as the monthly water samples. The sediment also included samples from the neighbouring fjord Isefjord, believed to be lesser polluted, for comparison. These fjord sediment samples were taken by a diver. All sediment samples were taken in the upper 2-5 cm of the sediment, with the exception of the core, which reached a depth of about 22 cm into the sediment. An overview of these samples is shown in Table 4.

The sampling methods are described more detailed in the Analytical Chapter.

Table 4 Overview of samples of fjord sediment taken 1996

Location	**Dir, km**	**n**
Roskilde Vig, near WWTP outlet	E 1	* 13
Roskilde Vig, Station 2	N 2	1
Roskilde Vig, Station 2044	N 4	1
Roskilde Bredning, Station 60	N 6	1
Isefjord, Tempelkrog & Bramsnæs		2

Dir = direction and distance from Roskilde n = number of samples
* including the core, counted here as one sample.

4 Analytical

The following substances were analysed:

NP, NPDE, DBP, DPP, BBP, DEHP, DnOP and DnNP.

The analytical methods used are improvement of the methods used in the previous parts of the project for water and soil *(Vikelsøe et. al. 1998 & 1999)*. A general problem encountered during analysis of phthalates is laboratory contamination, especially with DBP and DEHP, leading to a high analytical background (blank). The high background level impairs the precision of the analysis and elevates the limits of determination, which is a particularly severe problem for samples in very low concentrations, such as the fjord water. As shown in the previous studies, the main cause for this is contaminated glassware. Hence, exclusively new glassware, annealed at 450°C, was used for sampling and laboratory procedures. All solvents used were HPLC grade.

4.1 Sampling

The water was sampled in 2 l glass bottles, fastened in a special bottle holder mounted on a 3 m long pole. During sampling, the bottle mouth was kept upstream, and the bottle was rinsed twice in the water before the final sampling. During boat sampling, the boat was sailing slowly forward, and the sample taken near the prow. After the sampling, the volume was adjusted to about 1.2 l. The sample was frozen in the bottle in horizontal position, and stored in the bottles.

The sediment in the streams and the lake were sampled in new annealed thick-walled 1 l glass beakers fastened in a specially made beaker holder mounted on the pole. The bottom was scraped horizontally until the beaker was filled. The samples were stored in the beakers, covered with aluminium foil.

A diver sampled the fjord sediment, using stainless steel tubes 6.5 cm in internal diameter, reaching about 5 cm into the fjord bottom, and disregarding sand. These samples were transferred to glass bottles with screw caps for storage. The fjord sediment core 21 x 6.5 cm was sampled by hammering the stainless steel tube into the fjord bottom. It was stored in the steel tube.

All samples were frozen and stored at -20°C prior to analysis.

Before analysis, the fjord sediment core was carefully removed from the steel tube in the frozen state, and sawed in sections by means of saw blades cleaned by solvent rinsing. The operation was performed in the freezing room. The sections were 0.5 cm high for the upper 10 cm, and 1 cm sections for the lower 10 cm. The sediment was very hard, and difficult to slice. The uppermost 2 cm, which had a loose sandy texture, could not be sliced and was treated as an entity.

4.2 Extraction of water samples.

The water samples and their sampling bottles was treated as entities, since there may be a significant adsorption to the glass walls. Hence, it was not allowed to divide the samples, or to take subsamples. After thawing at room temperature, the volume of water present in the sampling bottle was measured. A volume of 0.1 ml extraction spike solution containing 0.1 µg of three deuterium labelled phthalates (Table 5) was added, the bottle was shaken and left for 15 min to equilibrate the extraction spikes with the water and the glass surfaces. The sample was extracted by shaking 5 min with 100 ml CH_2Cl_2 after addition of 2 ml 5M HCl. When the phases were separated, a sub-extract of 50 ml was taken, concentrated to near dryness by evaporation and the remanence dissolved in 0.1 ml syringe spike solution (Table 6) containing 0.1 µg D_4-DnOP.

4.3 Extraction of sediment samples

After thawing at laboratory temperature the samples were air-dried for 48 hours on filter paper. About 5 g of dried sample was weighed accurately into a 250 ml wide-necked Pyrex bottle. A volume of 0.1 ml extraction spike solution (Table 5) was added, distributed in the sample by shaking and left for 15 min to equilibrate the extraction spikes with the sample and the glass surfaces, and allow the ethanol in the spike solution to evaporate. A volume of 100 ml dichloromethane was added, and the bottle was closed by a screw-lid covered by aluminium-foil. The sample was extracted at laboratory temperature by shaking for 4 hours in a shaking apparatus (Heidolph Unimax 2010 at 200 shakes/min). When the phases were separated, a sub-extract of 10 ml was concentrated by careful evaporation under N_2, and the remanence re-dissolved in a volume of 1 ml syringe spike solution, Table 6.

The extracts were analysed directly by high-resolution GC/MS without further clean up. If necessary, the samples were diluted appropriately with syringe spike solution.

All sediment samples were extracted and analysed in duplicates.

4.4 Blanks

Every day empty laboratory glassware was extracted for determination of the blank values, i.e. one blank for about every 10 samples. Care was taken to treat the blanks in any way as samples, using same batches of solvents, glassware etc. The blanks were subtracted from the results on an amount per sample basis for each analytical series.

4.5 Standards and spikes

The labelled spikes are used for identification, quantification and for calculation of the extraction recovery. Extraction spikes are added before the extraction, syringe spikes before GC/MS analysis.

Table 5 Extraction spike solution

Substance	Acronym	Label	Water μg/ml	Sediment μg/ml
Dibutylphthalate	D_4-DBP	D_4	1.0	10
Benzylbutylphthalate	D_4-BBP			
Di-(2-ethylhexyl)phthalate	D_4-DEHP			
n-Hexane	Solvent			

Table 6 Syringe spike solution

Substance	Acronym	Label	Water μg/ml	Sediment μg/ml
Di(n-octyl)-phthalate	D_4- DnOP	D_4	1.0	0.1
n-Hexane	Solvent			

Standard solutions are used for quantification and identification (Table 7) analysed by GC/MS for about every 5 samples.

Table 7 Phthalate standard solutions for GC/MS

Substance	Acronym	Type	μg/ml low	μg/ml high
Nonylphenol	NP	Standard	0.01	0.1
Nonylphenol diethoxylate	NPDE	-	0.05	0.5
Di(n-butyl)phthalate	DBP	-	0.01	0.1
Dipentylphthalate	DPP	-	0.01	0.1
D_4-Dibutylphthalate	D_4-DBP	Extraction spike	0.1	0.1
Benzylbutylphthalate	BBP	Standard	0.01	0.1
D_4-Benzylbutylphthalate	D_4-BBP	Extraction spike	0.1	0.1
Di-(2ethylhexyl)-phthalate	DEHP	Standard	0.01	0.1
Di-(n-octyl)-phthalate	DnOP	-	0.01	0.1
Di-(n-nonyl)-phthalate	DnNP	-	0.01	0.1
D_4-Di-(2ethylhexyl)-phthalate	D_4-DEHP	Extraction spike	0.1	0.1
D_4-Di-(n-octyl)-phthalate	D_4-DnOP	Syringe spike	0.1	0.1
n-Hexane	Solvent			

The table sectioning indicate the spikes used for calculation of the results, thus NP, NPDE, DBP and DPP are calculated from D_4-DBP etc. Labelled NP and NPDE was not commercially available, hence, D_4-DBP was used as spike for these compounds in spite of the chemical difference. This is not quite as good as chemical identical spikes, as also shown in the analytical performance test described in section 4.7 and 4.8 and Appendix A.

4.6 Gaschromatography/mass spectrometry (GC/MS)

Gaschromatograph	Hewlett-Packard 5890 series II
Injection:	CTC autosampler. 2 µl split/splitless 270°C, purge closed 40 sec.
Pre-column:	Chrompack Retention Gap. Fused silica, 2.5 m x 0.32 mm i.Ø,
Column:	J&W Scientific DB-5MS. Fused silica, 30 m x 0.252 mm i.Ø, crosslinked phenyl-methyl silicone 0.25 µm film thickness
Carrier gas:	He, 120 Kpa
Temperature program:	40 sec at 80°C, 10°C/min to 290°C, 15 min at 290°C
Mass spectrometer:	Kratos Concept 1S high resolution
Resolution:	10,000 (10% valley definition)
Ionisation:	Electron impact 45 - 55 EV depending on tuning, ion source 270°C
Interface:	250°C direct to ion source
Calibration gas:	Perfluorokerosene (PFK)
Scan:	0.6 sec per scan (about 0.1 sec per ion) in Selected Ion Monitoring (SIM) mode (Table 8).

Table 8 Masses for high resolution mass spectrometry

Substance	Acronym	m/z
Nonylphenols	NP	135.0809
Unlabelled phthalates	PAE	149.0239
D$_4$-labelled phthalates (spikes).	D$_4$-PAE	153.0490
Lock mass	PFK	130.9920

4.7 Performance test of analytical method for water

The performance of the analytical method for water was evaluated by a repeated standard addition experiment carried out on fjord water sampled specifically for the test at the Risø pier at the East side of Roskilde Bredning. Since low concentrations were anticipated, the test was designed to study the range below 0.5 µg/l. A test standard solution in ethanol was prepared, containing the unlabelled substances in Table 7. This was added to 1 litre of the fjordwater in volumes of 0, 100 and 500 µl, respectively. The analysis was carried out in triplicates, making in total nine test samples and three laboratory blanks. The samples prepared in this way were analysed as described above.

In Table 9 the results of the test experiment are shown as the mean, standard deviation, and coefficient of variation. In the lower rows, the overall standard deviation is given, calculated from the pooled variance excluding zero variances, and the detection limits (calculation mentioned in Appendix A). In case of zero averages, the coefficient of variation is not defined. The levels in the Table 9 refer to the added µl test solution, which is approximately the concentration in ng/l. The blank has not been subtracted.

Table 9 Statistics of performance experiment for fjordwater

Statistics ng/l	**NP**	**NPDE**	**DBP**	**DPP**	**BBP**	**DEHP**	**DnOP**	**DnNP**
				Blank				
Blank mean	15	30	205	0	7	70	6	0
sd	13	9	42	0	3	26	6	0
CV%	85	31	20	u	41	38	100	u
				Level 0				
Added ng/l	0	0	0	0	0	0	0	0
Found mean	0	0	143	0	5	110	3	0
sd	0	0	25	0	2	28	1	0
CV%	u	u	17	u	34	26	21	u
				Level 100				
Added ng/l	123	929	80	82	95	37	87	49
Found mean	114	536	226	94	105	117	130	54
sd	7	40	2	3	2	4	12	4
CV%	6	7	1	3	2	3	10	7
				Level 500				
Added ng/l	613	4647	399	409	475	187	433	243
Found mean	345	2563	493	441	454	227	502	232
sd	79	855	28	25	36	38	23	17
CV%	23	33	6	6	8	17	5	7
				Summary statistics				
Pooled sd	46	494	28	18	18	27	13	12
Detection limits	10	40	30	3	3	25	9	4

u = undefined

It is noted from Table 9 that the coefficients of variation for the ”working levels “ 100 and 500, are 6-23 % for nonylphenols, about 17-38 % for DBP and DEHP and 2-7 % for the other phthalates. This difference occur even if the chemical properties of, say, DEHP and DnOP are virtually identical with respect to solubility in water, extraction efficiency, response factor in the mass spectrometer etc. These substances are just the ones which display a high blank (“high blank phthalates”). Hence, a significant part of the variation for these substances must be ascribed to random variations in the contamination background of the individual samples, in contrast to the “low blank phthalates”. Furthermore, for most substances the standard deviations increase with the concentration, except for DBP and DEHP, where it is higher and more constant. This is expected if the major part of the variation is due to the (concentration-independent) blank for these substances. It is further observed that the laboratory blanks in several cases are higher than the 0-level results. A chemical explanation for this may be that the phthalates contaminating the bottle is extracted more efficient in an empty bottle, which brings the solvent (dichloromethane) in closer contact with the glass surfaces than in a water filled bottle. For this reason is has previously been attempted to use distilled water or tap water in the blanks. However, it was not possible to obtain water with sufficiently low phthalate concentrations. *(Vikelsøe et al. 1998)*, hence the use of distilled-water blanks was abandoned.

No significant deviations from linearity were found as mentioned in Appendix A, which describes the performance experiment further.

4.8 Performance test of sediment method

The analytical method for sediment is essentially the same as the soil method described by *Vikelsøe et al. 1999*. The performance of the sediment method was evaluated by a similar repeated standard addition experiment as that for water, carried out on a sediment sample from the middle of Roskilde Vig. A test standard solution in ethanol 10 times stronger than that used for the water experiment was added to 5 g of wet sediment (about 3.5 g of dm) in volumes of 0, 150 and 300 µl, respectively.

Table 10 Statistics of performance experiment for fjordsediment

Statistics, ng/g		**NP**	**NPDE**	**DBP**	**DPP**	**BBP**	**DEHP**	**DnOP**	**DnNP**
					Blank				
Blank	**mean**	29	123	68	0	0	126	0	0
	sd	4	64	5	0	0	1	0	0
	CV%	15	52	7	u	u	1	u	u
					Level 0				
Added	**ng/g**	0	0	0	0	0	0	0	0
Found	**mean**	608	689	287	19	6	923	3	7
	sd	272	437	48	30	10	5	5	11
	CV%	45	63	17	160	173	1	173	173
					Level 500				
Added	**ng/g**	525	3983	342	351	407	160	371	208
Found	**mean**	959	2581	531	385	334	865	389	297
	sd	255	533	149	69	34	109	81	71
	CV%	27	21	28	18	10	13	21	24
					Level 1000				
Added	**ng/g**	1050	7966	685	702	814	320	742	417
Found	**mean**	1074	4209	781	803	663	1221	700	437
	sd	384	1242	188	298	114	234	47	61
	CV%	36	30	24	37	17	19	7	14
					Summary statistics				
Pooled sd		309	820	141	178	69	151	54	54
Detection limits		272	439	48	30	10	43	5	11

u = undefined

The analysis was carried out as described above in triplicates, making in total nine test samples and three blanks.

The statistics of the sediment performance experiment is given in Table 10 calculated in the same way as the water experiment. As seen, more substance is found than is added, certainly because of naturally occurring substances in the sample. Unlike the water experiment, these dominate over the blank. The coefficient of variation for the “working level” 500 is 10-28%, higher than for the water method. This may be due to differences in extraction efficiency, or to incomplete homogenisation of the sample.

No significant deviations from linearity were found. The analytical performance experiment is further described in Appendix A.

5 Results and statistics

5.1 Fjord water

5.1.1 Abundance of substances

The average concentrations and standard deviations measured in the fjord water for the total experiment is shown for each location in Table 11, which also contains the total mean and standard deviation for all samples.

Table 11 Concentration in Fjord water, all samples. Mean and standard deviation, ng/l

Location	n	Stat	NP	NPDE	DBP	DPP	BBP	DEHP	DnOP	DnNP
Roskilde Vig	9	mean	5	0	4	0.38	2.2	74	2.6	9.2
		sd	10	0	11	0.51	1.3	37	4.6	21
Roskilde Bredning	10	mean	9	0	2	0.16	2.5	71	1.0	1.5
		sd	15	0	5	0.18	2.1	25	0.9	2.8
Skuldelev	3	mean	0	0	0	0.28	1.5	97	2.5	6.6
		sd	0	0	0	0.30	2.1	75	1.7	7.5
Frederikssund	4	mean	8	0	31	0.11	7.1	191	4.0	15
		sd	16	0	43	0.14	9.9	211	5.5	30
Kulhuse	4	mean	0	0	5	0.13	2.0	76	0.7	1.4
		sd	0	0	9	0.11	1.6	62	0.9	0.9
Total	30	mean	6	0	6	0.23	2.9	91	2.0	6.1
	30	sd	12	0	18	0.32	3.9	87	3.3	16

0 = not detected

As noted from Table 11, DEHP was by far the most abundant phthalate, followed by considerably lower concentration of DBP, DnNP and DnOP, and minute amounts of BBP and DPP. NP is found on the same concentration level as DBP, but no NPDE was found. The total averages and standard deviations, i.e. of all fjordwater samples, are shown as bar graphs in Fig 3.

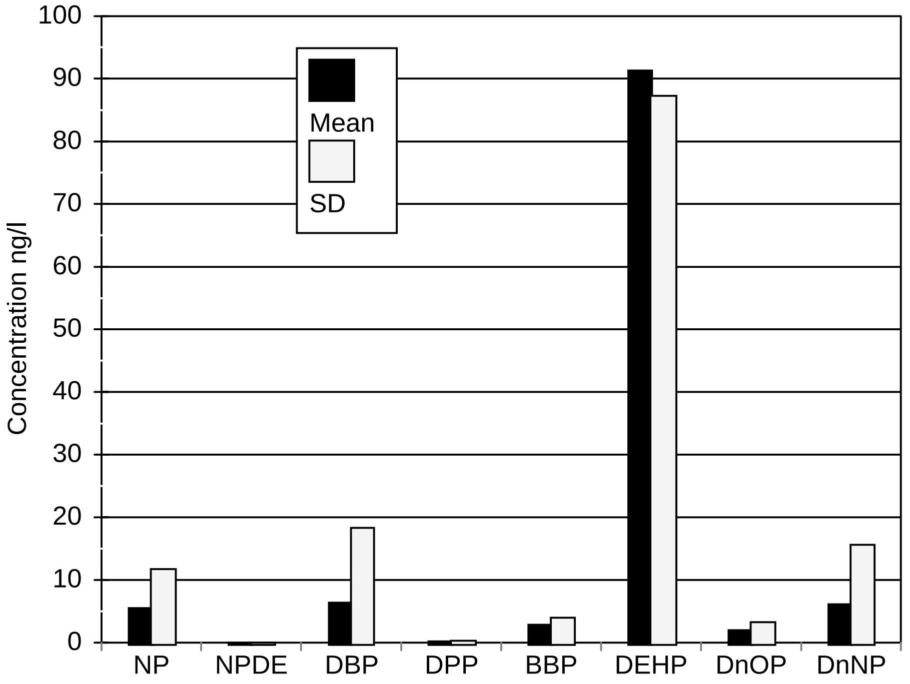

Figure 3 Mean and standard deviations for all samples of fjord water

It is evident from Figure 3 that only DEHP display a significant concentration, which may be of environmental significance. All other substances display concentrations that are extremely low, and can be detected only due to their considerable lower detection limits, which are due to their low laboratory blank. Furthermore, it is seen that the standard deviation for NP, DBP, and DnNP is about the double of the mean, whereas for DEHP, the standard deviation is of the same magnitude as the mean. It must be stressed that these standard deviations reflect as well the natural variation in the fjord water as the analytical error. The reason for the larger relative standard deviations of these substances may be that the concentrations are closer to the detection limits. Also, the natural variation in the fjord water might be larger for those substances compared to DEHP, but is difficult to see a rational reason why this should be the case. The correlation between different substances is evaluated in a correlation analysis described in section 5.1.6.

5.1.2 Temporal and spatial variation

In Figure 4, the spatial and seasonal variation of the DEHP concentration in the fjord water is shown as bar graphs. From the monthly samples taken in Roskilde Vig, those have been selected which are most close in time to the seasonal fjord samples. Station 2 is the innermost position, Frederikssund is located in a narrow passage, and Kulhuse is located at the mouth of the fjord. There are two June samples, taken in Frederikssund and Kulhuse the same day with 6 hours interval, corresponding to different tide, and hence current direction. The average of the locations is shown in the front right row and the average of seasons in the back right row (black).

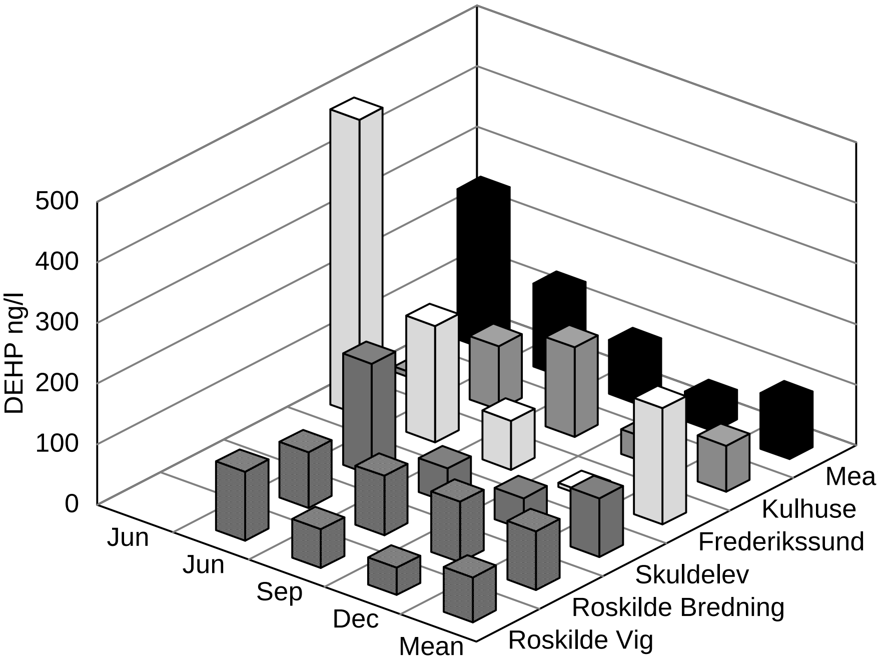

Figure 4 Seasonal and spatial variations of DEHP in fjord water.

As noted from Figure 4, the two June results from Frederikssund and Kulhuse sampled the same day during opposite current directions (North in the left row) indicate a significant short-term variation. At Frederiksund the passage is narrow and the current velocity is high, which probably also is the reason for the more pronounced pattern of seasonal variation observed at this location compared to the others. This observation may be caused by the suspension of sediments by turbulence. The sediment contains large amounts of substances, as mentioned in section 5.2.1. It is further noted that the two innermost locations at Station 2 in Roskilde Vig near Roskilde and Station 60 in Roskilde Bredning (6 km further North) seem to be more constant than the middle and mouth locations.

The means of all seasons for each location (front right row) are almost identical, showing that on an annual average scale the geographical differences are insignificant. On the other hand, in the means for each season (back right row) a maximum for June and a minimum for December is seen. This indicates that a seasonal variation is discernible. These seasonal and spatial variations are further tested statistically by an analysis of variance described in section 5.1.4.

Similar diagrams for DBP, DPP, BBP and DnOP are shown in Figs. 5 - 8.

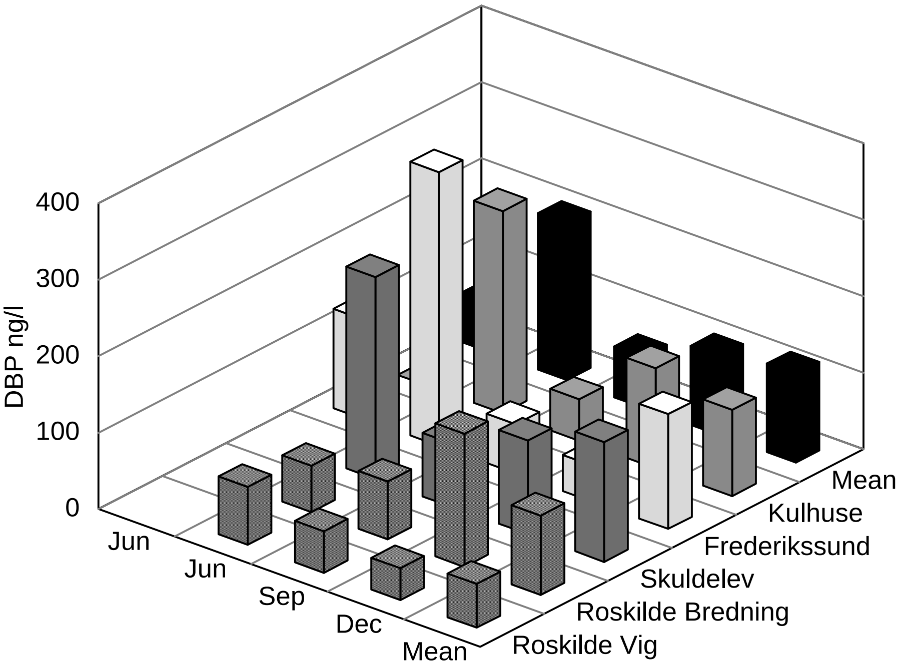

Figure 5 Seasonal and spatial variations of DBP in fjord water.

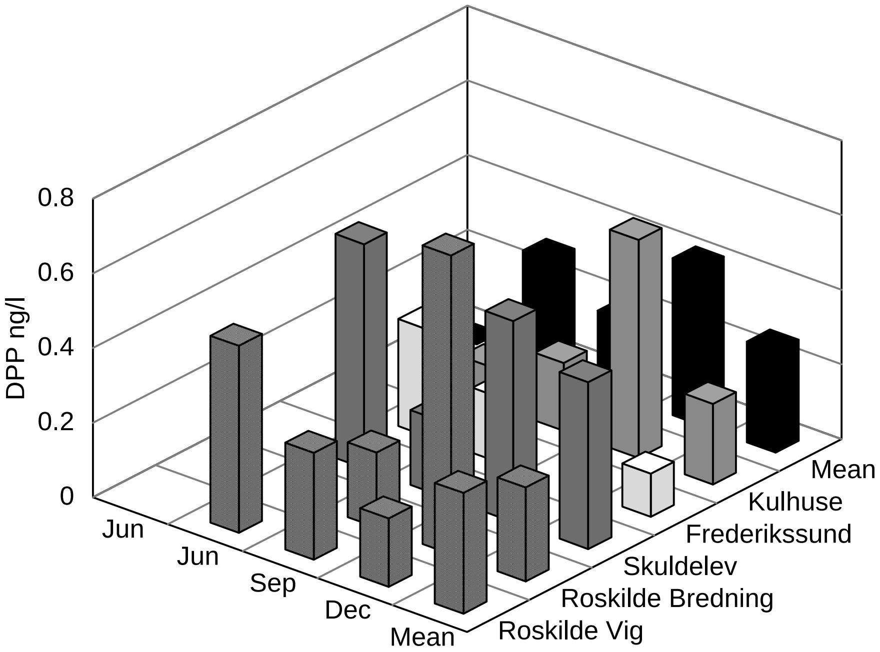

Figure 6 Seasonal and spatial variations of DPP in fjord water.

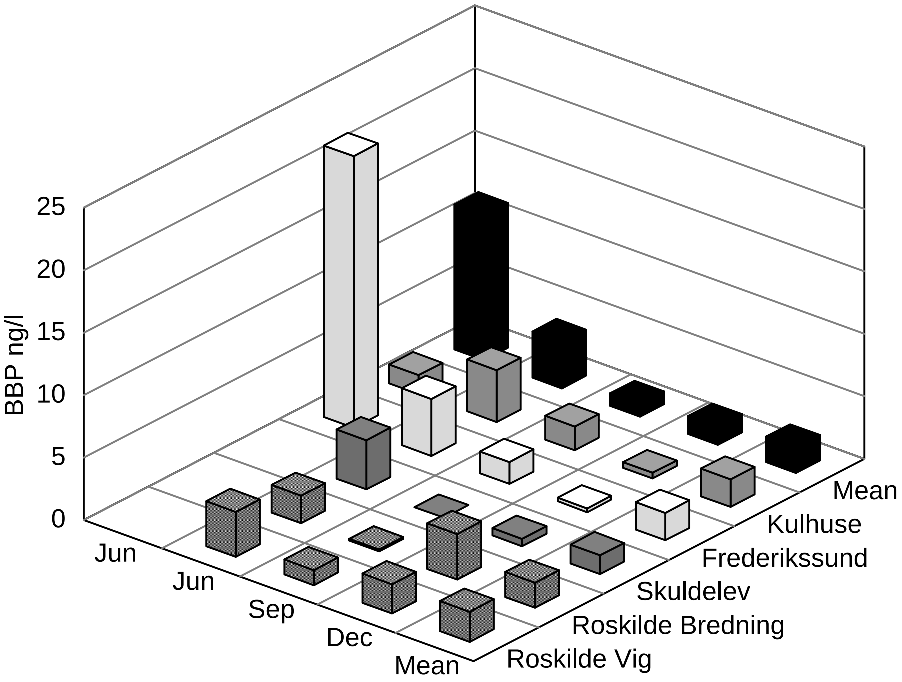

Figure 7 Seasonal and spatial variations of BBP in fjord water.

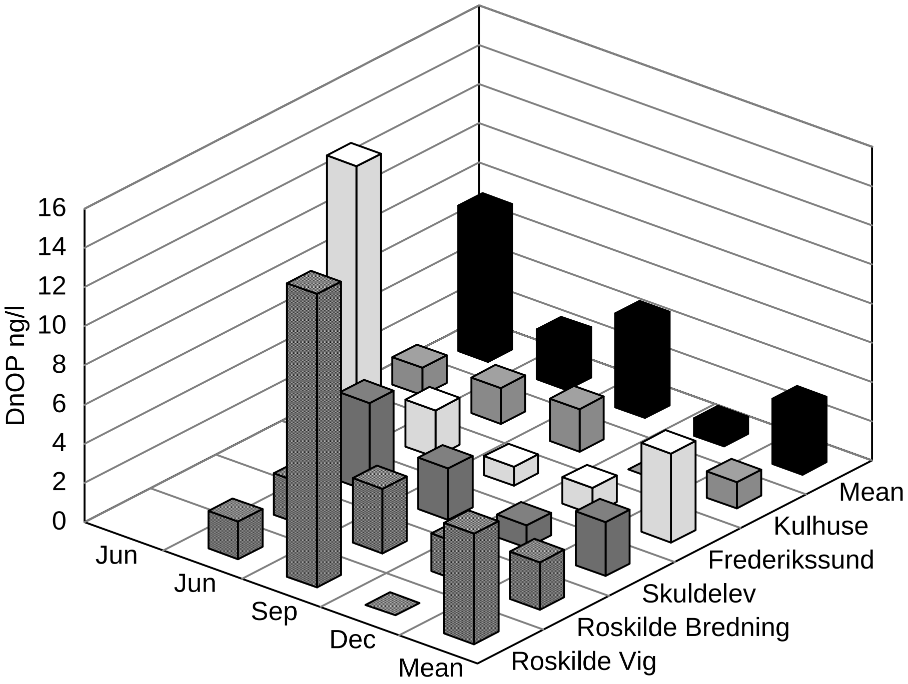

Figure 8 Seasonal and spatial variations of DnOP in fjord water.

As can be seen from Figs. 5 – 8, the seasonal and spatial variations displayed is considerably more erratic in comparison to DEHP in Figure 4, with the exception of BBP, Figure 7, which shows an almost identical pattern. This impression is confirmed by the statistical analysis mentioned below.

5.1.3 Monthly samples in Roskilde Vig and Bredning

Monthly samples were taken at the two southernmost locations at station 2 and 60. Station 60 near the middle of Roskilde Bredning is used by the Roskilde Amt Authority as a sampling station for monitoring other parameters, such as salinity, temperature, turbidity and many others. In Figure 9 the averages for Station 2 and Station 60 for all substances are shown.

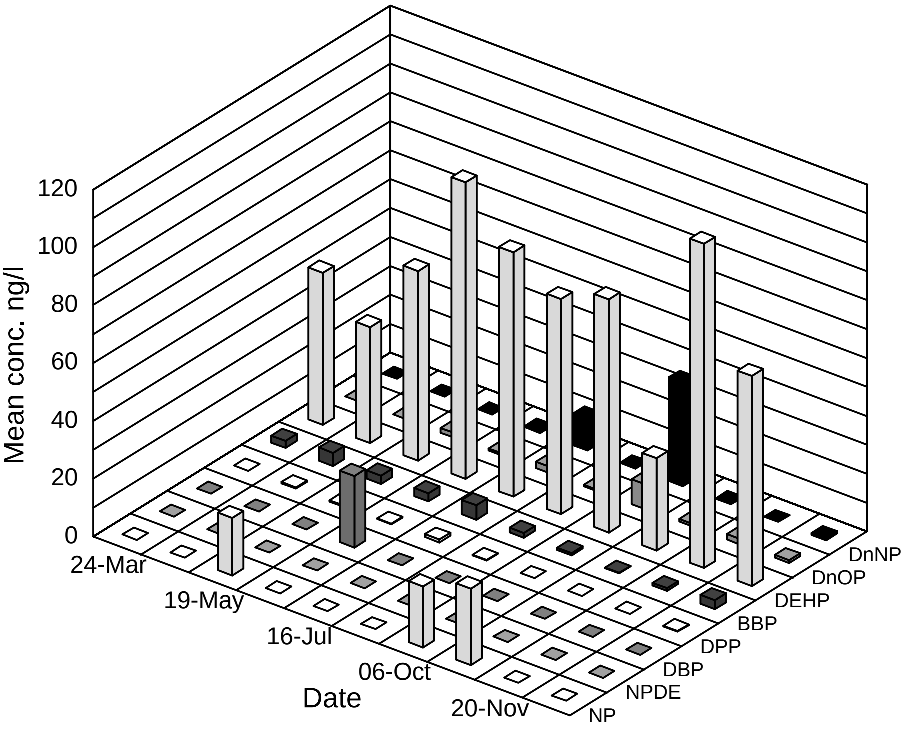

Figure 9 Temporal variation of all substances in fjordwater, mean concentrations of Station 2 and 60.

As noted from Figure 9, BBP and DEHP display a continuos pattern, whereas the patterns for the other substances are discontinuous and seemingly random. This impression is statistically confirmed in the correlation analysis mentioned below. Hence, the interest is concentrated on DEHP in the mathematical modelling, BBP being of lesser importance as a pollutant.

In Figs. 10 and 11 the individual results for Stations 2 & 60 are shown for DBP and DEHP, respectively, as a function of time.

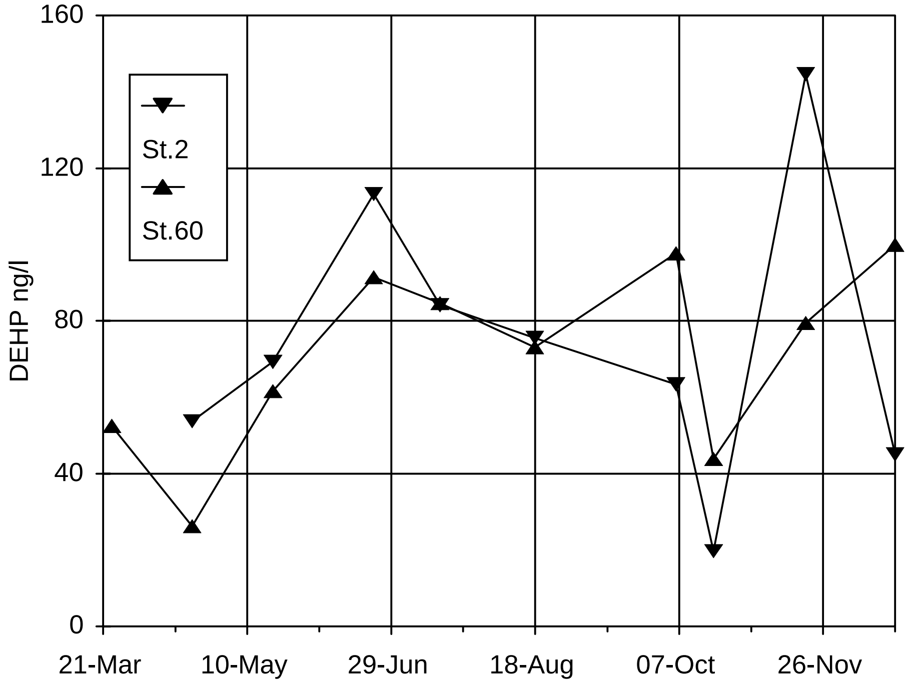

Figure 10 Temporal variation of DEHP in fjordwater at Station 2 and 60.

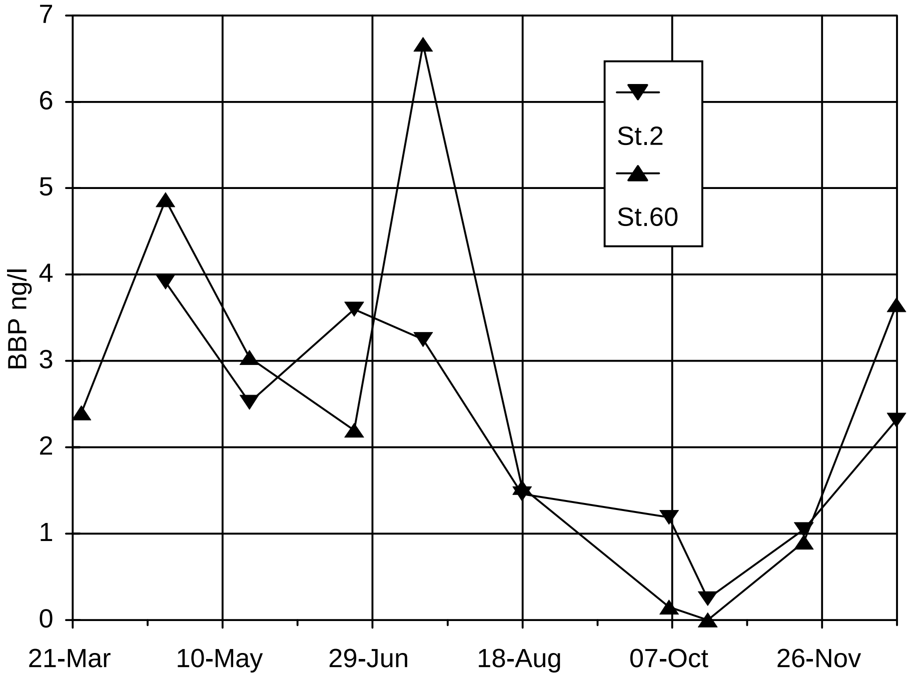

Figure 11 Temporal variation of BBP in fjordwater at Station 2 and 60.

As can be seen from Figs. 10 and 11, the concentrations at the two stations for a particular substance follow each other with few exceptions. This is evaluated statistically by a correlation analysis in a later section. Furthermore, the BBP curve has a pronounced minimum, whereas the DEHP-curve seems more erratic. However, a weak summer maximum can be seen.

5.1.4 Analysis of variance

To evaluate whether the temporal and spatial variations were statistically significant, an analysis of variance was performed. In Table 12, the results for the test of spatial variation is shown. In this case, all data for fjord water were used.

Table 12 Analysis of variance for spatial variation

Statistics	df	NP	NPDE	DBP	DPP	BBP	DEHP	DnOP	DnNP
Between locations variance	4	50	0	389	0.05	12	6605	5	99
Within locations variance	24	145	0	277	0.11	15	6913	11	254
F between/within	4/24	0.35	u	1.40	0.46	0.80	0.96	0.45	0.39
p		0.84	u	0.26	0.77	0.54	0.45	0.77	0.81

df = degree of freedom u = undefined

The between locations variance is the variance of the location-means, weighted by number of measurements at each location, an expression of the spatial variance for the fjord. The within location variance is calculated by pooling the seasonal variances for all locations. F is the ratio between these variances, which are compared by means of the F-test. If F is above a critical value it indicates significant ($p < 0.05$) spatial variation (i.e. a spatial variation so large that it can be seen in the “blur” of seasonal variation). p is the level of significance. Since all $p > 0.05$, no significant spatial variations were found for any substance.

The seasonal variation was tested by an analysis of variance comparing the variance of the season means (i.e. the between season variance) with the pooled within season variance, Table 13. In this case a subset had to be used for station 2 and 60, corresponding to the timing of the other locations, the same subset displayed in Figure 12 to Figure 16. Due to occurring zero variances, the analysis could not be carried out for NP and NPDE.

Table 13 Analysis of variance for seasonal variation

Statistics	df	NP	NPDE	DBP	DPP	BBP	DEHP	DnOP	DnNP
Between seasons variance	2	369	0	169	0.05	10	9664	12	341
Within seasons variance	8	u	0	188	0.05	2	2185	15	256
F between/within		u	u	0.90	1.15	6.02	4.42	0.82	1.33
p		u	u	0.44	0.36	0.03	0.05	0.47	0.32

df = degrees of freedom u = undefined

As noted from the p-row, statistically significant seasonal variations were found for BBP and DEHP. This may be seen in Figs. 4 and 7 in seasonal mean row (black), which as already mentioned display a visible time trend, summer maximum and winter minimum. This trend, of course, cannot be tested by the analysis of variance, since variances do not depend on sequence.

5.1.5 Discussion

The lack of spatial variation is surprising, since *a priori* a descending gradient was expected to occur from the innermost part of the fjord to the mouth. In chapter 6 on mathematical data interpretation this finding is taken *ad notam*.

The seasonal variations found for BBP and DEHP are characterised by higher summer concentrations. This should be expected due to a higher solubility at higher temperatures, and also a higher dissociation from the sediment at the fjord bottom, which is addressed in section 6.1. However, also the seasonal variation in the mass flow from the sources, and degradation rate must be taken into account for a complete understanding of the temporal variation. For these reasons, a mathematical model of the temporal variation would be very complicated, and it would furthermore be difficult to verify since many of the needed parameters would be unknown or only known approximately. Hence, such a model has not been attempted in the present investigation.

5.1.6 Analysis of correlation

An analysis of correlation was performed by calculating the coefficients of correlation for all locations and between all substances ("substance correlations"), Table 14. Correlation coefficients > 0.42 (r crit.) are significantly (p < 0.01) different from 0.

Table 14 Substance correlations for all fjord water samples (n = 30, r crit = 0.42, p<0.01)

r	**NP**	**NPDE**	**DBP**	**DPP**	**BBP**	**DEHP**	**DnOP**	**DnNP**
NP	1							
NPDE	u	1						
DBP	-0.00	u	1					
DPP	-0.10	u	0.04	1				
BBP	-0.20	u	**0.80**	0.19	1			
DEHP	-0.17	u	**0.80**	0.09	**0.86**	1		
DnOP	0.09	u	**0.44**	0.09	**0.51**	**0.59**	1	
DnNP	0.07	u	**0.52**	0.17	**0.57**	**0.58**	**0.97**	1

u = undefined Significant correlations (p<0.01) in **bold**

As seen in Table 14, significant correlations were found between all phthalates from BBP and up (BBP, DEHP, DnOP and DnNP). The correlations found between DBP and the higher phthalates are somewhat misleading due to un-detects in DBP. No significant correlations were found between NP or NPDE and the other substances.

For the Station 60 in Roskilde Bredning monthly measurements of salinity and temperature ("parameters") existed. Hence, for this station it was possible to study correlations between substance concentrations and parameters ("parametrical correlations"). Furthermore, assuming the same temperature and salinity at Station 2 because of the short distance, it was possible to include this station in the parametrical correlation analysis. Finally, the parallel sampling at the two stations made possible to evaluate the correlation for the same substance between the two stations ("positional correlations"). The results of this analysis are shown in Table 15. NP and NPDE have been omitted from the table due to many undetects.

Table 15 Correlations at Stations 2 & 60 (n=10, r crit = 0.71, p<0.01)

r		**Temp**	**Sal**	**DBP**	**DBP**	**DPP**	**DPP**	**BBP**	**BBP**	**DEHP**	**DEHP**	**DnOP**	**DnOP**
	St.	60	60	2	60	2	60	2	60	2	60	2	60
Temp °C	60	1											
Salin °/y	60	0.09	1										
DBP	2	0.34	0.20	1									
DBP	60	0.35	0.19	u	1								
DPP	2	0.45	0.27	0.09	0.09	1							
DPP	60	-0.02	*-0.59*	-0.36	-0.36	0.20	1						
BBP	2	0.29	-0.02	0.42	0.42	*0.57*	0.52	1					
BBP	60	0.16	-0.05	-0.06	-0.06	**0.78**	**0.71**	**0.80**	1				
DEHP	2	0.08	0.19	0.39	0.39	0.16	-0.34	0.16	-0.01	1			
DEHP	60	0.04	0.23	0.27	0.27	0.01	-0.20	-0.07	-0.09	0.38	1		
DnOP	2	-0.09	0.31	-0.19	-0.19	-0.09	-0.33	-0.30	-0.31	-0.01	0.48	1	
DnOP	60	0.26	-0.10	-0.09	-0.09	-0.10	-0.39	-0.41	-0.47	0.09	0.27	**0.78**	1

Significant correlations (p<0.01) in **bold,** (p<0.05) in *Italics*

As noted from Table 15 only few significant correlations were found. No significant correlations with temperature were seen. A weakly significant negative correlation was found between DPP and the salinity. This result could be caused by the presence of the substance in the wet deposition. However, the most abundant phthalates in the deposition are DBP and DEHP as described in section 5.4 which do not display negative correlations with salinity.

Significant substance correlations were only found between BBP and DPP.

Finally, significant positional correlations were found between Stations 2 and 60 for the substances BBP and DnOP.

Thus, only weak correlations were found in the southern part of the fjord, and only between “outsider” substances. The reason for the weak correlations is the limited concentration variation at this part of the fjord.

Selected examples of the correlations are illustrated in the following. In Figs. 12 and 13 are shown two examples of not significant parametrical correlations, plots of DEHP versus temperature and salinity, respectively. Regression lines and correlation coefficients are shown for Station 2 and Station 60, respectively, in the figures.

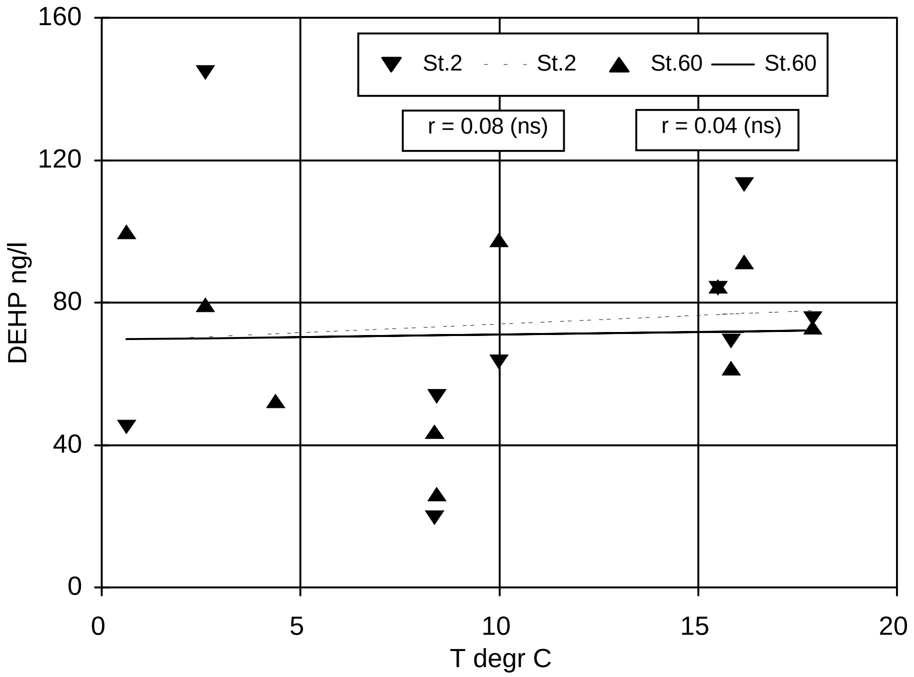

Figure 12 DEHP versus temperature at station 2 & 60. No significant correlations were found

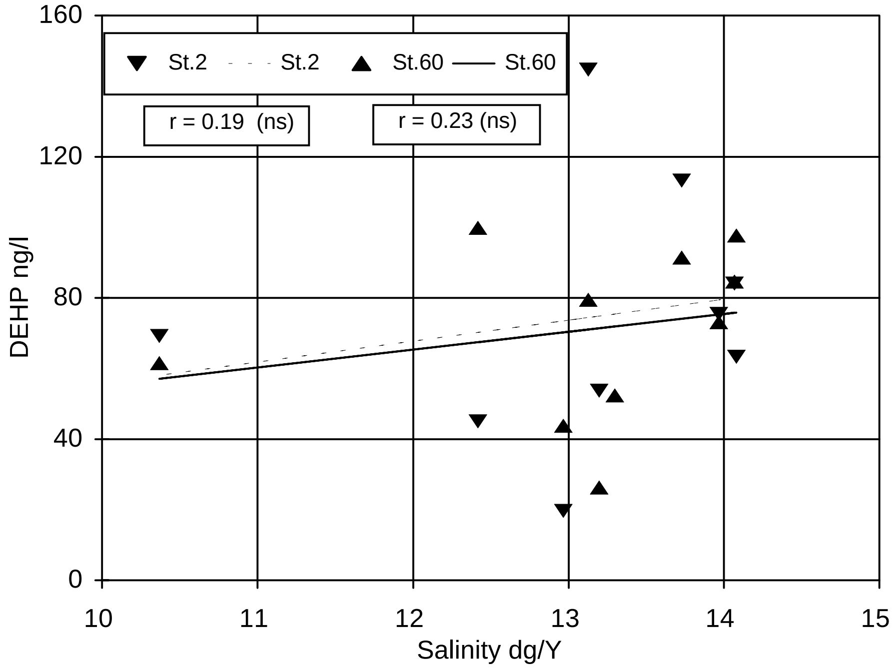

Figure 13 DEHP versus salinity at Station 2 & 60. No significant correlations were found

It is noted that the DEHP concentrations are evenly scattered over the temperature range. In contrast, they are clumped together in the higher salinity range, with exception of two low points.

Significant substance correlations are shown in the following figures between DEHP and BBP and DnOP, respectively.

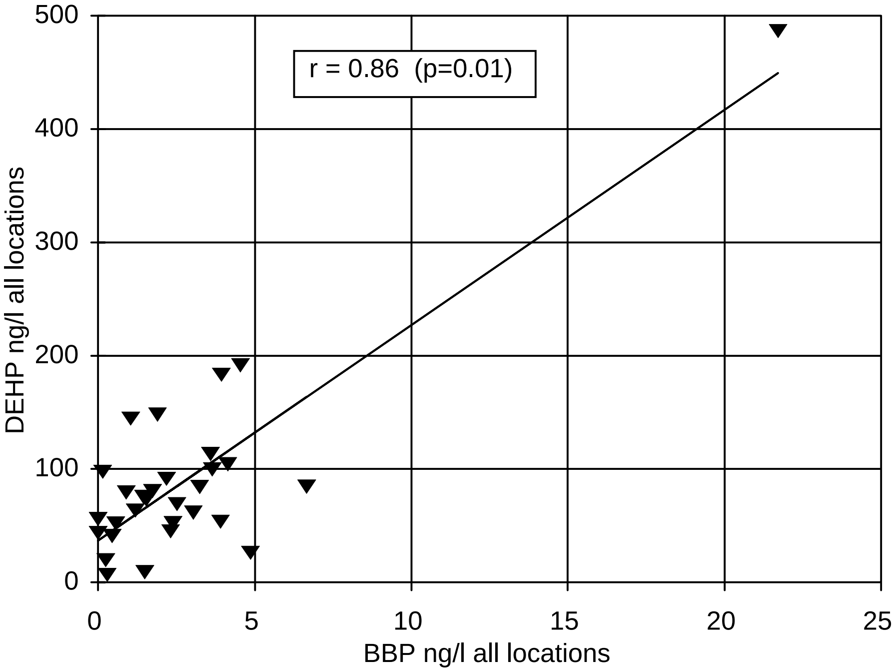

Figure 14 DEHP versus BBP for all locations. Highly significant correlation due to one point.

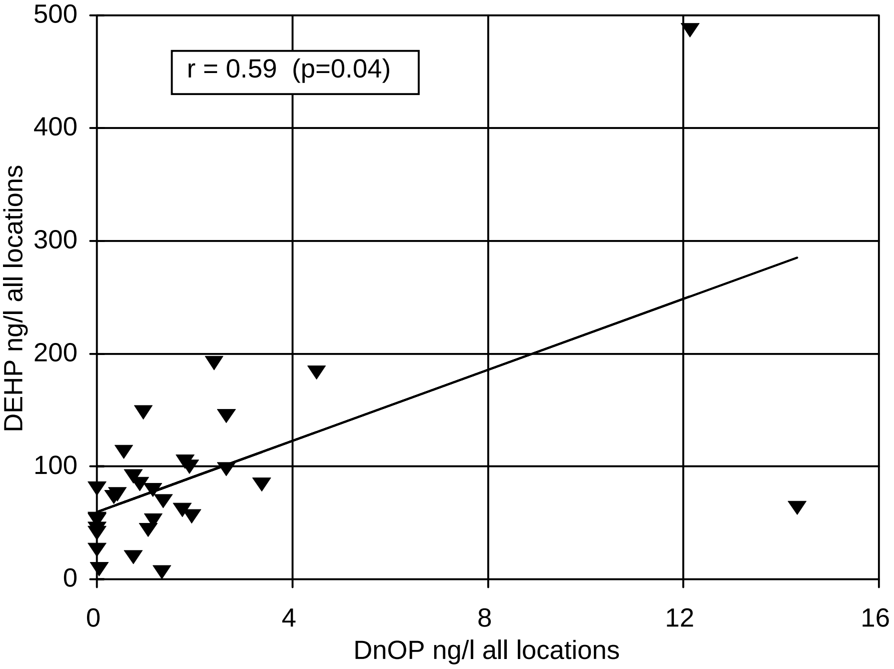

Figure 15 DEHP versus DnOP for all locations. Significant correlation.

As can be seen from Figure 14 and Figure 15, the data points clumps together in the lower left corner. The high correlation coefficient are in these cases due to only one high point. Hence, in spite of the high significance the correlation is uncertain, since one high point in a dataset may be an outlyer.

In Figure 16 is shown a positional correlation between Station 2 and Station 60 for BBP.

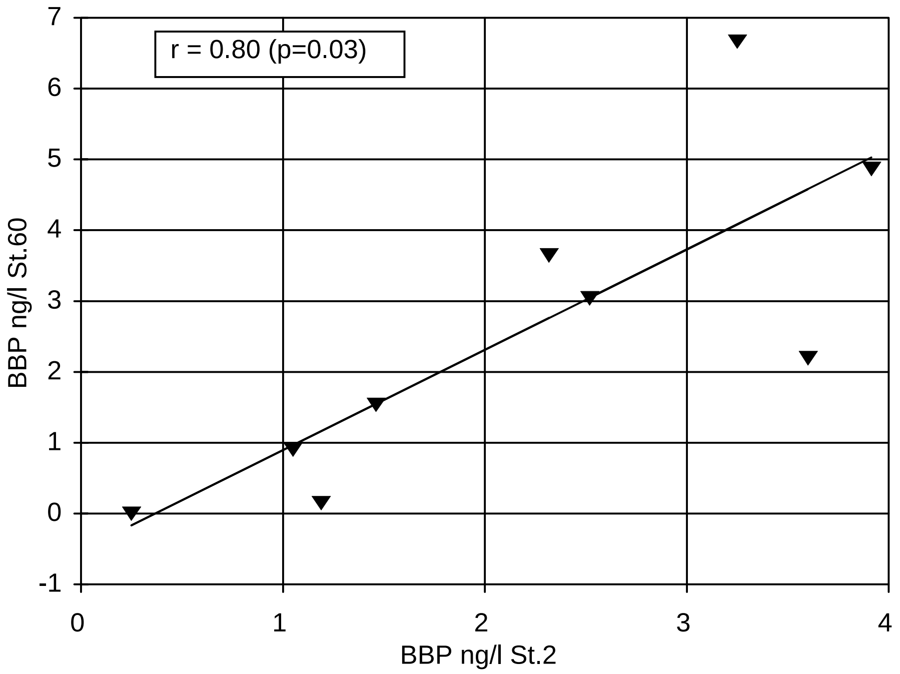

Figure 16 Station 60 versus Station 2 for BBP. Significant correlation.

As can be seen from Figure 16, a good linear relationship exists for BBP between the two locations. It is somewhat surprising that this is found for BBP, and not for the much more abundant substances DBP and DEHP. There is no obvious environmental explanation for this observation.

5.2 Fjord sediment

5.2.1 Abundance of substances

In the sediment much higher concentrations were found than in the water. In Table 16, the results for the sediment are shown as mean and standard deviation for the Roskilde Vig near the WWTP outlet, and average for the positions further away Station 2, Station 2044 and Station 60. Furthermore, the results for the two stations in the Isefjord are shown for comparison. “d” is the mean distance from the WWTP outlet in meters.

Table 16 Concentrations in fjord sediment, ng/g dm, mean and standard deviation

Location	Station	d, m	n	Stat	NP	NPDE	DBP	DPP	BBP	DEHP	DnOP	DnNP
Vig	WWTP	210	26	mean	147	180	143	0.4	7.0	724	8.9	17
				sd	150	133	178	0.5	4.7	375	10.2	11
Vig	St 2	1883	2	mean	347	276	78	0.6	5.4	161	9.9	25
				sd	22	68	18	0.6	4.0	37	4.6	19
Bredning	St 2044	3981	2	mean	176	118	59	0	3.6	133	5.7	8.1
				sd	23	30	21	0	3.0	53	1.8	2.3
Bredning	St 60	6374	2	mean	149	23	46	0.8	4.4	52	1.8	1.7
				sd	45	32	6	0.5	0.3	5	0.7	2.4
Isefjord	Bramsnæs		2	mean	214	0	44	0	2.7	80	1.1	0.6
				sd	9	0	5	0	0.3	28	0.1	0.9
Isefjord	Tempelkrog		2	mean	49	0	43	2.0	4.6	21	2.4	2.4
				sd	9	0	4	0.5	2.0	12	0.2	0.2
Total			36	mean	158	153	118	0.5	6	548	8	15
				sd	139	134	156	0.6	4	429	9	12

d = distance from WWTP outlet

As seen from Table 16, DEHP and DBP were the most abundant phthalates in the fjord sediment. The mean of DEHP in Roskilde Vig was 724 ng/g dm, but the individual concentrations ranged up to nearly 2000 ng/g dm. NP was found in higher concentrations than DBP, and in contrast to the fjordwater, also NPDE was found, in concentrations almost identical to those of NP.

5.2.2 Horizontal distribution

The mean concentrations for all phthalates - with the exception of DPP - displayed a general decreasing tendency from the locations nearest to the WWTP outlet through station 2 and 2044 average 3 km away to the farthest location Station 60 6 km to the North. The concentrations at Station 60 are comparable with the concentrations found in Isefjord, where the lowest concentrations are found in the inner part, Tempelkrog.

The individual results for DEHP in sediments of Roskilde Fjord are shown in Figure 17 and for NP and NPDE in Figure 18 versus the distance to the WWTP outlet. The point labels e, m and w refer to the East, middle and West positions, respectively, of the fan-shaped sampling layout (shown on map in Figure 2).

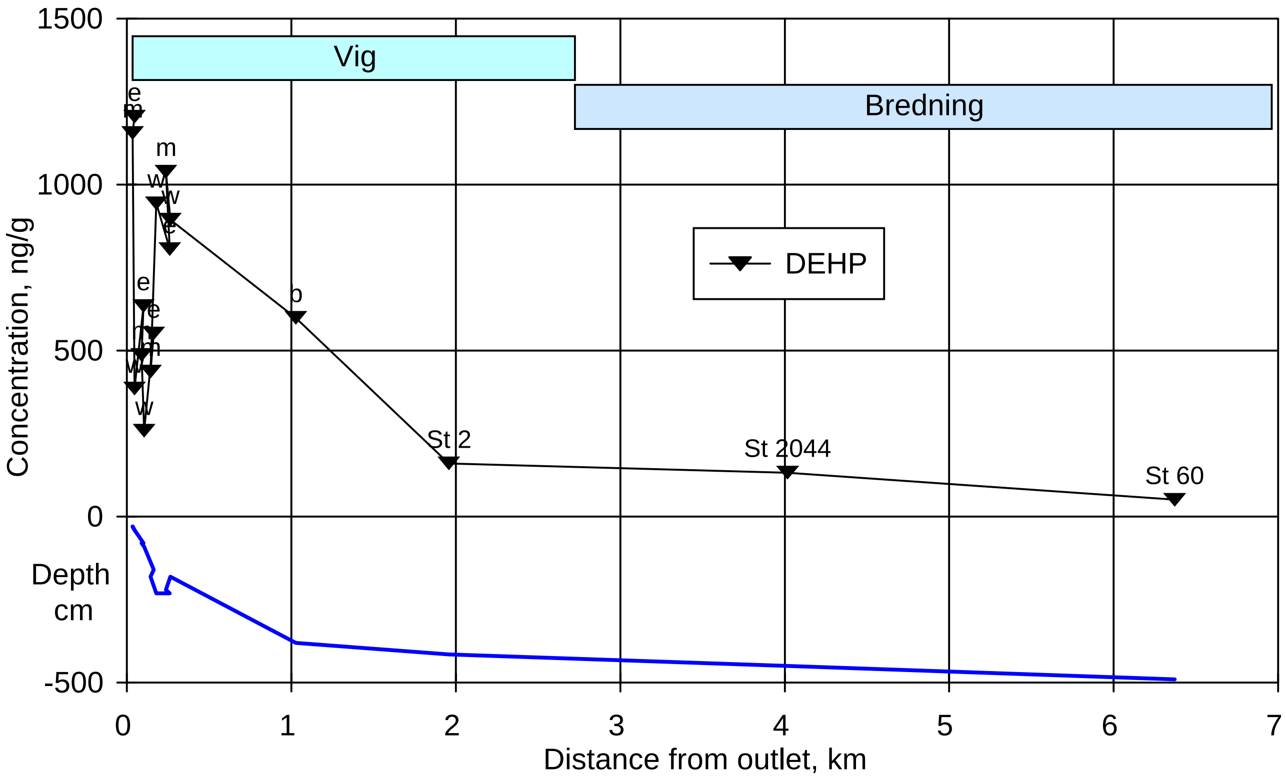

Figure 17 DEHP in sediments of Roskilde Fjord versus distance to WWTP outlet.

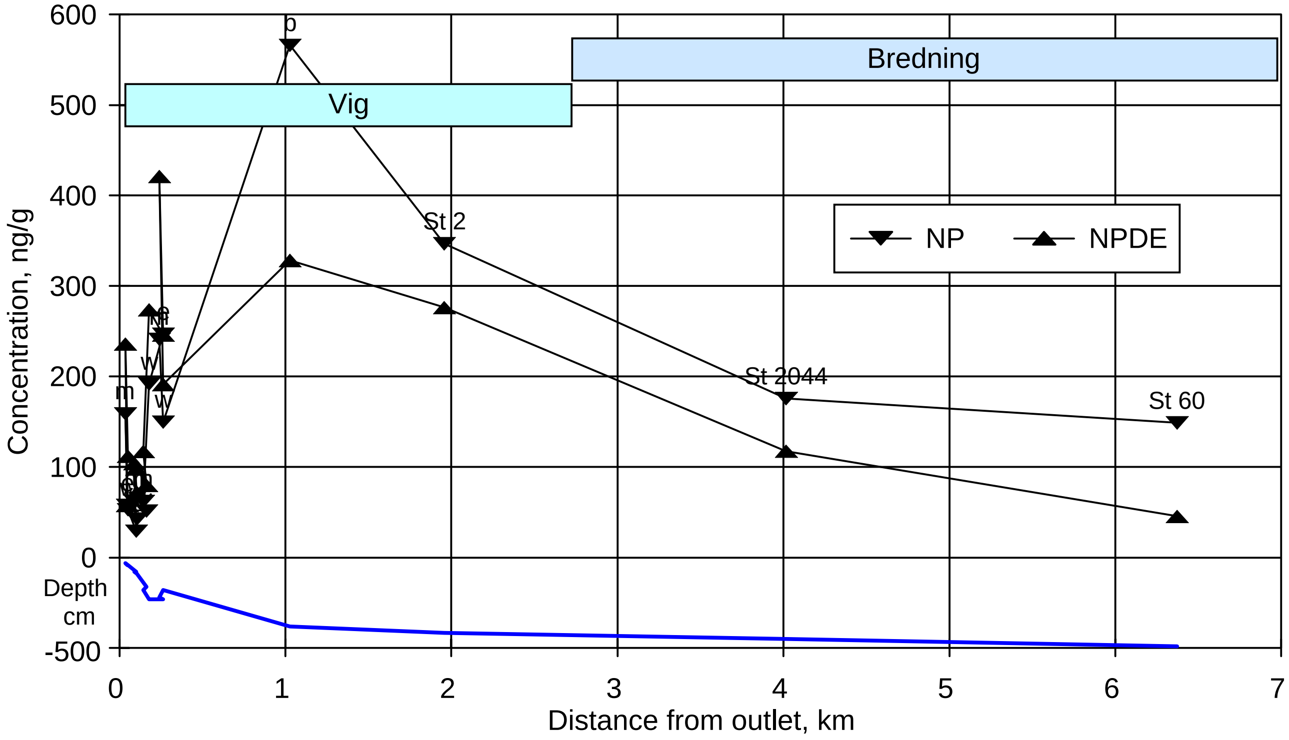

Figure 18 NP and NPDE in sediments of Roskilde Fjord versus distance to WWTP outlet.

In Figure 17 an almost monotonous descending gradient is observed for DEHP. Thus, for the sediments a significant spatial variation can be seen, unlike the fjordwater, where no such gradient was found. An important process going on is thus sedimentation of substances bound to particles and binding of dissolved substances to sediment in the fjord bottom. It is seen that essentially all DEHP has been carried to the bottom within the shallow depths of the first few kilometres. Further away the concentration levels off, ultimately approaching a level comparable with the reference sediment samples in the less polluted Isefjord. This concept is to be evaluated in further detail in the mathematical model described in section 6.1.3.

The horizontal transport of particle bound DEHP is thus short-ranged and seems to be insignificant on a geographical scale larger than some kilometres. This observation is consistent with the very hard texture of the sediments: As soon as the substances are incorporated into the sediments, they are essentially fixed in position. Neither does DEHP dissolved in the water significantly contribute to the horizontal transportation, since this would have resulted in a levelling of the concentrations at different locations. This is consistent with the low concentrations occurring in the water.

NP and NPDE shown in Figure 18 display a more complicated pattern, since a concentration maximum is found a distance of about 1 km from the outlet, followed by a monotone decline at larger distances. Also in this case, the concentrations at large distances approach those in Isefjord. In the lake sediment mentioned in section 3.5.2, an analogous pattern for NP and NPDE is seen. It seems that the NP/NPDE is carried to the bottom sediments more slowly than DEHP, perhaps because these substances are detergents which exist in micelle form, keeping them suspended in the water. The micelles are eventually broken by dilution in the water, but this is a slow process.

In the sediments very close to the WWTP outlet (the “near-field”), a complicated pattern is observed in Figs. 17 and 18. To illustrate the concentrations found at the individual sample positions in that region, Figure 19 shows a column-map plot of the DEHP concentrations, seen from South. The WWTP outlet is located on the East-axis near the 100 m position.

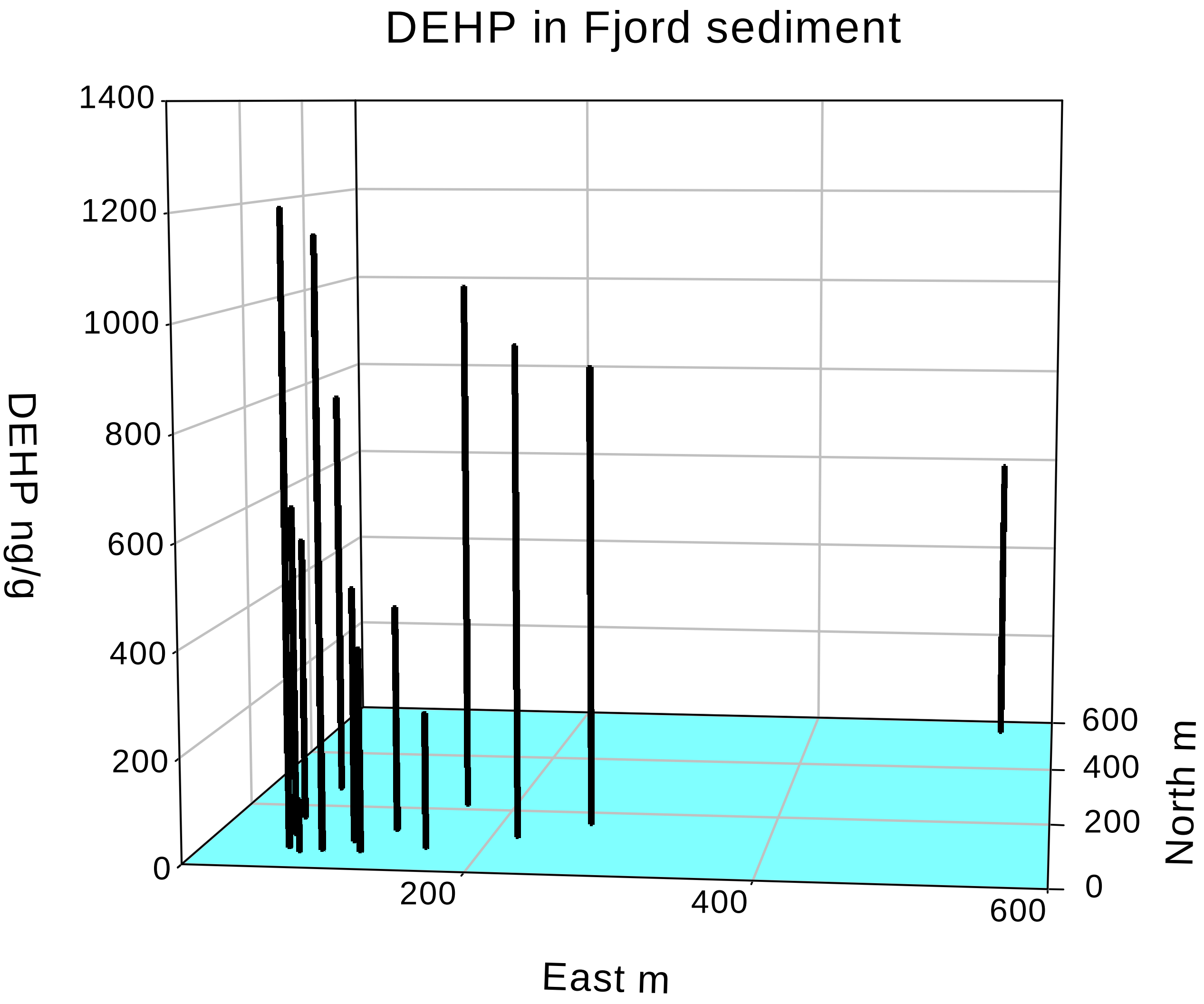

Figure 19 South view of DEHP concentrations in fjord sediment in Roskilde Vig near WWTP outlet located at the 100 m position on the East axis.

As observed in Figure 19, a subset of points forms a monotonous descending gradient, interspersed with points of lower concentrations. This pattern is probably generated by the action of currents and waves near the shore, which lead fresh water with low concentration into the area, and probably suppress sedimentation by the action of turbulence in some point. This can also be the reason for the large fluctuations near the shore in Figs. 17 and 18. The current in the area is primarily from west to east, driven by the predominantly western wind *(Roskilde County & Municipality 1994).*

5.2.3 Vertical distribution in sediment core

The results for the most abundant substances in the fjord sediment core, DEHP, BBP and NP are shown in Figs. 20 to 22. Tentative time scales are shown below the x-axis, based on the 0.25 cm/y sedimentation rate found by ^{210}Pb dating (*Madsen & Larsen 1979*). This scale probably underestimates the age of the oldest sediments, since a compression takes place in the deeper layers.

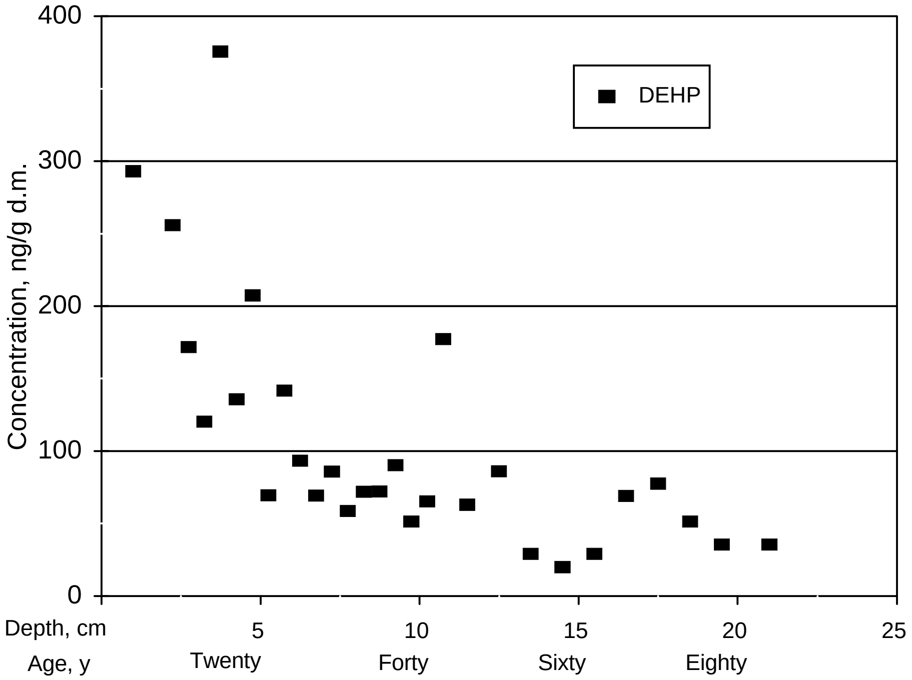

Figure 20 DEHP in the core of fjord sediment near the WWTP outlet.

In Figure 20 a general decreasing tendency of DEHP concentration with depth can be observed. There is a large scatter of the points, and there seem to be weak local maxima occurring at depths of 11 and 17 cm. It is evident that old sediment layers contain lesser xenobiotic substance than newer ones, reflecting a history of increasing pollution.

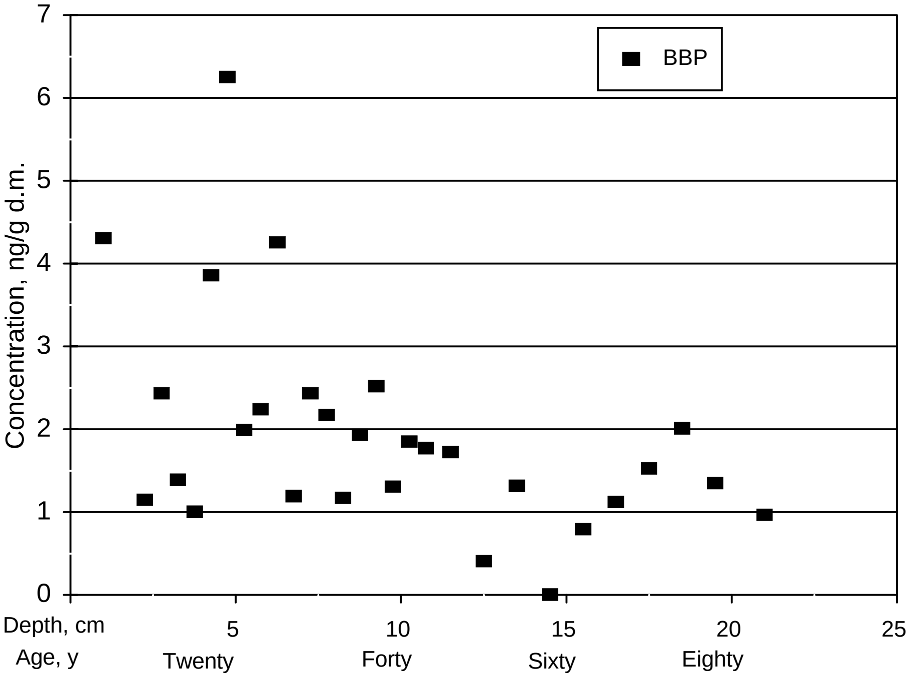

Figure 21 BBP in sediment core

As observed in Figure 21, BBP display the same general pattern as DEHP, but with more random variation. More pronounced maxima are seen, occurring roughly at the same depths as for DEHP.

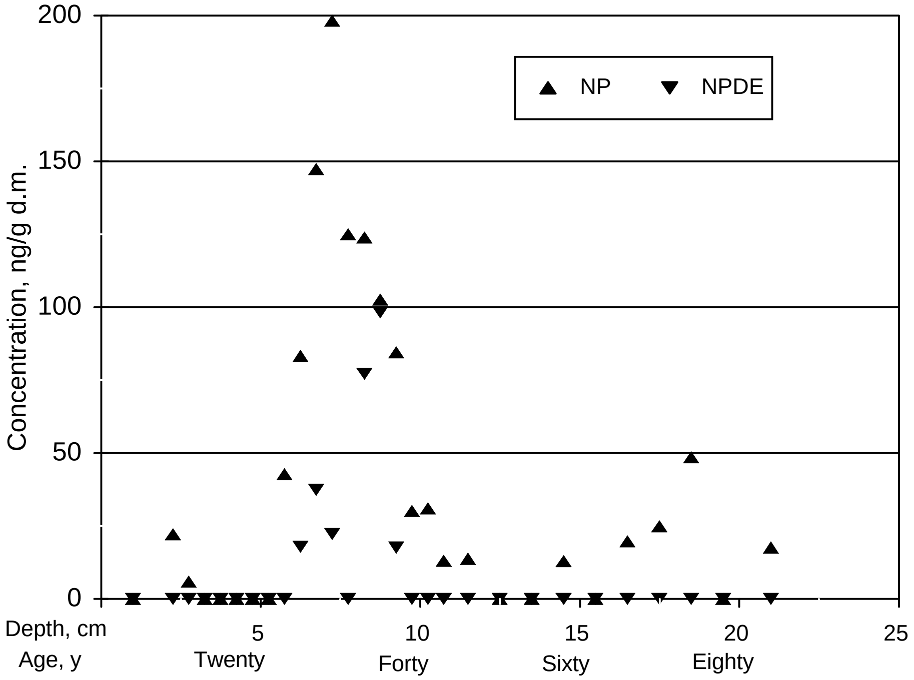

Figure 22 NP and NPDE in sediment core

For NP and NPDE, a very different and interesting pattern is observed in Figure 22, which display two pronounced maxima occurring at depths of 7 and 18 cm, respectively. These maxima coincides approximately – but not precisely - with those observed for DEHP and BBP. A probable explanation for this observation may be a long-term variation in the consumption of NPE, since these by an agreement between the detergent industry and the environmental authorities has been phased out in 1989.

For the variation with depth, another factor of significance is the new and more efficient WWTP, taken into operation in 1995. The current efficiency is described by *Fauser et al. (2000)*.

For a more complete understanding of the variation with depth, a model taking care of the transport, adsorption and desorption as well as degradation will be described in section 6.1.4. The model treats only the fate of DEHP, being the most abundant substance.

5.3 Streams and lake

5.3.1 Water

In Table 17 the abundances of the substances in the stream and the lake water are shown as mean and standard deviation of all samples

Table 17 Abundance of substances in stream and lake water. Mean and standard deviation all samples, ng/l

Water, ng/l	n	Stat	NP	NPDE	DBP	DPP	BBP	DEHP	DnOP	DnNP
Hove Å upstream lake G.	4	mean	17	201	0	0.4	2.3	313	4.1	0.5
		sd	33	402	0	0.8	2.7	218	3.7	1.0
Lake Gundsømagle Sø	5	mean	19	230	11	1.6	13	408	20	8
		sd	43	514	21	2.2	19	428	39	16
Hove Å downstream lake G.	4	mean	0	0	0	1.3	4.5	405	108	699
		sd	0	0	0	1.0	5.4	510	216	1399
Maglemose Å near mouth	2	mean	0	0	0	0.2	2.3	158	0.7	0
		sd	0	0	0	0.1	1.5	139	1.0	0
Helligrenden near mouth	4	mean	13	0	0	0.1	1.9	107	1.3	0
		sd	26	0	0	0.1	1.3	140	2.7	0
Total	19	mean	11	103	3	0.8	5.1	298	29	149
		sd	28	313	11	1.3	9.7	336	100	641

0 = not detected.

The total means and standard deviations from Table 17 of all stream and lake water samples are shown as bar graphs in Figure 23.

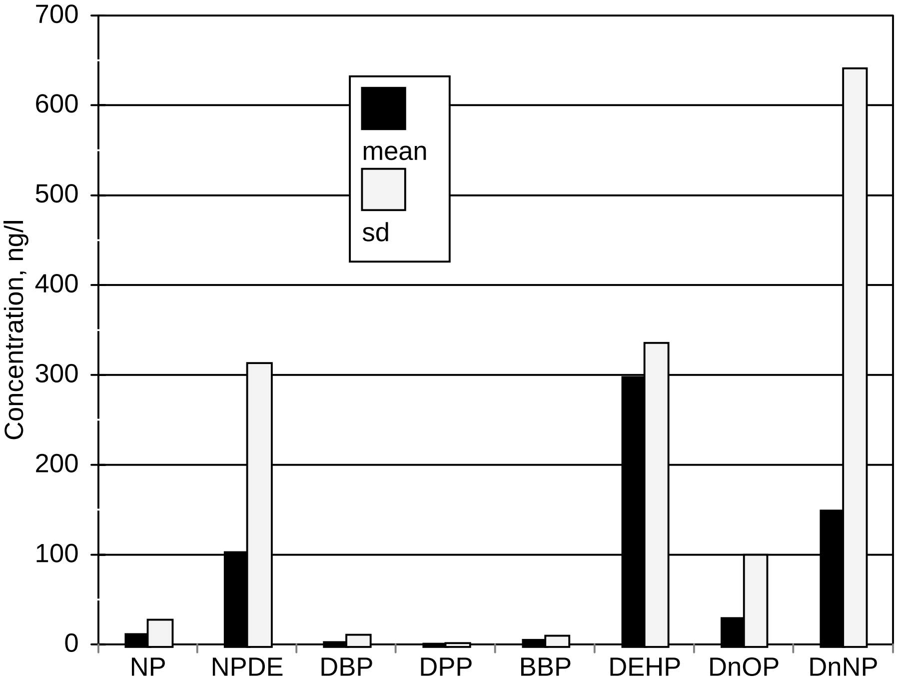

Figure 23 Total mean and standard deviations of water in streams and lake.

In the water of the streams and the lake, the most abundant phthalates was DEHP, DnNP and DnOP followed by very low amounts of BBP and DBP as seen from Table 17 and Figure 23. DEHP occurred overall in about the triple concentrations of those occurring in the fjord. NP occurred in significant concentration, and in contrast to the fjord water, also NPDE was found.

NPDE was found in Lake Gundsømagle and in Hove Å upstream the lake. These substances thus seem to be removed by sedimentation in the lake, a view supported by the sediment measurements mentioned below. DBP occurred only in the lake and only at low concentrations. Contrary to expectations, an increasing concentration gradient for most phthalates was observed in the flow direction in the Hove Å system through the lake. Remarkably, DnOP and DnNP were found at very high concentrations in Hove Å downstream the lake (near the mouth), indicating a local pollution.

The water of the nearby stream Maglemose Å displayed significantly lower concentrations of all substances measured (about the half for DEHP). The water in Helligrenden on the other side of the fjord located in a more rural area displayed still lower abundances, approaching the level in the fjord water. The spatial and temporal variation of DEHP is shown in Figure 24 and for BBP in Figure 25.

The spatial and temporal variations of DEHP and BBP in the water of the streams as seen from Figs. 24 and 25 were more pronounced and seemed more random in comparison to the fjord water. This must be expected since the streams – unlike the fjord – are hydraulic separate entities located in different geographical areas, fed by different sources and having different flows, which display large variations due to the deposition.

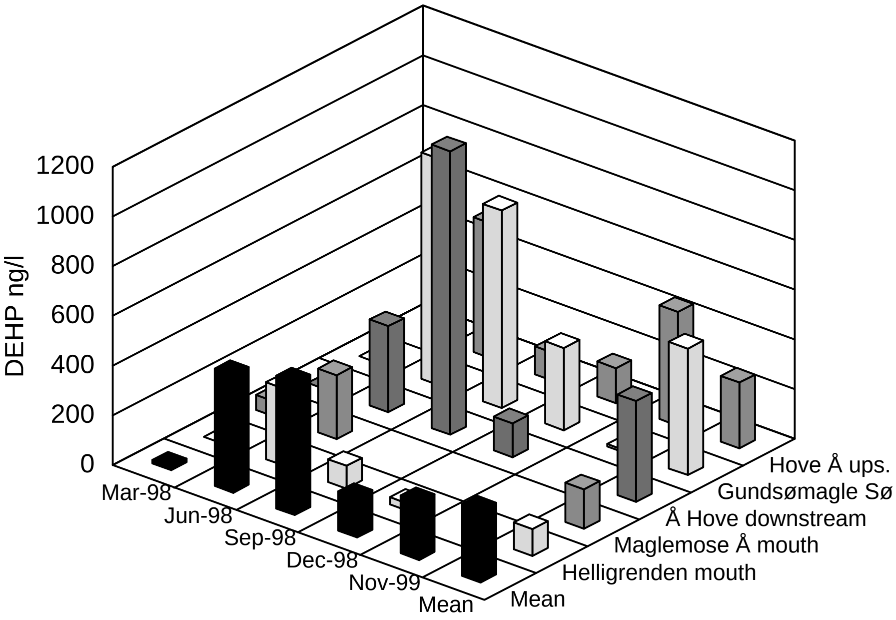

Figure 24 Spatial and temporal variation of DEHP in water of streams and lake

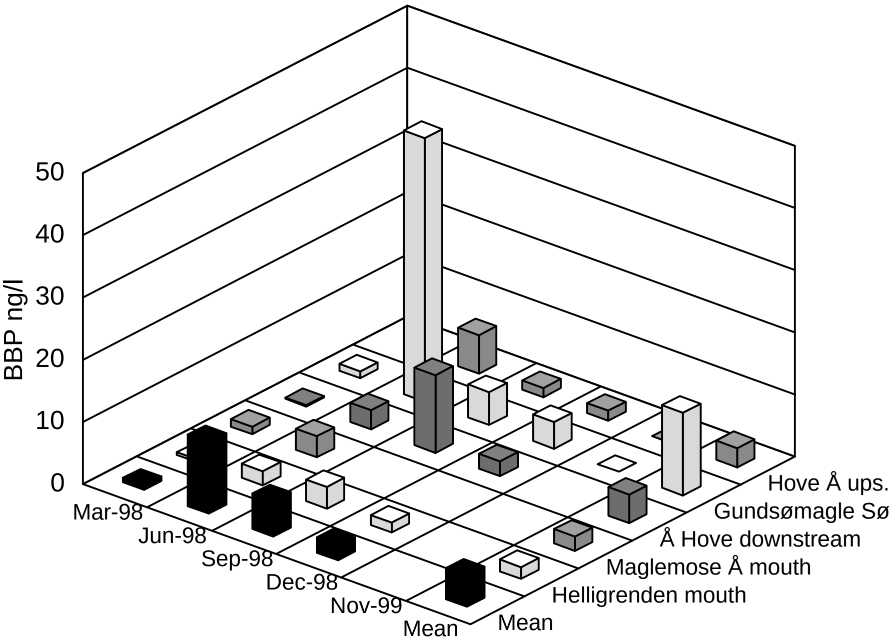

Figure 25 Spatial and temporal variation of BBP in water of streams and lake

5.3.2 Sediment

In Table 18 the abundances of the substances in the stream and the lake sediments are shown as mean and standard deviation of all samples. Only sediment from the Hove Å system was sampled. Within the lake there are three sampling positions at different distances from the inlet of Hove Å (in the East end of the lake) and near the South bank, respectively.

Table 18 Abundance of substances in stream and lake sediment. Mean and standard deviation, all samples, ng/g dm

Sediment, ng/g dm	n	Stat	NP	NPDE	DBP	DPP	BBP	DEHP	DnOP	DnNP
Hove Å upstream lake G.	2	mean	32	9	17	0.9	3.8	75	3.6	7.0
		sd	5	13	23	1.3	0.01	20	0.02	2.3
Gundsømagle Sø 100 m W	2	mean	416	341	38	0.4	5.5	93	2.7	5.8
		sd	19	113	14	0.6	0.5	11	2.1	4.3
Gundsømagle Sø 200 m W	2	mean	2362	2278	67	0	2.2	124	1.0	4.2
		sd	335	425	42	0	0.3	3.7	1.4	1.7
Gundsømagle Sø S bank	2	mean	223	0	3	0	1.4	14	1.5	0
		sd	57	0	2	0	2.0	6.6	2.2	0
Hove Å downstream lake G.	6	mean	110	240	3	0.8	1.7	180	2.6	9.2
		sd	47	251	5	1.5	3.1	115	1.6	6.2
Total	14	mean	480	479	19	0.5	2.6	121	2.4	6.4
		sd	812	797	28	1.1	2.5	94	1.6	5.2

0 = none detected

The total means and standard deviations from Table 18 of all sediment samples from the streams and the lake are shown as bar graphs in Figure 26.

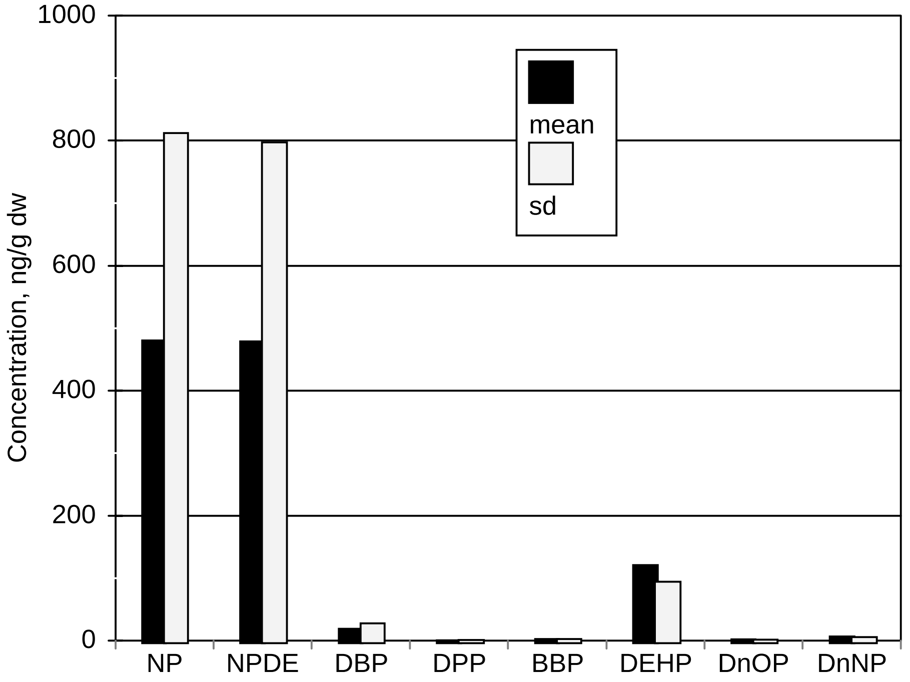

Figure 26 Mean and standard deviations of all sediment samples in streams and lake.

A prominent feature in Figure 26 is the very high almost equal abundance of NP and NPDE in the stream and lake sediment, followed by DEHP and much lower concentrations of DBP, DnNP and DnOP.

The spatial and temporal variations of DEHP, NP and NPDE in the stream and lake sediment are shown in Figs. 27 to 29, respectively.

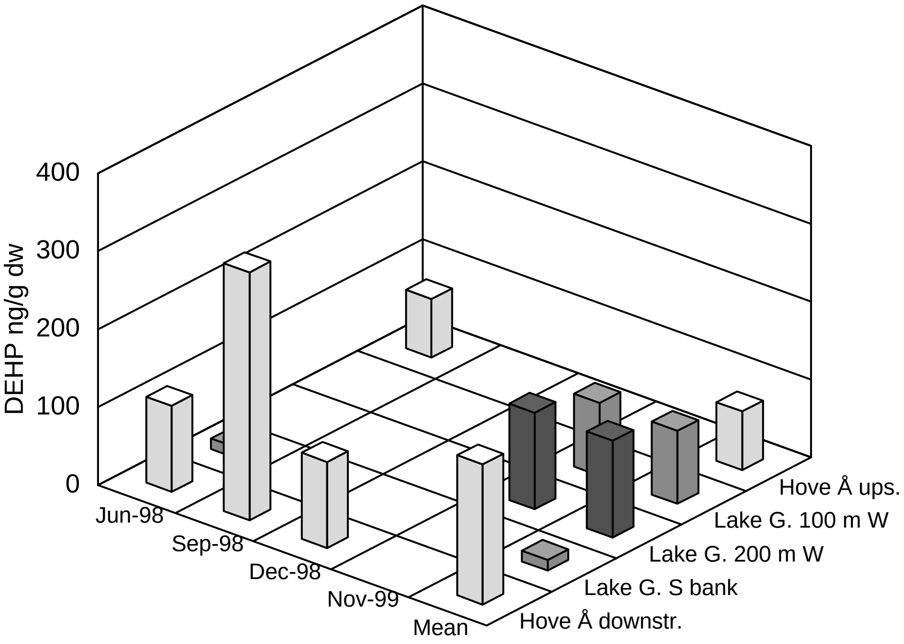

Figure 27 Seasonal and spatial variations of DEHP in stream and lake sediment

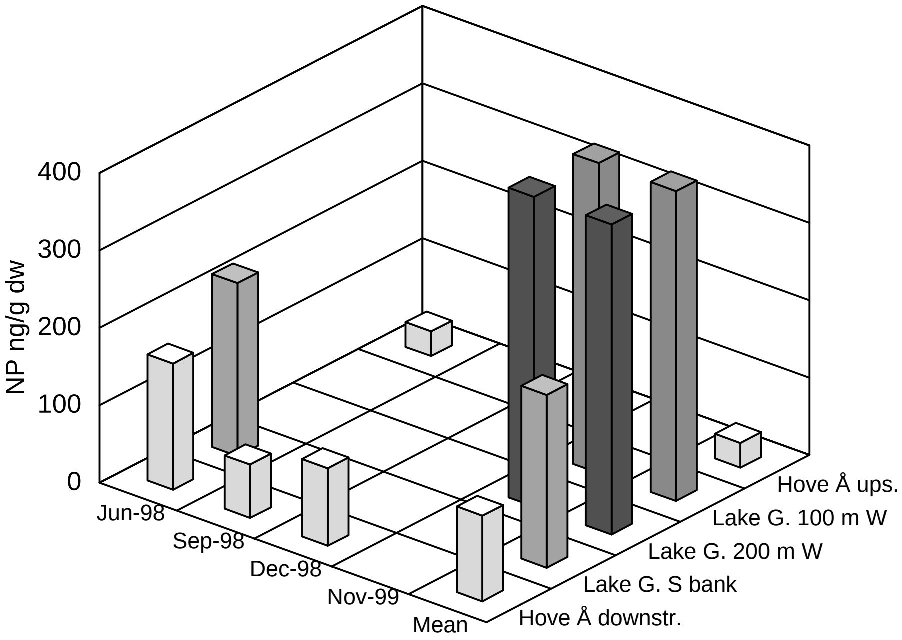

Figure 28 Seasonal and spatial variations of NP in stream and lake sediment

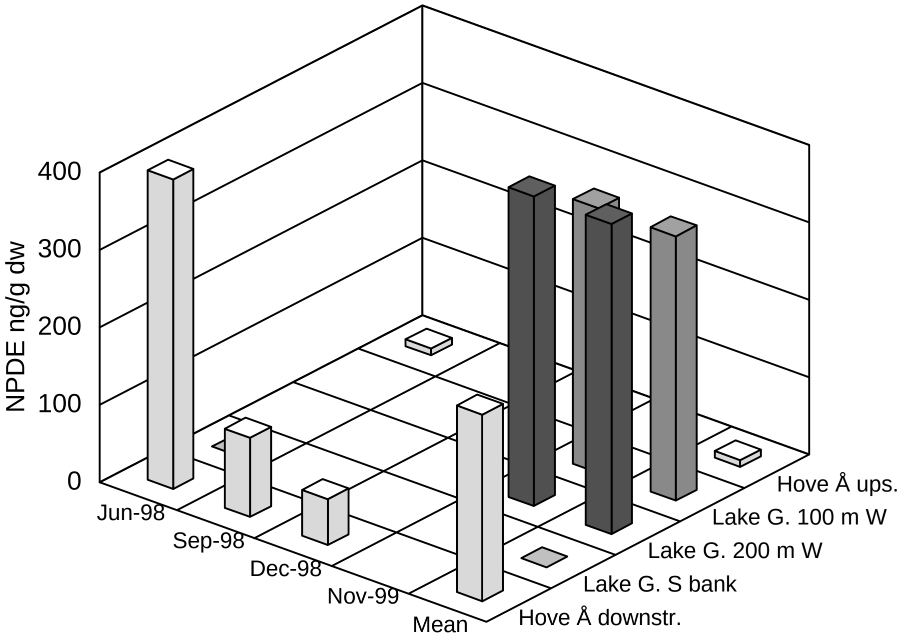

Figure 29 Seasonal and spatial variations of NPDE in stream and lake sediment

Temporal variation

As seen from Figs. 27 - 29, there is a significant temporal variation of the concentrations in Hove Å downstream the lake Gundsømagle Sø, which is the only complete seasonal series. Such a variation was also observed for the water. The variation of the concentration in the sediment at that position must be due to a large exchange of substances between water and sediment due to the high flow velocity, causing suspension of the sediment by turbulence.

Stream gradient

The mean, shown in the front right row of Figs 27-29, is an expression of the spatial variation. This spatial variation in sediment is further illustrated in Figure 30, showing the mean and standard deviation of NP, NPDE and DEHP in the Hove Å system as bar graphs for the sampling positions in the flow direction (East to West).

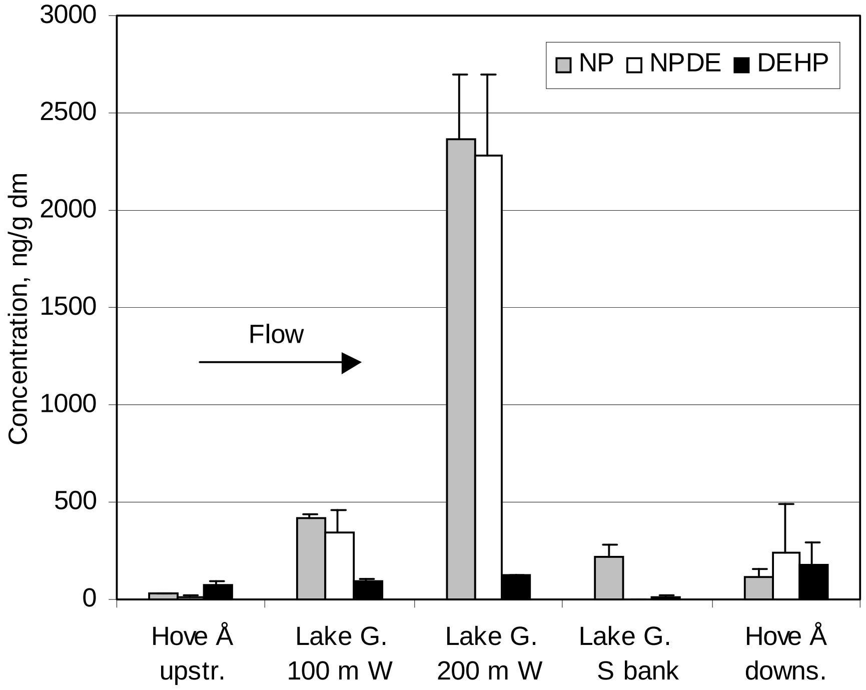

Figure 30 Mean and standard deviation of most abundant substances in sediment along the flow direction of Hove Å system.

As noted from Figure 30, DEHP follows a monotonously increasing tendency in the flow direction, with the exception of the South bank, in which very low amounts of all substances occur. This is probably due to the sandy character of the bottom at that position, in contrast to the organic character at the two other lake positions. The difference may be due to the action of waves near the bank. Furthermore, assuming the main input to the lake is through Hove Å, the main sedimentation should occur in the line connecting the inlet and outlet in the lake, which is a distance to the North of the South bank. Remarkably, the tendency for NP and NPDE is strongly increasing until the 200 m position in the lake, followed by much lower amounts downstream. The same tendency is seen for DBP and BBP in Table 18.

The same trend for these substances was found in the water. An interpretation of these observations would be that the main sedimentation process of all substances occurs at the 200m position in the lake, where the lake is broad and deepest and the water velocity low. Hence, the substances are depleted downstream the lake, occurring in considerably lower concentrations in water as well as sediment. DEHP, however, deviates from this pattern, since larger amounts are found downstream. Probably new sources downstream the lake are present.

5.3.3 Correlation analysis of streams and lake

In Table 19 the significant correlations between substances in all lake and stream water samples are shown (N=19, r crit. = 0.53, $p < 0.01$). It appears that the higher phthalates from BBP and up are correlated with DEHP. The same correlations are found in the fjord water, but for that matrix, some more correlations were found. This is hardly surprising, given the more diverse character of the different streams, which - unlike the fjord – are hydraulic separate entities.

Table 19 Significant substance correlations in water of streams and lake

r	**BBP**	**DnOP**	**DnNP**
DEHP	0.65	0.71	0.61

p<0.01

In Table 20 the significant correlations between substances in all lake and stream sediment samples are shown (N=14, r crit. = 0.61, $p < 0.01$). A pattern deviating from that of water is found, since NP, NPDE and DBP are significantly intercorrelated, and DnOP is correlated with DnNP.

Table 20 Significant substance correlations in sediment of streams and lake

r	**NP**	**NPDE**	**DnOP**
NPDE	0.97	1	
DBP	0.71	0.65	
DnNP			0.64

p<0.01

Since there is no reason to expect positional correlations between the different streams, no such correlation analysis has been done.

5.4 Deposition

The deposition was measured one year at Lille Valby meteorological station during 1996-1997. The annual deposition is given in Table 21 in µg/m^2/y (= g/km^2/y). The station is believed to be representative for the fjord *(Vikelsøe et al. 1998 & 1999).*

Table 21 Deposition at Lille Valby 1996-1997

µg/m²/y	**NP**	**NPDE**	**DBP**	**DPP**	**BBP**	**DEHP**	**DnNP**	**DnOP**	**DiNP**
mean	61	0.3	206	0.1	17	228	2.6	13	17
sd	105	2.2	313	0.3	15	207	6.9	20	26
min	0	0	1.3	0	0	25	0	0	0
max	438	9.2	945	1.0	49	789	26	66	109

As seen, DEHP and DBP are the most abundant substances in the deposition, the mean annual deposition of DBP and DEHP being 206 and 228 g/km^2/y, respectively. This corresponds to a total annual deposition over Roskilde Vig and Bredning, which has an area of about 16 km^2 of 3.3 kg DBP and 3.6 kg DEHP.

In Figure 31 the deposition is shown for the most abundant substances versus sampling date.

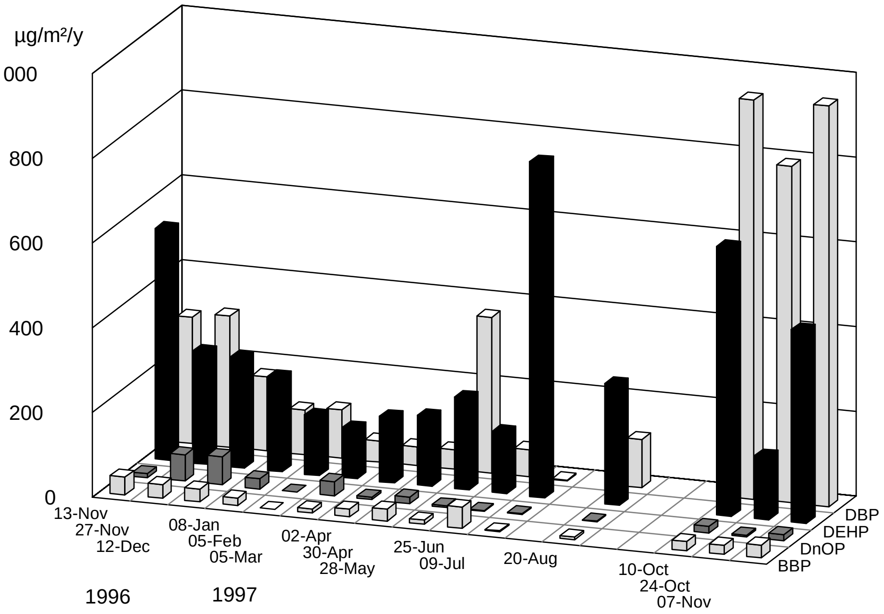

Figure 31 Deposition of most abundant substances at Lille Valby meteorological station.

As observed from Figure 31, for DEHP a minimum occurred in February and a maximum in July. For DBP the minimum and maximum seem to occur later. This variation reflects the air concentration, which probably primarily is driven by the evaporation depending on the temperature. However, also the use of the substances may be of importance.

As discussed by *Vikelsøe et al. (1999)*, wind speed and direction seemed to be of lesser significance for the phthalate deposition. This indicated that point sources and other local differences played a minor role, long range transport being more important. Hence, the deposition is approximately distributed evenly over the fjord. Further, the specific deposition of the phthalate per area unit g/km^2/y seemed to be rather independent of the wet deposition (rainfall).

The mean wind speed and direction is shown for the 1 year sampling period in the rosette diagram Figure 32.

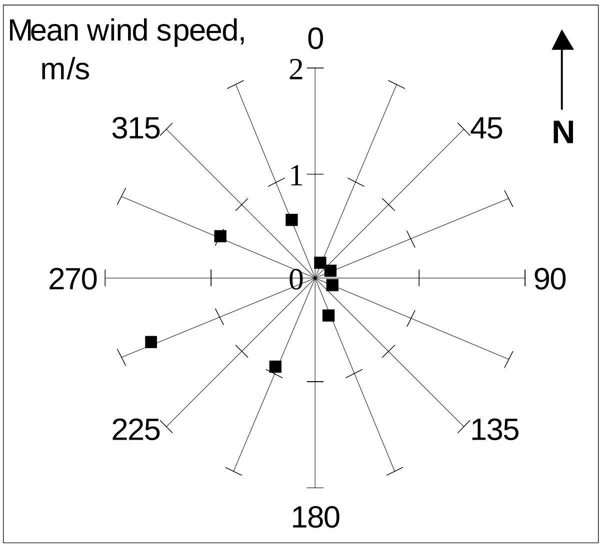

Figure 32 Wind rosette diagram for period of deposition sampling.

The wind is primarily blowing from the West across Roskilde Bredning. The single sampling station is therefore believed to represent the deposition of nonylphenols and phthalates in the Bredning with good approximation.

6 Mathematical data interpretation

In this section the experimental data is interpreted through model simulations. The experimental results show that only DEHP occur in a concentration that is of environmental significance. Therefore the physico-chemical processes determining the fate of xenobiotics in the water-sediment system are identified only for DEHP.

Numerical models are set up to assess the fate of DEHP in the sediment and water compartment of the fjord, respectively. The experimental sediment core measurements are used to calibrate the sediment model and a theoretical validation is performed with analytical solutions. A steady-state mass balance for the water compartment, comprising the DEHP fluxes in the fjord system, is validated with the experimental fjord water concentrations.

6.1 Physico-chemical processes

The considered physico-chemical processes that involve the fate of DEHP in the water and sediment systems respectively are (cf. Figure 33)

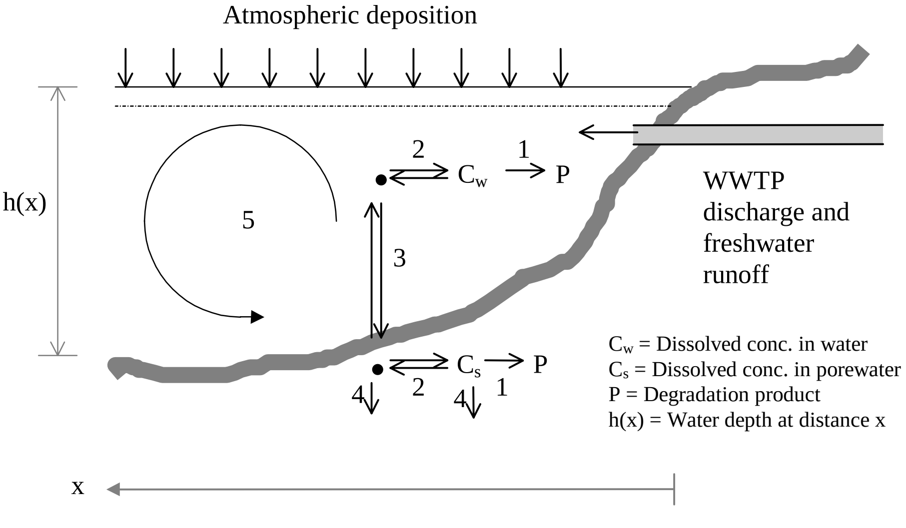

Figure 33 Physico-chemical processes in Roskilde Fjord.

1. Microbial degradation.
2. Adsorption of molecular xenobiotics to suspended particulate matter.
3. Sedimentation of particulate matter.
4. Vertical transport of molecular substances and particulate matter in sediment.
5. Mixing of water volume and transport of molecular substances and particulate matter in water.

6.1.1 Microbial degradation

The substance can occur in different phases: As free dissolved molecules, as micelles or microdroplets, as adsorbed to dissolved organic matter (DOM) or adsorbed to fixed organic matter. Only the free dissolved compound is accessible for microbial degradation. The phthalates primarily occur as micelles due to low solubility and high hydrophobicity and hence only a small fraction of the total substance is biodegradable.

The bio-degradation rate is based on the Monod-expression *(e.g. Schnoor, 1996)* and can be expressed through 1st order reaction kinetics

$$\frac{dC}{dt} = - k_1 \cdot C \quad \left[\frac{mg}{liter \cdot sec.}\right] \tag{1}$$

where

k_1 is the pseudo 1st order degradation rate [sec^{-1}].

C is the dissolved free molecular concentration of the substance [$mg \cdot litre^{-1}$].

The 1st order kinetic holds under the following conditions

- The concentration of the dissolved degradable substance is much smaller than the half saturation constant.

- The biomass specific to the actual substance is assumed to be active at all times and the concentration is constantly low in time and homogeneous in the different compartments.

- The yield coefficient of the micro-organisms is constant regardless of the biomass and substance concentrations. This approximation is very rough and is only true within narrow concentration limits *(Mikkelsen, 1994).*

Different reaction rates can be employed for the degradation of DEHP in the Fjord water and sediment respectively. In the water phase the concentration of active biomass is very small and as a rough estimate a reaction rate equal to a factor of 1000 *(Furtmann, 1996)* lower than the aerobic rate found in the WWTP, $k_{1N} = 10^{-5}\ sec^{-1}$ (*Fauser et al. 2000)* is expected.

In the aerobic sediment surface layer about the same degradation rate as in the WWTP is expected. This layer originates from oxygen diffusion from the water to the sediment and/or from mixing through bioturbation of benthic macro-fauna under favourable conditions. The thickness of the layer can be varying, mainly due to wind conditions and a probable mean value will be around 5 cm.

Below this layer anoxic (nitrate or sulphate reducing) conditions prevail and a degradation rate of 10% of the aerobic rate is anticipated.

6.1.2 Sorption and solvation

In the model set-up it is assumed that the adsorption-desorption processes are instantaneous, reversible and linear in concentrations. Compared to other processes in the system the sorption reactions reach chemical equilibrium quickly and the kinetic relationships related to adsorption can therefore be assumed to be steady-state. The reversibility is true in some cases, but for the phthalates the adsorption is very strong and it is questionable whether the desorption is of any importance. 1st order irreversible adsorption has been shown to describe soil adsorption more satisfactorily *(Sørensen, 1999)*.

Different regimes for simulating adsorption capacities can be employed. The Langmuir adsorption model is defined by a maximum adsorption capacity that is related to a monolayer coverage of surface sites, which is representative of a wide range of equilibrium sorption isotherms for organic adsorbates in natural waters *(Schnoor, 1996)*.

When the number of available sites is large compared to the number of occupied sites there is usually a linear relationship between the concentration of dissolved substance, C (mg · litre^{-1}), and the concentration of adsorbed substance, C_X (mg · litre^{-1}). For a specific adsorbate the concentration of available sites can be expressed through the particulate dry matter concentration, C_{XB} (kg DM litre^{-1}). The adsorption constant specific for this adsorbate, is expressed through the constant K_d.

$$C_X = K_d \cdot C \cdot C_{X_B} \quad \left[\frac{\text{mg}}{\text{litre}}\right] \tag{2}$$

K_d [litre · $(\text{kg DM})^{-1}$] is a measure of the actual partition in natural waters that can be empirically derived from the fraction of organic carbon present in the particulate matter, f_{oc}, and the organic carbon/water partition coefficient for the compound, K_{oc}. This is valid when the organic carbon content is larger than 0.05 - 0.1 % in environmental matrices. When the organic content is lower there is an increasing tendency for adsorption to the inorganic parts of the matrix. This phenomenon is more pronounced for polar organic substances.

The K_d value is characteristic for specific adsorbates. It is assumed that there exist different “species” of particulate matter in the system, i.e. at the WWTP outlet and in the water phase of the Fjord the organic fraction of the particulate matter is relatively high and in the sediment it is lower due to degradation. This implies a lower K_d value in the sediment. However, K_d is defined under steady-state conditions and since it is questionable whether the retention time in the water is long enough for steady-state to occur, a reduction of K_d is appropriate here. On the other hand, the substance entering the Fjord through discharge and deposition will already be adsorbed to DOM and therefore it is more a problem of desorption in the diluted Fjord water.

At the sediment surface the organic fraction will be higher than in the deeper layers. The sediment density is, however, assumed to be constant throughout the depth although there will be an increase caused by pressure build-up. The former will result in a decreasing retention factor and the latter in an increasing retention factor for increasing depths.

Microbial degradation of organic matter can release adsorbed substance. Digestion of organic matter by benthic organisms will remove adsorbed substance and degrade or incorporate it in the tissue. The substance will then be released as adsorbed substance when the organism dies. The former process will result in a decreasing K_d value and the latter an increasing K_d value.

As a consequence of these complex interactions only one K_d value is assigned to the total system. In the WWTP a K_d value for DEHP was found to be approximately 13000 litre · $kgDM^{-1}$ *(Fauser et al., 2000)*. In this work K_d is set to 10000 due to the lower organic fraction in the particulate matter.

For substances that are only sparingly soluble, such as the phthalates, it is necessary to consider the solubility properties in relation to micelle formation that removes the compound from its molecular unimeric dissolved state to a state of non-degradability. Due to the hydrophobicity of the phthalates the dissolved state generally comprises micelles (or microdroplets) even at very low concentrations *(Thomsen et al., 2000).* The presence of detergents will, however, increase the apparent solubility by micelle formation. With densities close to that of water these micelles will not form a bulk phase but rather form a colloidal suspension in the aqueous phase.

Based on the definition of the dissolved fraction, the regimes in Table 22 can be set up.

Table 22 Influence of definition of dissolved fraction on the degradation and diffusion processes.

"Dissolved" fraction	**Degradation**	**Diffusion**
Free molecules Micelles Adsorbed to DOM	Overestimated	Overestimated
Free molecules Micelles	Overestimated	Realistic
Free molecules	Realistic	Underestimated

The experimentally found concentrations in the water and sediment are *total* concentrations. A differentiation in dissolved and adsorbed fractions in the model is based on the K_d value found in *Fauser et al. (2000)* where the samples are centrifuged yielding a settled fraction comprising substance adsorbed to large and small particles (DOM) and a dissolved fraction comprising free molecules and micelles. In the model calculations this will result in an overestimation of the degradation and a realistic estimation of the diffusion in the sediment, cf. Table 22.

6.1.3 Sedimentation

Sedimentation is a transport mechanism where particles are brought to the sediment surface by gravitational settling. Due to turbulence resuspension of surface layer particles will occur. The resuspended particles are assumed to comprise the same concentration of adsorbed substance as the particles in the water phase. It is therefore sufficient to consider the net sedimentation.

Different standard methods can be used to define the vertical transport of matter through the water phase. The *sedimentary* fraction can be found from standing in e.g. 2 hours (DS/R 233 1973) and the *suspended* fraction from filtering (DS/R 233 1973). The remaining amount is either dissolved (molecular) or colloid. No standardised methods exist that can identify the transition between these last two groups.

The *total sedimentary* fraction is obtained through centrifugation where the sedimentary fraction, suspended fraction and some of the colloidal matter is comprised. If the particulate matter is defined as particles with diameters larger than 1 µm the following materials are the predominant contributors in the sedimentation process.

Table 23 Properties for suspended particulate matter *(Harremoës et al., 1990).*

		Diameter [µm]	Density [g · cm^{-3}]
Inorganic:	Clay particles	1 - 2	2.5 - 2.7
	Silt, fine	2 - 6	2.5 - 2.7
	Silt, medium	6 - 20	2.5 - 2.7
	Silt, coarse	20 - 60	2.5 - 2.7
Organic:	Algae	1 - approx. 50	1.01 - 1.03

The sedimentation process can be described by a pseudo 1st order removal of particulate matter from the water phase. Thus, the removal of adsorbed xenobiotics is

$$\frac{dC_w}{dt} \cdot X_w \cdot K_{dw} = -k_{1sed} \cdot C_w \cdot X_w \cdot K_{dw} \quad \left[\frac{mg}{litre \cdot sec.}\right] \tag{3}$$

where

$$k_{1sed} = \frac{v_{sed}}{h} \approx \frac{1\,\frac{m}{hour}}{3\,m} = 0.33\,\frac{1}{hours} = 8\,\frac{1}{days}$$

is the sedimentation constant and v_{sed} is the sedimentation velocity suggested by *Harremoës et al., (1990)*, h is the water depth. X_w is the concentration of particulate matter in the water. In the following a sedimentation constant fitted for the present data is found.

Extraction is a process whereby the non-sedimentary organic matter can be transported to the sediment. It comprises adsorption of colloids to the sediment and absorption of molecular substances in micro-organisms present in the sediment. The resulting concentration gradient across the boundary layer is followed by a vertical diffusive transport from the totally mixed water to the sediment.

The extraction process can be described by a pseudo 1st order removal of dissolved and colloid matter from the water phase

$$\frac{dC_w}{dt}\cdot\theta = -k_{1ext}\cdot C_w\cdot\theta \quad \left[\frac{mg}{litre\cdot sec.}\right] \tag{4}$$

where

$$k_{1ext} = \frac{v_{ext}}{h} \quad \frac{0.5 - 2\,\frac{m}{day}}{3\,m} = 0.17 - 0.67\,\frac{1}{days}$$

is the extraction constant and v_{ext} is the extraction velocity *(Harremoës et al., 1990).*

The overall vertical transport can be expressed as

$$\frac{dC_w}{dt}\cdot(\theta + X_w\cdot K_{dw}) = -C_w\cdot(k_{1ext}\cdot\theta + k_{1sed}\cdot X_w\cdot K_{dw}) \quad \Rightarrow$$

$$\frac{dC_w}{dt}\cdot(\theta + X_w\cdot K_{dw}) =$$

$$-\,C_w\cdot k_{1vert}\cdot(\theta + X_w\cdot K_{dw}) = -C_w\cdot k_{1vert}\cdot R_w \quad \left[\frac{mg}{liter\cdot sec.}\right]$$

The retention factor R_w will be close to unity, i.e. low particulate concentrations prevail in the water, and therefore k_{1vert} is approximately equal to k_{1ext}.

The extraction process is defined for organic matter that is present in abundant concentrations in the water compartment such as proteins, sugars and other easily degradable and hydrophilic compounds. For these compounds the predominant removal mechanism in the sediment is 1st order microbial degradation and accordingly this can be related to a 1st order transfer from the water to the sediment (cf. Equation 4).

In this work xenobiotics that appear in very low concentrations and that are practically insoluble are investigated. The degradation rates are low and the governing removal/transport mechanism in the sediment is diffusion, which in turn is related to a similar removal rate from the water phase. The approach is therefore to define the vertical transport of non-sedimentary substance in terms of a “suction” caused by molecular concentration-gradient conditioned diffusion in the sediment (cf. Equation 19).

The transport of sedimentary adsorbed substance can be derived from Equation 3, where the sedimentation of particles is

$$\frac{dX_w}{dt} = -k_{1sed}\cdot X_w \quad \left[\frac{mg}{liter\cdot sec.}\right] \tag{5}$$

Introducing the concentration of sedimentary particulate matter $X_w = 10 \cdot 10^{-6}$ kg dm · litre^{-1} *(Larsen, 1999)* and an adjusted sedimentation constant, $k_{1sed} = 0.36$ days^{-1}, the sedimentation rate becomes

$$\frac{dX_w}{dt} =$$

$$-0.36 \quad 365 \frac{1}{\text{year}} \quad 10 \quad 10^{-6} \frac{\text{kg dm.}}{\text{litre}} = -13.2 \quad 10^{-4} \frac{\text{kg dm}}{\text{litre} \quad \text{year}}$$

The 23 cm sediment core taken at a position 130 meters from the shore and WWTP outlet is divided into 0.5 cm sections. It shows a mean water content of $\theta = 0.55 \pm 0.13$ litre water · (litre total)$^{-1}$ and a mean dry matter content of $X_s = 1.06 \pm 0.26$ kg dm · (litre total)$^{-1}$ yielding a solids density of 1.06 / 0.45 = 2.35 kg dm · (litre dm)$^{-1}$.

The sedimentation interacts with resuspension and assuming a net sedimentation rate of 13.2 · 10^{-4} kg dm · (litre · year)$^{-1}$ the annual net accumulation rate, S, at the sediment surface amounts to

$$S = \frac{13.2 \quad 10^{-4} \dfrac{\text{kg dm}}{\text{litre} \quad \text{year}} \quad 30\,\text{dm}}{1.58 \dfrac{\text{kg dm}}{\text{litre}}} = 2.5 \frac{\text{mm}}{\text{year}} \tag{6}$$

Where the water depth is 3 m and the dry matter content at the surface is 1.58 kg org. dm · litre^{-1}. *Madsen et al. (1979)* found linear accumulation rates in the inner Fjord in the interval 1.2 - 5.8 mm · year^{-1}. The historical substance load and hence the substance accumulation rate can be derived from the particle accumulation rate and the substance concentration in the sediment. However, this is beyond the scope of this report.

The total downward transport of substance is thus found from a combination of diffusive concentration gradient conditioned transport and sedimentation of adsorbed particulate substance.

6.1.4 Vertical transport in the sediment

Once the substances have reached the sediment the dissolved fraction can be transported further vertically and horizontally. The flux in the sediment is governed by molecular diffusion. Advection and convection are negligible processes that are primarily relevant in connection with hydraulic gradients in groundwater studies. Diffusion is not only relevant for dissolved substances but it has been suggested that also substance adsorbed to dissolved organic matter (DOM) is susceptible to macro molecular diffusion. This will probably have diffusion coefficients that are considerably smaller than the free molecules. According to the previous definition only the free molecules and micelles are comprised in the dissolved fraction in the experimental measurements and adsorption to DOM will therefore not be dealt with here.

The diffusivity of a molecule depends on the random movements (Brownian motion) which again is dependant on the kinetic (or internal) energy. The kinetic energy is defined as ½ · m · v^2 stating that larger molecules have lower mean velocities than smaller molecules, given equal energy levels. Furthermore the increased cross sectional areas reduce the mean free path in the carrier medium resulting in a lower mobility of larger molecules compared to smaller molecules.

This relationship between molecular size and diffusivity can be used to predict diffusivities of compounds from known diffusivities of other compounds based alone on the molecular masses, cf. Equation 7 *(Schwarzenbach et al., 1993)*

$$\frac{D_{\text{unknown}}}{D_{\text{known}}} \approx \sqrt{\frac{\text{mass}_{\text{known}}}{\text{mass}_{\text{unknown}}}} \tag{7}$$

This requires that the carrier media are the same and that the chemical structures are related. Benzene can be used as a model compound for calculating the diffusivity of DEHP that also contain a benzene ring in addition to the alkyl chains and ester groups. *Schwarzenbach et al. (1993)* have found a diffusion coefficient in water for benzene (M_w = 78 $g \cdot mol^{-1}$) of approximately $10^{-9}\ m^2 \cdot sec^{-1}$.

$$D_{\text{DEHP}} = D_{\text{benzene}} \cdot \sqrt{\frac{m_{\text{benzene}}}{m_{\text{DEHP}}}} = 1 \cdot 10^{-9}\ \frac{m^2}{\text{sec.}} \cdot \sqrt{\frac{78}{391}} = 5 \cdot 10^{-10}\ \frac{m^2}{\text{sec.}}$$

Fick's 1st law can describe the vertical substance flux in the sediment

$$N_{sz} = \theta \cdot D_{\text{disp},sz} \cdot \frac{dC_S}{dz} \quad \left[\frac{mg}{m^2 \cdot \text{sec.}}\right] \tag{8}$$

where θ is the porosity of the sediment and $D_{\text{disp},sz}$ is the dispersion coefficient, defined as

$$D_{\text{disp},sz} = \alpha \cdot v_p + D_{sz} \quad \left[\frac{m^2}{\text{sec.}}\right] \tag{9}$$

where α is the longitudinal dispersivity, v_p is the advective pore water velocity (≈ 0) and D_{sz} is the molecular diffusion coefficient.

Schwarzenbach (1993) suggests the following empirical relationship

$$D_{\text{disp},sz} = D_{sz} \quad {}^{1.5} = 5 \quad 10^{-10} \quad 0.55^{1.5} = 2 \quad 10^{-10}\ \frac{m^2}{\text{sec.}} \tag{10}$$

Additionally, under favourable conditions, the redistribution of sediment particles by benthic macro fauna can occur by a variety of processes. This bioturbation can influence the transport and fate of hydrophobic xenobiotics in the surface layer. The particle reworking and the pumping of pore water can create a mixed layer where the adsorbed and dissolved substances migrate more rapidly than can be accounted for by molecular diffusion.

The extension of the mixing layer is dependent on the macro organism. For lugworm *Arenicola marina*, which is the predominant benthic organism in the inner Fjord, a 5 to 10 cm bioturbation zone in depths of approximately 15 cm can be expected. However, the sediment core was extremely hard and therefore it is expected that the influence from bioturbation is negligible. This is confirmed by the DEHP concentration profile in the sediment core.

Thus neglecting the influence from bioturbation, the horizontal concentration gradient is much smaller than the vertical concentration gradient and the horizontal diffusion can be omitted in the mass balance for a model sediment volume.

6.1.5 Horizontal transport in the water

The hydraulic effect from the sea will cause a high flow through the narrow parts in the middle of the Fjord. This combination of saline intrusions and fresh water discharges causes a salinity gradient ranging from 20 ‰ in the northern entrance to 14.5 ‰ in the inner parts of the Fjord *(Harremoës et al., 1990).*

In the preceding section it is assumed that the convective flow in the sediment is zero. This excludes the influence of percolation of groundwater through the sediment into the Fjord. This is an assumption that will not hold at local spots where freshwater intrusions will enter the saline Fjord and lower the salinity on a local scale. The approach in this work is to consider net deposition, streams and anthropogenic outlets as the only freshwater sources to the fjord.

Due to an effective large scale mixing of the water volumes, which enhances the vertical transport of dissolved and particulate matter, the vertical concentration gradient is negligible, resulting in a mean depth integrated concentration in the water column. The large scale mixing, which is caused by a combination of turbulence and convection, is also the predominant process in the horizontal transport of water and substances in the shallow Fjord.

The salinity mixing data can be used to calculate an effective longitudinal dispersion coefficient for the narrow part of the Fjord. Assuming a uniformly distributed freshwater supply along the shore of $1.16 \cdot 10^{-4}\ \mathrm{m}^3 \cdot (\mathrm{m} \cdot \mathrm{sec})^{-1}$, a mean cross sectional area of $2610\ \mathrm{m}^2$, a length of 28 km and salinities of 20 ‰ in the northern entrance and 14.5 ‰ in the Bredning, the effective dispersion coefficient can be calculated from the salinity gradient *(Harremoës et al., 1990)*

$$D_{wx} = \frac{1.16 \cdot 10^{-4}\ \frac{\mathrm{m}^2}{\mathrm{sec.}} \cdot (28000\ \mathrm{m})^2}{2 \cdot 2610\ \mathrm{m}^2 \cdot \ln\frac{20.0}{14.5}} = 54\ \frac{\mathrm{m}^2}{\mathrm{sec.}} \tag{11}$$

The longitudinal salinity gradient is only constant in the narrow part of the Fjord and therefore the dispersion coefficient is only representative of this section. In the inner Fjord the salinity is approximately constant and the horizontal transport is based on other criteria, such as turbulence and convective mixing.

In the inner Fjord, i.e. Roskilde Vig and Bredning, where the discharge from Bjergmarken WWTP is situated, the horizontal velocity will be minor due to the larger surface areas. Hydraulic effects from wind and freshwater sources will govern the mixing. Strong western winds are able to create water level fluctuations up to 170 cm above mean sea level in the inner Fjord compared to only ± 10 cm resulting from tidal variations.

Therefore, it is not relevant to consider the transport in the Vig and Bredning in relation to dispersion, but rather to consider them as mixed basins.

6.2 Sources

Different sources contribute to the DEHP concentrations in the Fjord (cf. Figure 2).

- The wastewater treatment plant (WWTP) effluent is discharged as a point source to the surface water at the shore in the inner part of Roskilde Fjord (Vig). The flow is 492 ± 356 $m^3 \cdot day^{-1}$ with a mean concentration of 0.7 µg DEHP · m^{-3} *(Fauser et al., 2000).*

- The point sources to the Bredning and narrow passage of the Fjord, i.e. WWTP discharges from four smaller cities, are estimated to account for the same concentration (C_{WWTP}) and flow rate (Q_{WWTP}) as the WWTP in the Vig. The total load from the point sources is distributed uniformly along the horizontal axis (cf. Table 24 and Figure 34).

- For Roskilde Bredning and the narrow passage contributions from freshwater sources from streams and lakes must be included. The freshwater runoff is higher per length unit in the Bredning than in the narrow passage.

- Atmospheric deposition is considered to be uniformly distributed with respect to time and surface area. The dry deposition rate is 230 µg DEHP · $(m^2 \cdot year)^{-1}$ (cf. Table 21).

- For a period of 25 years, ending in 1991, all of the sludge produced in earlier WWTP's in Roskilde was used for amendment on an agricultural field adjacent to the WWTP discharge in the shore. Since 1991 the produced sludge has been stored in an intermediary deposit close to the sludge amended area and shore. Leaching from the sludge amended soil as well as wash out from the sludge deposit, in case of heavy rainfall, will contribute to the load in to the Fjord *(Vikelsøe et al., 1999).*

- In 1969 in connection with work on the Roskilde harbour, the sediment was dumped on the site marked ∇ on the map in Figure 2. This has since then been a source of leaching to the Fjord water. The load has decreased with time and is today estimated to be negligible compared to the WWTP discharge.

- The flux of saline water from the sea to the Fjord is 3 to 4 times larger than the freshwater flux to the Fjord *(Hedal et al, 1999)*. In Table 24 the three water exchange rates are stated.

6.3 Model parameters

The following model parameters are required in the models.

Calculated and measured state variables

C_w: Concentration of dissolved substance in water phase [$\text{mg} \cdot \text{litre}^{-1}$].
C_s: Concentration of dissolved substance in sediment phase [$\text{ng} \cdot \text{g}^{-1}$].

Measured model inputs

X_w: Concentration of suspended particulate matter in water phase
$= 10 \cdot 10^{-6}$ kg DM · (litre total)$^{-1}$
X_s: Concentration of dry matter in sediment
$= 1.06$ kg DM · (litre total)$^{-1}$
θ_s: Water fraction in sediment
$= 0.55$ litre water · (litre total)$^{-1}$
Q_{WWTP}: Discharge flow from WWTP
$= 492 \pm 356\ \text{m}^3 \cdot \text{hour}^{-1}$
C_{WWTP}: Concentration of dissolved DEHP in WWTP discharge
$= 0.7$ µg DEHP · litre^{-1}
R_{WWTP}: Retention factor for WWTP discharge
$= 1.05$
$C_{tot,dep}$: Atmospheric bulk deposition
$= 7.29 \cdot 10^{-15}$ kg DEHP · $(\text{m}^2 \cdot \text{sec})^{-1}$
$C_{tot,f}$: Concentration of mean total substance in freshwater from streams
$= 0.2$ µg DEHP · litre^{-1}

Calibration parameters

K_d: Distribution coefficient between water and organic matter in water or sediment [litre water · (kg DM)$^{-1}$].
k_{1N}: Aerobic pseudo 1st order removal rate [sec^{-1}].
k_{1D}: Anaerobic pseudo 1st order removal rate [sec^{-1}].
S: Annual sediment accumulation rate [$\text{mm} \cdot \text{year}^{-1}$].

Estimated model inputs

Parameters in Table 24.
D_{wx}: Horizontal dispersion coefficient in narrow part of Fjord
$= 54\ \text{m}^2 \cdot \text{sec}^{-1}$
D_{sz}: Molecular diffusion coefficient in sediment
$= 2 \cdot 10^{-10}\ \text{m}^2 \cdot \text{sec}^{-1}$

The hydraulic and geographical key data for Roskilde Fjord are shown in Table 24.

Table 24. Data for Roskilde Vig, Bredning and narrow passage.

	Vig	**Bredning**	**Narrow passage**
Surface area	A_{vig} = 4 km^2	A_{bred} = 48 km^2	A_{narr} = 73 km^2
Length	-	L_{bred} = (10 km)	L_{narr} = 28 km
Mean depth	h = 3 m	h = 3 m	h = 3 m
Diffuse freshwater flow	$Q_{f,vig}$ = 0	$Q_{f,bred}$ = 3.60 $m^3 \cdot sec^{-1}$	$q_{f,narr}$ = $1.16 \cdot 10^{-4}$ $m^3 \cdot (m \cdot sec)^{-1}$
Point source flow	$Q_{p,vig}$ = $136.7 \cdot 10^{-3}$ $m^3 \cdot sec^{-1}$	$Q_{p,bred}$ = $36.0 \cdot 10^{-3}$ $m^3 \cdot sec^{-1}$	$q_{p,narr}$ = $3.60 \cdot 10^{-6}$ $m^3 \cdot (m \cdot sec)^{-1}$
Water exchange	$Q_{bred\text{-}vig}$ = $(0.5 \cdot Q_{f\text{-}sea})$3.4 $m^3 \cdot sec^{-1}$	$Q_{narr\text{-}bred}$ = $(2 \cdot Q_{f,sea})$13.7 $m^3 \cdot sec^{-1}$	$Q_{sea\text{-}narr}$ = $(3 \cdot Q_{f,sea})$20.5 $m^3 \cdot sec^{-1}$

The mean residence time for the entire Fjord is approximately 3 months.

6.4 Model set-up

Roskilde Vig and Bredning are considered to be totally mixed whereas the transport in the narrow part of the Fjord is more appropriately described with dispersion.

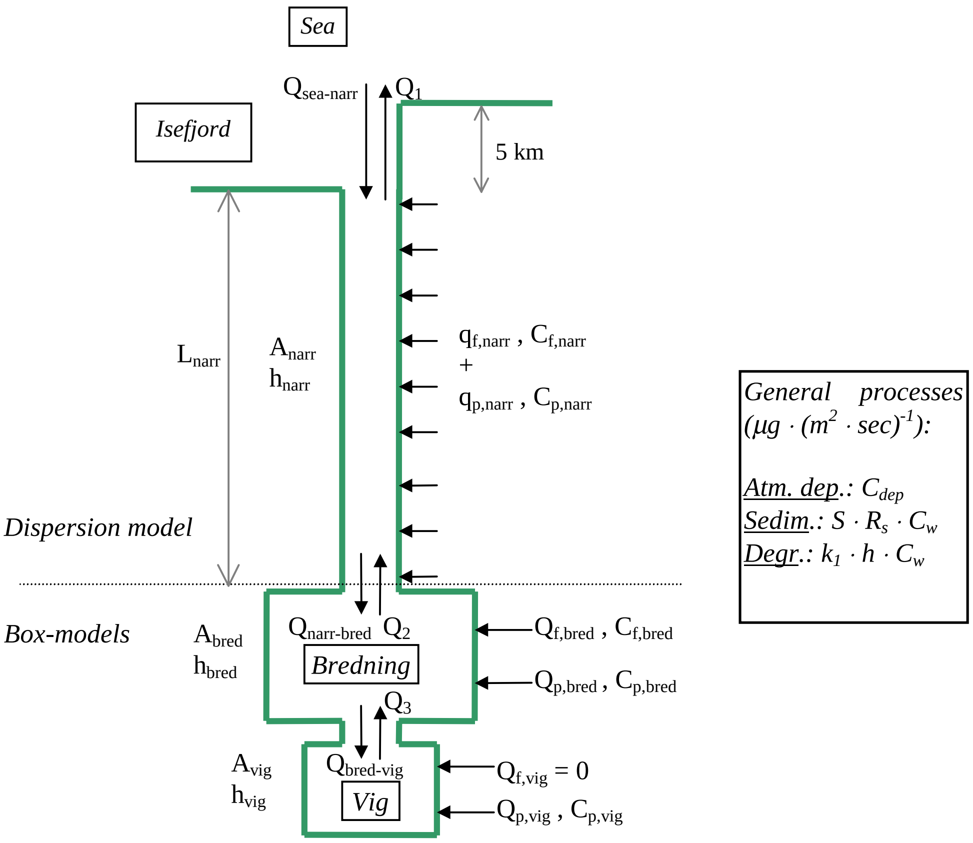

$$Q_1 = Q_{sea\text{-}narr} + (q_{f,narr} + q_{p,narr}) \cdot L_{narr} + Q_{f,bred} + Q_{p,bred} + Q_{p,vig}$$

$$Q_2 = Q_{narr\text{-}bred} + Q_{f,bred} + Q_{p,bred} + Q_{p,vig}$$

$$Q_3 = Q_{bred\text{-}vig} + Q_{p,vig}$$

Figure 34 Schematic view of Roskilde Fjord. Symbols and notations are explained in Table 24.

Two model scenarios are set-up that in combination will describe the dynamic and steady-state concentrations based on the processes in the water and sediment of Roskilde Fjord.

Water model: Steady-state box-models of Roskilde Vig and Bredning combined with a dynamic numerical model of the narrow passage of the Fjord. Experimental results are used to validate the model. The models are designed to account for the overall mass balances in the different regions of the Fjord.

Sediment model: Numerical model including diffusion, sedimentation and degradation. Analytical expressions and experimental results are used to validate the model.

The models are set up based on the following assumptions

- Constant discharge flow (Q_{WWTP}), freshwater flow (Q_f) and deposition (Q_{dep}).
- Constant discharge concentration (C_{WWTP}), freshwater concentration (C_f) and deposition concentration (C_{dep}).
- Constant water depth (h).

- Constant concentrations of suspended matter in water and sediment (X_w, X_s).
- Equilibrium between dissolved and adsorbed substance (K_d).
- Water volume is totally mixed along the vertical axis.
- Only vertical diffusive flows in sediment (D_{sz}).
- Dissolved concentration in sediment surface layer is equal to the dissolved water concentration.
- 1st order degradation of dissolved substance in water and sediment (k_1).
- Increasing sediment depth in time due to sedimentation (S).

6.4.1 Steady-state box-model

The values in Table 24 and the model parameters are inserted in the general steady-state Equation 12.

$$\begin{aligned} 0 = {} & \text{Point sources} + \text{Freshwater sources} + \\ & \text{Water exchange} + \\ & \text{Atmospheric deposition} + \text{Sedimentation} + \text{Degradation} \quad \Rightarrow \end{aligned} \tag{12}$$

For Roskilde Vig the mass balance becomes

$$\begin{aligned} 0 = {} & C_{WWTP} \cdot R_{WWTP} \cdot Q_{WWTP} + C_{tot,f} \cdot Q_{f,vig} - \\ & C_{w,vig} \cdot R_w \cdot \left(Q_{bred\text{-}vig} + Q_{p,vig} + Q_{f,vig}\right) + \\ & C_{tot,dep} \cdot A_{vig} - C_{w,vig} \cdot S \cdot A_{vig} \cdot R_s - k_1 \cdot C_{w,vig} \cdot A_{vig} \cdot h_{vig} \end{aligned} \tag{13}$$

The equations for Roskilde Bredning and narrow passage are described analogously. In the Vig equation $C_{w,bred}$ is unknown. In the Bredning equation $C_{w,vig}$ and $C_{w,narr}$(boundary) are unknown and in the equation for the narrow passage $C_{w,bred}$ is unknown. Through iteration in the water model the unknowns are determined.

The calculated contributions and mean water concentrations are summarised in Table 25.

6.4.2 Numerical models (water and sediment model)

The mass balance for the water compartment of the Vig and Bredning are as shown in Equation 13. The water balance in the narrow passage is described with the expressions below. Transport in the sediment is described below irrespective of the model for the water.

In Figure 35 a vertical section of the water-sediment system is shown. The considered horizontal and vertical mass fluxes are stated for each compartment.

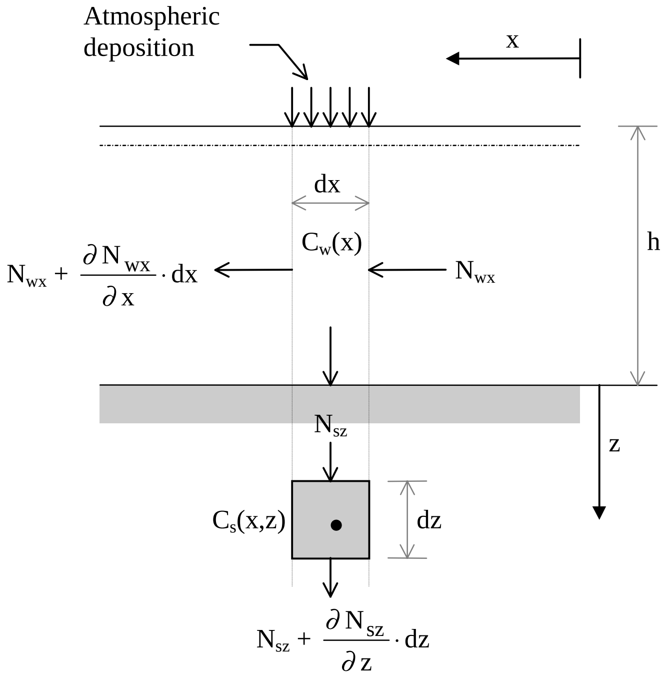

Figure 35 Vertical sectional view of the water-sediment system in the narrow passage of Roskilde Fjord.

The time incremental mass balance for a water volume dx · b · h and a sediment volume dx · b · dz is

$$\begin{aligned}
&\frac{dC_A}{dt} \cdot R \cdot dx \cdot b \cdot dz = \\
&N_x \cdot b \cdot dz - \left(N_x + \frac{dN_x}{dx} \cdot dx \right) \cdot b \cdot dz + \\
&N_z \cdot dx \cdot b - \left(N_z + \frac{dN_z}{dz} \cdot dz \right) \cdot dx \cdot b + \\
&\sum k_{1i} \cdot C_A \cdot dx \cdot b \cdot dz \quad \Rightarrow
\end{aligned} \tag{14}$$

$$\frac{dC_A}{dt} = -\frac{dN_x}{dx} \cdot \frac{1}{R} - \frac{dN_z}{dz} \cdot \frac{1}{R} - \sum \frac{k_1}{R} \cdot C_A \tag{15}$$

where N_x and N_z are the mass fluxes $[g \cdot (m^2 \cdot sec)^{-1}]$ along the x and z axis respectively of substance A with dissolved concentration C_A. k_1 is a pseudo 1^{st} order process constant. Equation 15 is the result of two-dimensional modelling assumptions and can be formulated for the water and sediment compartment respectively.

Water (narrow passage):

The horizontal flux is a result of advection and dispersion

$$N_{wx} = \frac{Q_{narr}}{b \cdot h} \cdot C_{w,narr} \cdot R_w - D_{wx} \cdot \frac{\partial C_{w,narr}}{\partial x} \cdot R_w \tag{16}$$

where (cf. Figure 34)

$$Q_{narr} = Q_{f,bred} + Q_{p,bred} + Q_{p,vig} + (q_{f,narr} + q_{p,narr}) \cdot x$$

The vertical flux is a combination of sedimentation of particles, extraction of molecular substance through sediment suction, atmospheric deposition and freshwater sources.

$$N_{wz} = - D_{sz} \cdot \left.\frac{\partial C_s}{\partial z}\right|_{z=0} - S \cdot R_s \cdot C_{w,narr} + C_{tot,dep}$$

$$+ \frac{q_{f,narr}}{b} \cdot C_{tot,f} + \frac{q_{p,narr}}{b} \cdot C_{tot,p} \qquad (17)$$

The first term in Equation 17 is the boundary condition at the sediment surface caused by sediment "suction" of substance. The total mass balance for the water compartment furthermore includes 1st order degradation and thus becomes

$$\frac{\partial C_{w,narr}}{\partial t} = \frac{Q_{narr}}{b \cdot h} \cdot \frac{\partial C_{w,narr}}{\partial x} + \frac{\left(q_{f,narr} + q_{p,narr}\right)}{b \cdot h} \cdot C_{w,narr} +$$

$$D_{wx} \cdot \frac{\partial^2 C_{w,narr}}{\partial x^2} - \frac{D_{sz}}{R_w \cdot h} \cdot \left.\frac{\partial C_s}{\partial z}\right|_{z=0} +$$

$$\frac{C_{dep}}{R_w \cdot h} - \frac{S \cdot R_s \cdot C_{w,narr}}{R_w \cdot h} - \frac{k_1}{R_w} \cdot C_{w,narr}$$

$$\frac{q_{f,narr}}{b \cdot h \cdot R_w} \cdot C_{tot,f} + \frac{q_{p,narr}}{b \cdot h \cdot R_w} \cdot C_{tot,p} \qquad (18)$$

Boundary conditions:
$C_{w,narr} = C_{w,bred}$ for $x = 0$
$C_{w,narr} = C_{w,sea} = 0$ for $x = L_{narr} + 5$ km

Sediment:
The horizontal flux is negligible. The vertical flux arises from molecular diffusion and advection from sediment build-up

$$N_{sz} = - D_{sz} \cdot \frac{\partial C_s}{\partial z} + S \cdot R_s \cdot C_w \qquad (19)$$

The total mass balance for the sediment compartment is

$$\frac{\partial C_s}{\partial t} = \frac{D_{sz}}{R_s} \cdot \frac{\partial^2 C_s}{\partial z^2} - S \cdot \frac{\partial C_s}{\partial z} - \frac{k_1}{R_s} \cdot C_s \qquad (20)$$

In the upper 5 cm the aerobic degradation rate, k_{1N}, is used and further down the anoxic degradation rate, k_{1D}, is used.

The two coupled 2nd order differential Equations 18 and 20 each having two independent variables, x and t for the water model and z and t for the sediment model respectively, can be solved numerically using a grid consisting of discrete nodes for the (x,t) and the (z,t) system respectively, and by employing a forward time central space scheme (cf. Figure 36).

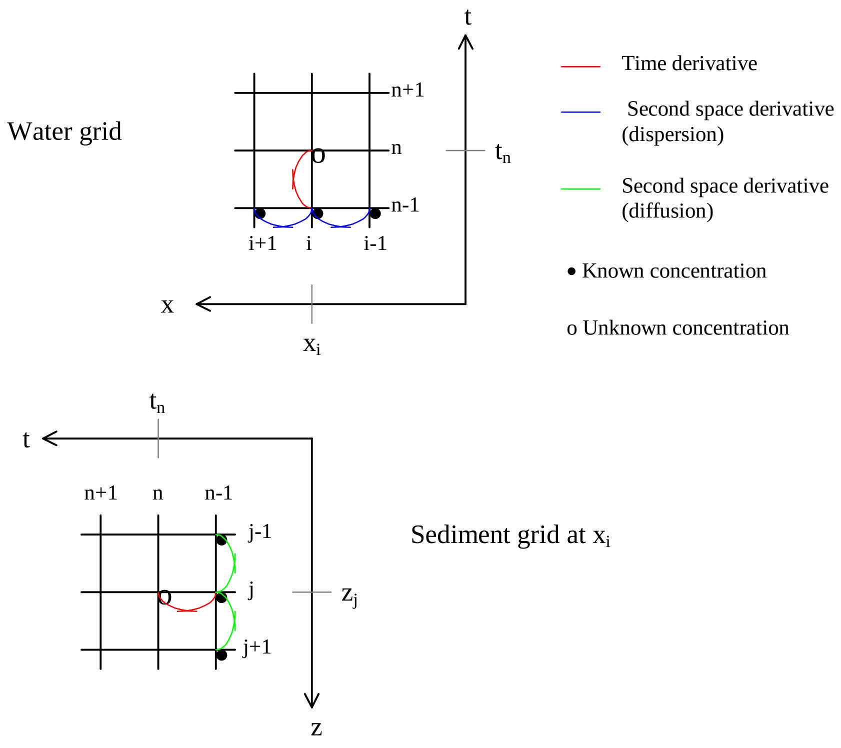

Figure 36 Time-space grids for the water and sediment models respectively.

The numerical interpretation of the sedimentation term $S \cdot R_s \cdot C_w$ is accounted for by increasing the sediment thickness with an extra layer, dz, each time

$$t_{sed} = \frac{dz}{S} \tag{21}$$

is fulfilled. With a step size of dz = 0.01 m and an accumulation rate of S = 2.5 mm · year^{-1}, cf. Equation 6, an additional layer with thickness dz must be added every 4 years. In doing so the entire concentration profile is moved downward one grid point. The sediment difference equation below does therefore *not* comprise a sedimentation term.

Water (narrow passage):

$$
\begin{aligned}
C_w^{n+1}(i) \;&=\; C_w^n(i) \\
&+ dt \cdot \left(\frac{Q_{narr}}{b \cdot h} \cdot \frac{\left(C_w^n(i+1) - C_w^n(i)\right)}{dx} + \frac{\left(q_{f,narr} + q_{p,narr}\right)}{b \cdot h} \cdot C_w^n(i) \right) \\
&+ dt \cdot \left(D_{wx} \cdot \frac{\left(C_w^n(i+1) - 2 \cdot C_w^n(i) + C_w^n(i-1)\right)}{dx^2} \right) \\
&- dt \cdot \left. \left(\frac{D_{sz}}{R_w \cdot h} \cdot \frac{\left(C_s^n(i,j+1) - C_s^n(i,j)\right)}{dz} \right) \right|_{j=0} \\
&+ dt \cdot \left(\frac{C_{dep}}{R_w \cdot h} - \frac{S \cdot R_s}{R_w \cdot h} \cdot C_w^n(i) - \frac{k_1}{R_w} \cdot C_w^n(i) \right) \\
&+ dt \cdot \left(\frac{q_{f,narr}}{b \cdot h \cdot R_w} \cdot C_{tot,f} + \frac{q_{p,narr}}{b \cdot h \cdot R_w} \cdot C_{tot,p} \right)
\end{aligned}
\tag{22}
$$

Sediment:

$$
\begin{aligned}
C_s^{n+1}(i,j) \;&=\; C_s^n(i,j) \\
&+ dt \cdot \left(\frac{D_{sz}}{R_s} \cdot \frac{\left(C_s^n(i,j+1) - 2 \cdot C_s^n(i,j) + C_s^n(i,j-1)\right)}{dz^2} \right) \\
&- dt \cdot \left(\frac{k_1}{R_s} \cdot C_s^n(i,j) \right)
\end{aligned}
\tag{23}
$$

For j = 0 the second space derivative in Equation 23 is

$$
\frac{\left(C_s^n(i,1) - 2 \cdot C_s^n(i,0) + C_s^n(i,0)\right)}{dz^2}
\tag{24}
$$

At time step n: The input sediment surface concentration $C_s(i,0)$ to the sediment equation, is calculated from the water equation at the same time step, because of the faster dispersion in the water phase compared to the diffusion in the sediment.

At time step n + 1: The input sediment surface concentration $C_s(i,0)$ to the water equation is calculated from the sediment equation at time step n.

The models are validated with analytical solutions. The experimental and analytical concentration profiles will be aggregated and discussed in sections 6.5 and 6.6 for the sediment and the water compartments respectively.

6.4.3 Dynamic solution to the diffusion and sedimentation problem in the sediment

The combined dynamic diffusion, sedimentation and degradation problem is complex to solve analytically. The determination of the concentration profile in the sediment at any given position in the Fjord, is therefore simplified to a problem of diffusion and sedimentation in a semi-infinite medium, where the boundary (water) is kept at a constant concentration. It is acceptable to consider the water concentration as constant in time due to the high horizontal dispersion and vertical mixing that prevail in the water phase compared to the slower sedimentation to and diffusion in the sediment.

The boundary condition is thus

$C_s(x,0) = C_w(x)_{\text{steady-state}}$ for $t > 0$

Initial condition

$C_s(x,z) = 0$ for $t = 0$

The solution of the one-dimensional diffusion and sedimentation equation, i.e.

$$\frac{\partial C_s}{\partial t} = \frac{D_{sz}}{R_s} \cdot \frac{\partial^2 C_s}{\partial z^2} - S \cdot \frac{\partial C_s}{\partial z} \tag{25}$$

with the initial and boundary conditions stated above, is *(Sørensen et al., 2000)*

$$C_s = 0.5 \cdot C_w \cdot \left(\begin{array}{l} \operatorname{erfc}\left(0.5 \cdot \sqrt{\dfrac{R_s}{D_s}} \cdot \left(\dfrac{z}{\sqrt{t}} - S \cdot \sqrt{t} \right) \right) + \\ e^{\frac{S \cdot R_s}{D_s}} \cdot \operatorname{erfc}\left(0.5 \cdot \sqrt{\dfrac{R_s}{D_s}} \cdot \left(\dfrac{z}{\sqrt{t}} + S \cdot \sqrt{t} \right) \right) \end{array} \right) \tag{26}$$

where erfc ( ) is the complementary error function.

6.4.4 Steady-state solution to the diffusion, sedimentation and degradation problem in the sediment

Under steady-state conditions the following linear homogeneous second order equation is valid in the sediment compartment

$$\frac{D_{sz}}{R_S} \cdot \frac{d^2C_S}{dz^2} - S \cdot \frac{dC_S}{dz} - \frac{k_1}{R_S} \cdot C_S = 0 \quad \Leftrightarrow$$

$$\frac{d^2C_S}{dz^2} - \frac{S \cdot R_S}{D_{sz}} \cdot \frac{dC_S}{dz} - \frac{k_1}{D_{sz}} \cdot C_S = 0 \tag{27}$$

It can be solved according to Spiegel (1968) with the boundary conditions

$C_s \rightarrow 0$ for $z \rightarrow \infty$

$C_s = C_w(\text{steady-state})$ for $z = 0$

And the solution becomes

$$C_s(z) = C_w(\text{steady}-\text{state}) \cdot e^{\left(\frac{S \cdot R_s}{D_{sz} \cdot 2} - \sqrt{\left(\frac{S \cdot R_s}{D_{sz} \cdot 2}\right)^2 + \frac{k_1}{D_{sz}}}\right) \cdot z} \qquad (28)$$

6.5 Discussion of experimental and analytical results in the sediment

In Figure 37 the numerical model is validated with the analytical solution to the diffusion and sedimentation problem, cf. Equation 26. The degradation is set to zero in the numerical model. The input values are characteristic for DEHP and are as stated in the discussion of Figure 38.

The simulated time is 50 years and the optimum time step, with respect to run time and precision, is dt = 10^5 sec. The vertical step size is dz = 1 cm.

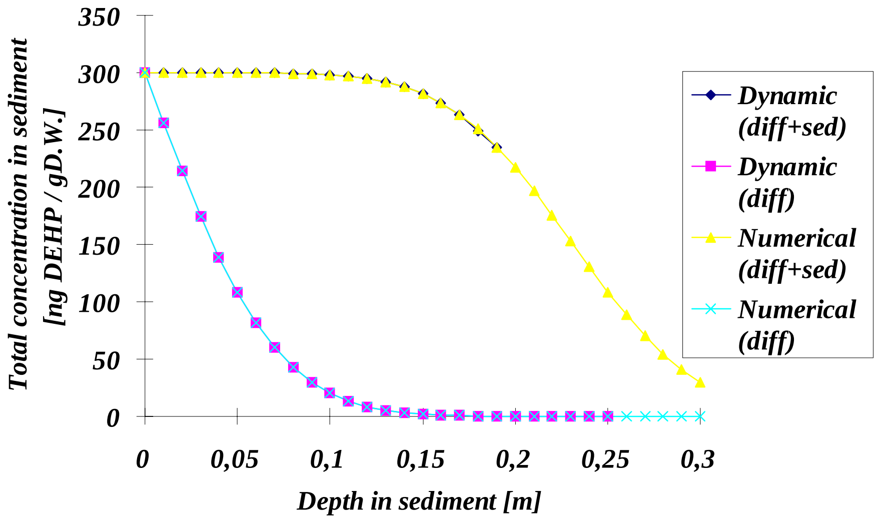

Figure 37 Validation of numerical sediment model (Equation 23) with analytical solution (Equation 26).

Two cases are considered; diffusion combined with sedimentation and diffusion alone. For diffusion combined with sedimentation the analytical curve is only calculated to a depth of 20 cm due to mathematical instabilities at larger depths. The sedimentation process in the numerical model, where discrete layers of thickness 1 cm are added, is seen to be satisfactorily described compared to the analytical solution. A situation of sedimentation alone will produce a horizontal curve through 300 ng DEHP · g DM, that will extend to a depth of S · 50 years ≈ 12 cm.

The two diffusion curves and the two diffusion + sedimentation curves are coincident, which implies that the numerical sediment model is considered to be properly validated.

In Figure 38 the validated numerical model is calibrated with the experimental sediment concentration profile sampled 130 m from the WWTP discharge, cf. section 5.2.3.

The model simulations uses the following parameters
$S = 2.5\ \text{mm} \cdot \text{year}^{-1}$
$k_{1N} = 2 \cdot 10^{-5}\ \text{sec}^{-1}$
$k_{1D} = 8 \cdot 10^{-6}\ \text{sec}^{-1}$ (below a depth of 5cm)
$K_d = 10000$ litre water · (kg dm)$^{-1}$

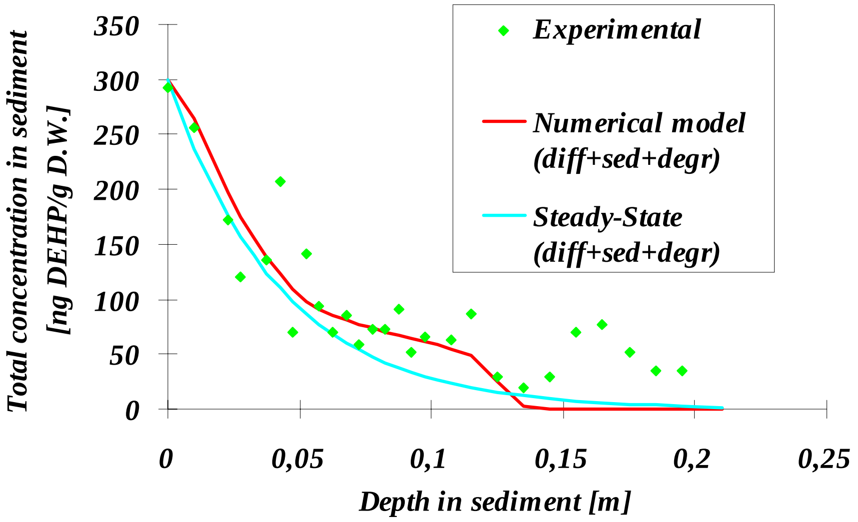

Figure 38 Experimental sediment core concentrations at distance 130 from discharge, numerical sediment model (Equation 23) and steady-state solution (Equation 28).

The curve in the upper 5 cm decreases according to the typical transport-degradation situation with a constant degradation rate. The high degradation rate indicates aerobic conditions. This rate is the same order of magnitude as the aerobic rate found in the WWTP although the biomass and oxygen concentrations are considerably lower in the sediment.

Deeper down in the sediment the profile flattens out and decreases with only 10 % in 5 cm. The oxygen concentration is probably negligible. A degradation rate of $8 \cdot 10^{-6}\ \text{sec}^{-1}$ points to either anoxic or anaerobic conditions.

The periodic fluctuations from 12 to 20 cm are probably experimental noise but bioturbation by lugworm *(Arenicola marina)* could produce a zone in depths around 10 to 20 cm corresponding to the experimentally found. As mentioned previously circumstances that disconfirm this suggestion are the hardness of the sediment core.

The interpretation of the experimental data leads to two cases; The fluctuations below approximately 12 cm are noise and the concentrations are zero. This gives a sedimentation rate of 2.5 mm · year^{-1}. Alternatively the concentration profile below 10 cm is approximately constant down to a depth of minimum 20 cm. In this case the sedimentation is equal to or larger than 4.5 mm · year^{-1}, since diffusion alone can not transport this amount of substance down to these depths.

In the model set-up the sedimentation is described as a discontinuous process where a layer of dz = 1 cm is added every 4 years but in reality the sedimentation occurs in two annual maxima, one in the spring and one in the autumn. The differences in sediment application rate have been investigated in the numerical model and the results are identical.

The organic concentrations in the sediment and in the particulate material in the outlet from the WWTP and from atmospheric deposition are lower compared to the biomass in the bio-reactors in the WWTP. The adsorption coefficient, K_d, is therefore lower than the adsorption coefficients in the WWTP.

The last curve in Figure 38 is the steady-state profile, cf. Equation 28. From observing the profile development for increasing time and from flux considerations by *Sørensen et al. (2000),* it can be seen that the time needed to achieve steady-state is governed by the accumulation rate. With S = 2.5 mm · year^{-1} steady-state is reached in the upper 2.5 cm after 10 years. It is only in the immediate theoretical upstart of the process, t = 0, that the concentration gradient at the sediment surface will be infinitely high and that diffusion will dominate the flux *(Sørensen et al., 2000).*

This fact can be further substantiated by calculating the flux at the sediment surface during steady-state, from differentiating Equation 28 for z = 0 and inserting it in Equation 19.

$$N_{sz} = C_w(\text{steady}\quad\text{state})\quad S\quad R_s\qquad 0.5+\sqrt{0.25+\frac{k_1\quad D_{sz}}{(S\quad R_s)^2}} \tag{29}$$

In Figure 39 the ratio $\text{flux}_{\text{sedimentation}} \cdot (\text{flux}_{\text{total}})^{-1}$ is plotted for realistic values of the products $k_1 \cdot D_{sz}$ and $S \cdot R_s$.

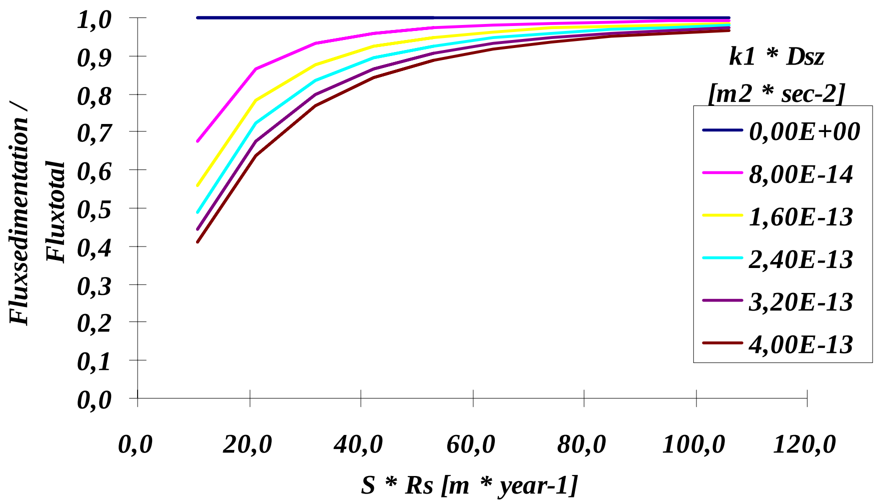

Figure 39 The importance of sedimentation with respect to the flux of substance to the sediment.

Higher degradation rates yield increasing concentration gradients and thus higher diffusion rates through the sediment. Higher adsorption coefficients, K_d, and therefore higher retention factors, R_s, result in higher adsorption to particulate matter, SOM and DOM, and accordingly in higher sedimentation rates of adsorbed substance.

Therefore hydrophobic substances are transported to the sediment at higher rates than hydrophilic substances.

For DEHP the ratios $k_{1N} \cdot D_{sz} = 2.0 \cdot 10^{-15}$ $m^2 \cdot sec^{-2}$ and $S \cdot R_s = 26.5$ $m \cdot year^{-1}$ result in a sedimentation flux comprising about 95 % of the total flux to the sediment.

The sediment concentration profiles of NP and NPDE in Figure 22 differ from the DEHP profile. The concentrations are approximately zero in the upper 5 cm after which a maximum occurs at a depth of 8 cm. The qualitative profile can not be simulated analogously to DEHP, where a constant input concentration in the water is assumed. It is necessary to introduce a water concentration that varies in time, either as a consequence of changing emissions or because a new and more efficient WWTP were taken into operation in 1995. The exact emission pattern of NP and NPDE is not known and therefore it is not relevant, with respect to model calibration, to try to simulate this, in order to achieve the concentration profiles in Figure 22.

6.6 Discussion of experimental and analytical results in the water compartment

Experimental measurements in the water compartment at the marked sampling sites, cf. Figure 1 yield a mean DEHP concentration of 91 ± 81 ng DEHP $\cdot$ litre^{-1} that is approximately constant throughout the fjord.

To obtain an estimate of the DEHP mass flows in the Fjord system an integrated mass balance, cf. Equation 12, comprising the two box models and the dispersion model is performed in an iterate process. The calculations assume constant flows and concentrations for the DEHP sources. Steady-state will occur already after a few months in the water compartment and it is therefore appropriate to consider the steady-state situation alone.

For simplicity reasons the diffusive suction by the sediment is omitted, which is in accordance in steady-state considerations. The biomass concentration in the water is a factor of 100 lower than in the WWTP and furthermore it is not adapted to optimum DEHP degradation, therefore the degradation rate per litre is set to be a factor of 1000 lower than in the WWTP, $k_1 = 2 \cdot 10^{-8}$ sec^{-1}. This is probably still too high but it is compensated by the removal by volatilisation.

Apart from the degradation rate, there are no adjustments of the model parameters in order to fit the modelled results to the experimental findings.

In Table 25 and Figure 40, the steady-state DEHP contributions (+) and removals (-) to the fjord water compartment, are shown in μg DEHP · sec^{-1}.

Table 25 Mass contributions in μg DEHP · sec^{-1} for the Vig, Bredning and narrow passage calculated from the water model.

	Vig	Bredning	Narrow passage
Point sources	+ 100 (37 %)	+ 30 (1 %)	+ 70 (3 %)
Freshwater sources	0 (0 %)	+ 720 (33 %)	+ 650 (26 %)
Net water exchange	- 30 (11 %)	- 80 (4 %)	- 250 (10 %)
Atmospheric deposition	+ 30 (11 %)	+350 (16 %)	+ 530 (21 %)
Sedimentation	- 100 (37 %)	- 950 (43 %)	- 940 (38 %)
Degradation	- 10 (4 %)	- 70 (3 %)	- 70 (3 %)

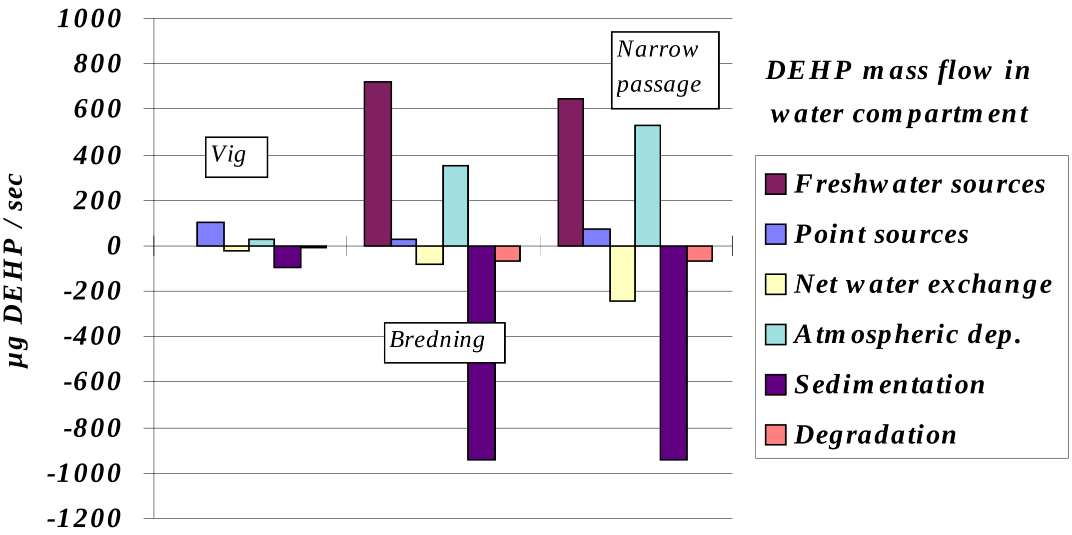

Figure 40 Mass contributions in µg DEHP · sec^{-1} for the Vig, Bredning and narrow passage calculated from the water model.

The calculated total mean steady-state concentrations for the three regions of the Fjord are

Vig:	32 ng DEHP · $litre^{-1}$
Bredning:	26 ng DEHP · $litre^{-1}$
Narrow passage:	19 ng DEHP · $litre^{-1}$ (mean, cf. figure 41)

It can be seen that the freshwater sources from streams are the main contributors to DEHP in the Fjord water followed by atmospheric deposition and WWTP discharges. The removal processes are highly dominated by sedimentation, followed by water exchange with the sea and degradation balances the contributions.

The experimental sediment surface concentrations increase towards the inner parts of the Fjord. In the Vig the DEHP concentration is a factor of 2 higher than in the Bredning and a factor of 10 higher than in the narrow passage. In the narrow passage the flow and turbulence are considerably higher and the net sedimentation rate is reduced.

By using the calculated steady-state concentration for the Bredning as boundary condition in the numerical solution for the narrow passage, the water concentration profile in Figure 41 is obtained.

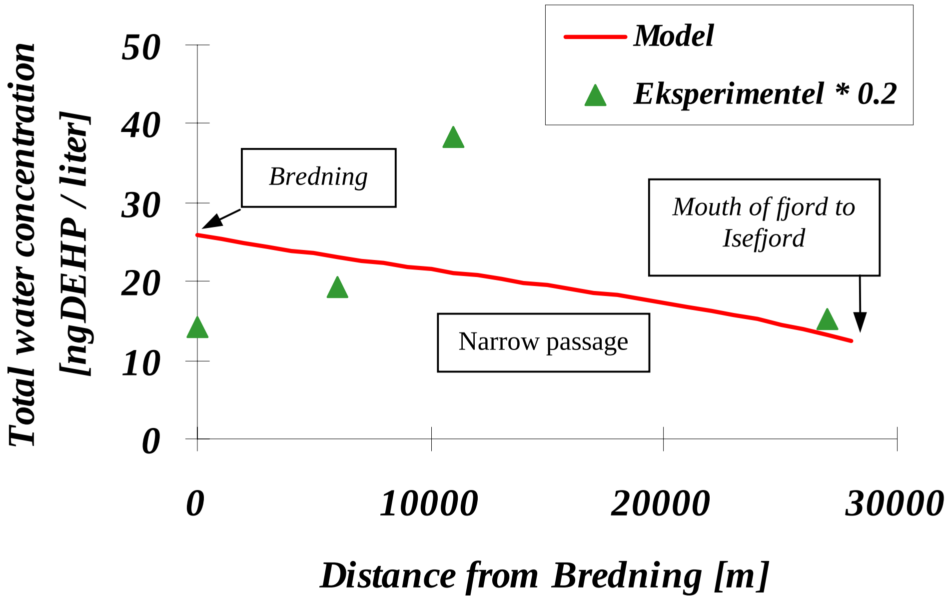

Figure 41 Total DEHP concentrations in the water in the narrow passage. Numerical model (Equation 22) and experimental measurements divided by a factor of 5, cf. Table 9.

The experimental concentrations in the water compartment are approximately constant in all sections of the Fjord (5 sampling sites), cf. Figure 4 and do therefore not display the characteristic decrease caused by dispersion as seen in Figure 41. The experimental concentration peak around 11 km (Frederiksund), arise from an area with very high current and resuspension of settled material with adsorbed DEHP is a possible explanation to the high water concentration. A reason for the underestimation of the calculated concentrations could be missing contributions from sources such as boats, spills from industrial activities or leaching from dumped slag which is reported to have taken place in the Vig.

With a mean experimental water concentration of 91 ng DEHP · litre^{-1}, there is a discrepancy by a factor of 3 – 5 compared to the modelled water concentrations. This is considered to be acceptable as a model result, but in order to use the model as a risk assessment tool the deviation must be taken into account in calculating the predicted environmental concentration (PEC).

7 Conclusions

DEHP was the most abundant substance found in the fjord water, followed by a much lower concentration of DBP, and minute amounts of BBP, DPP and NP. NPDE was not detected. The concentrations were very low, about a third of deposition and half of the small streams.

No significant spatial variation of the concentration for any substance was found in the fjord water on a large geographical scale. A significant seasonal variation was found for DEHP and BBP having maximum in June and minimum in December. The variation was lesser at the inner part compared to the middle and the outer part of the fjord. At the narrow middle part the seasonal variation was highest, and a significant short-term variation was observed having a time-scale of hours.

For the streams, the concentrations in the water were about the triple of the fjord, the spatial and temporal variations being more pronounced and random.

In the fjord sediment DEHP and DBP were most abundant, occurring in much higher concentrations than in the water. The concentrations decreased about 20 times depending on distance from the WWTP outlet. In a 22 cm deep core of fjord sediment, the DEHP concentrations decreased about 10 times from top to bottom.

The concentrations found in the fjord water seem too low to adversely affect the environment, whereas the substances found in the sediments may influence the bottom living organism, and through them enter the food chain.

The experimental results were used to calibrate numerical models that were set up for the water and sediment system respectively. Additionally, analytical solutions were used to perform a theoretical validation. The generic compartment model, SimpleBox, comprised in the European Union System for the Evaluation of Substances, EUSES, was evaluated with respect to sediment uptake of the hydrophobic compound DEHP.

In the water compartment, a mass balance for the annual mean DEHP concentrations, comprising contributions from wastewater treatment plants, atmospheric deposition and freshwater contributions and removals from microbial degradation and sedimentation, was performed. It revealed that the main removal process in the fjord is sedimentation of particle bound substances, or binding of dissolved substances to sediments, whereas horizontal transport through the water seems to be of lesser significance. The main contributors are freshwater sources from streams followed by atmospheric deposition and discharges from wastewater treatment plants.

The fate of xenobiotics, exemplified with DEHP, in the sediment compartment has been described with sedimentation, diffusion and 1st order degradation. However, diffusion will only be significant in the upstart phase and can therefore be omitted in model calculations when steady-state conditions are concerned. Such situations typically occur in the surface layer after about 10 years. As concluded by *Sørensen et al. (2000)* the insignificance of gradient conditioned diffusion in the surface layer, justifies the use of a sediment description comprising a totally mixed sediment compartment, such as the set-up used in the mathematically more simple SimpleBox.

The used modelling approach, where the water and sediment compartments are treated separately only connected through substance exchange through sedimentation, seems appropriate in describing the fate of DEHP in the complex multi media fjord system.

8 References

Berger, W.H. & Heath, G.R. (1968): Vertical Mixing in Pelagic Sediments. Journal of Marine Research, *26*, 134 – 143.

Carbonell, G, Ramos, C., Pablos, M.V., Ortiz, J.A. & Tarazona, J.V. (2000): A System Dynamic Model for the Assessment of Different Exposure Routes in Aquatic Ecosystems. The Science of the Total Environment, *247*, 107 – 118.

Fauser, P., Sørensen, P.B., Vikelsøe, J. & Carlsen, L. (2000): Phthalates, Nonylphenols and LAS in Roskilde Wastewater Treatment Plant – Fate Modelling Based on Measured Concentrations in Wastewater and Sludge. Ministry of Environment and Energy, National Environmental Research Institute, Department of Environmental Chemistry, Research Report submitted for publication.

Fischer, H.B. (1972): Mass Transport Mechanisms in Partially Stratified Estuaries. Journal of Fluid Mechanic, *53*, 671 – 687.

Fischer, H.B., Imberger, J., List, E.J., Koh, R.C.Y. & Brooks, N.H. (1979): Mixing in Inland and Coastal Waters. Academic Press.

Flindt, M., Madsen, M. & Sørensen, P.S. (1992): Modelsystem for Fjorde og Bugter. Havforskning fra Miljøstyrelsen, *9*.

Flindt, M.R., Kamp-Nielsen, L., Marques, J.C., Pardal, M.A., Bocci, M., Bendoricchio, G., Salomonsen. J., Nielsen, S.N. & Jørgensen, S.E. (1997): Ecological Modelling, *102*, 17 – 31.

Flindt, M., Pedersen, C.B., Hansen, L.R. & Hedal S. (1998): Hydrografisk Modellering af Typeområdet Roskilde Fjord 1998. NOVA 2003 Årsrapport, Roskilde og Frederiksborg Amter.

Furtmann, K. (1996): Phthalates in the Aquatic Environment. Landesamt für Wasser und Abfall Nordrhein-Westfalen.

Harleman, D.R.F. & Thatcher, M.L. (1974): Longitudinal Dispersion and Unsteady Salinity Intrusion in Estuaries. La Houille Blanche, *½*, 25 – 33.

Harremoës, P. & Malmgren-Hansen, A. (1990): Lærebog i Vandforurening. Polyteknisk Forlag.

Hedal, S., Hansen, L.R., Thingberg, C. & Jensen, K.B. (1999): Overvågning af Roskilde Fjord 1998. Roskilde Amt, Teknisk Forvaltning og Frederiksborg Amt, Teknik og Miljø.

Holley, E.R., Harleman, D.R.F. & Fischer, H.B. (1970): Dispersion in Homogeneous Estuary Flow. Journal of the Hydraulics Division, Proceedings of the American Society of Civil Engineers, 1691 – 1709.

Larsen M. (1999): Personal communication.

Larsen, T. & Hansen, T.B. (1998): Modellering af Næringssalte i Fjorde. Vand & Jord, *3*, 120 – 123.

Madsen, P.P. & Larsen, B. (1979): Bestemmelse af Akkumulationsrater i Marine Sedimentationsområder ved Pb-210 Datering. Vand, *5*, 2 - 6.

McCall, P.L. & Tevesz, M.J.S. (1982): Animal-Sediment Relations, The Biogenic Alteration of Sediments. Plenum Press, New York and London.

Mikkelsen, J. (1994): Matematisk Modellering af Kemikaliers Skæbne i Renseanlæg. Danmarks Tekniske Højskole, Lyngby, Denmark.

Møhlenberg, F. (1995): Regulating Mechenisms of Phytoplankton Growth and Biomass in a Shallow Estuary. Ophelia, *42*, 239 – 256.

Peters, H. (1999): Spatial and Temporal Variability of Turbulent Mixing in an Estuary. Journal of Marine Research, *57*, 805 – 845.

Pilegaard, K. (1997): Risø National Laboratory. Data collected during the RIMI project (Risøs Integrerede Miljøprojekt). Private communication.

Remberg, M. (1999): Analysis of phthalate esters in Swedish lakes and rivers. Presented at Phthalate Esters Environmental Analysis Workshop, arr. ECPI, Kortrijk, Belgium, 4-5 Nov. 1999.

Roskilde County & Municipality (1994): Hydrografic investigation of Roskilde Fjord. Reports from Danish Hydraulic Institute and Water Consult.

Roskilde County (1999): Rambøll, Hydrometriske beregninger 1998 Roskilde Amt

Schnoor, J.L. (1996): Environmental Modelling – Fate and Transport of Pollutants in Water, Air and Soil. Environmental Science and Technology. A Wiley-Interscience series of texts and monographs. John Wiley & Sons, inc.

Schwarzenbach, R., Gschwend, P.M. & Imboden, D. (1993): Environmental Organic Chemistry. John Wiley & Sons, Inc.

Shang, D.Y, MacDonald, R.W. & Ikonomou, M.G. (1999): Persistence of Nonylphenol Ethoxylate Surfactants and Their Primary Degradation Products in Sediments from near a Municipal Outfall in the Strait of Georgia, British Columbia, Canada. Environmental Science and Technology, *33*, 1366 – 1372.

Smith, R. (1986): Mixing and Dispersion in Estuaries: Which Mathematical Model and When? International Conference on Water Quality Modelling in the Inland Natural Environment, Bournemouth, England: 10 – 13 June, 1986, 375 - 385.

Spiegel, M.R. (1968): Mathematical Handbook of Formulas and Tables. Schaum's outline series. McGraw-Hill Book Company.

Sørensen, P.B., Fauser, P., Carlsen, L & Vikelsøe, J. (2000): Evaluation of Sub-Process Validity in the TGD in Relation to Hydrophobic Substances. Ministry of Environment and Energy, National Environmental Research Institute, Department of Environmental Chemistry, Research Report submitted for publication.

Sørensen, P.B. (1999): Personal communication.

Thomsen, M., Carlsen, L. & Hvidt, S. (2000): Solubilities and Surface Activities of Phthalates Investigated by Surface Tension Measurements. Environmental Toxicology and Chemistry, in press.

Toppari, J., Larsen, J.C., Christiansen, P., Giwercman, A., Grandjean, P., Guilette Jr, L.J., Jégou, B., Jensen, T.K., Jouannet, P., Keiding, N., Leffers, H., McLachlan, J.A., Meyer, O., Müller, J., Meyts, E.R.-D., Scheike, T., Sharpe, R., Sumpter, J., & Skakkebæk, N.E. (1995): Male reproductive health and environmental chemicals with estrogenic effects. Miljøstyrelsen, Miljøprojekt nr. 292.

van der Velde, E.G., de Korte, G.A.L. Linders, S.H.M.A. & Hijman, W.C (1999): Method development for the analysis of phthalates in environmnetal samples with GC-MS. Presented at Phthalate Esters Environmental Analysis Workshop, arr. ECPI, Kortrijk, Belgium, 4-5 Nov. 1999.

Vikelsøe, J., Thomsen, M. & Johansen, E. (1998): Sources of phthalates and nonylphenols in municipal waste water. NERI technical report No. 225.

Vikelsøe, J., Thomsen, M., Johansen, E. & Carlsen, L. (1999): Phthalates and Nonylphenols in Soil – A Field Study of Different Soil Profiles. Ministry of Environment and Energy, National Environmental Research Institute, Department of Environmental Chemistry, Technical Report No. 268.

Wheatcroft, R.A., Jumars, P.A., Smith, C.R. and Nowell., A.R.M. (1990): A Mechanistic View of the Particulate Biodiffusion Coefficient: Step Lengths, Rest Periods and Transport Directions. Journal of Marine Research, *48*, 177 – 207.

9 Abbreviations

Analyte	Substance analysed
BBP	Butylbenzylphthalate
D	Deuterium (^2H, heavy isotope of hydrogen)
D_4-BBP	BBP deuterium-labelled in ring
D_4-DBP	DBP deuterium-labelled in ring
D_4-DEHP	DEHP deuterium-labelled in ring
D_4-DnOP	DnOP deuterium-labelled in ring
DBP	Di(n-butyl)phthalate
DEHP	Di(2-ethylhexyl)phthalate
DnNP	Di(n-nonyl)phthalate
DnOP	Di(n-octyl)phthalate
DPP	Dipentylphthalate
dm %	Content of dry matter in weight percent of total
dm	Dry matter
GC	Gaschromatography
GC/MS	GC combined with MS
HRMS	High resolution MS (high ability of MS to discriminate between masses)
LD	Limit of determination, concentration below which the result is uncertain
mg/kg dw	Milligram per kg dry weight (Parts Per Million, PPM)
µg/kg dw	Microgram per kg dry weight (Parts Per Billion, PPB)
MS	Mass spectrometry
nd	Not detected, non-detect
non-detect	Result < 0 after subtraction of the blank
DEPA	Danish Environmental Protection Agency
NERI	National Environmental Research Institute

NP	Nonylphenol
NPDE	Nonylphenol-diethoxylate
NPE	Nonylphenol-ethoxylates
PAE	Phthalate ester
PFK	Perfluoro kerosene (calibration gas for HRMS)
Phthalate	Di ester of phthalic acid (1,2-benzene dicarboxylic acid)
sd	Standard deviation
SIM	Selected ion monitoring (MS operating mode)
Spike	Labelled substance added during the analytical procedure for quality control
Steady-state	Situation with constant conditions
WWTP	Wastewater treatment plant
ww	Wet weight

10 Variables

A_{bred}	Surface area of Roskilde bredning (km^2)
A_{narr}	Surface area of narrow passage (km^2)
A_{vig}	Surface area of Roskilde Vig (km^2)
b	width of fjord compartment (m)
C	Dissolved concentration (ng pr. litre)
C_A	Dissolved concentration of substance A (ng A pr. litre)
C_s	Dissolved DEHP concentration in sediment pore water (ng pr. g dm)
C_s(x or i,z or j)	Dissolved DEHP concentration in sediment at position (x or i, z or j) (ng pr. g dm)
$C_{tot,dep}$	Atmospheric bulk deposition (kg pr. ($m^2 \cdot$ sec))
$C_{tot,f}$	Dissolved and adsorbed DEHP concentration in freshwater sources (µg pr. litre)
C_w	Dissolved DEHP concentration in water (ng pr. litre)
C_w(x or i)	Dissolved DEHP concentration in water at position x or i (ng pr. litre)
$C_{w,bred}$	Dissolved DEHP concentration in water in bredning (ng pr. litre)
$C_{w,narr}$	Dissolved DEHP concentration in water in narrow passage (ng pr. litre)
$C_{w,sea}$	Dissolved DEHP concentration in water in sea (ng pr. litre)
$C_{w,vig}$	Dissolved DEHP concentration in water in vig (ng pr. litre)
C_{WWTP}	Dissolved DEHP concentration in WWTP discharge (µg pr. litre)
C_X	Concentration of adsorbed substance (ng pr. litre)
C_{XB}	“Concentration” of available sites on dry matter (µg pr. litre)
dx	Horizontal step in water (m)
dt	Time step (sec)

dz	Vertical step in sediment (m)
$D_{benzene}$	Diffusion coefficient of benzene (m^2 pr. sec)
D_{DEHP}	Diffusion coefficient of DEHP (m^2 pr. sec)
$D_{disp,sz}$	Vertical dispersion coefficient in the sediment (m^2 pr. sec)
D_{known}	Diffusion coefficient of known substance (m^2 pr. sec)
D_{sz}	Vertical diffusion coefficient in sediment (m^2 pr. sec)
$D_{unknown}$	Diffusion coefficient of unknown substance (m^2 pr. sec)
D_{wx}	Horizontal dispersion coefficient in water (m^2 pr. sec)
DOM	Dissolved organic matter
h(x)	Water depth at distance x (m)
i	Number of horizontal steps
j	Number of vertical steps
k_1	Pseudo 1st order degradation rate (sec^{-1})
k_{1D}	Pseudo 1st order anoxic degradation rate (sec^{-1})
k_{1ext}	Extraction constant ($days^{-1}$)
k_{1N}	Pseudo 1st order aerobic degradation rate (sec^{-1})
k_{1sed}	Sedimentation constant ($days^{-1}$)
k_{1vert}	Vertical sedimentation constant ($days^{-1}$)
K_d	Partition coefficient between water and particulate matter (litre pr. kg dm)
K_{dw}	Partition coefficient between water and particulate matter in water (litre pr. kg dm)
$mass_{benzene}$	Mass of benzene (g pr. mol)
$mass_{DEHP}$	Mass of DEHP (g pr. mol)
$mass_{known}$	Mass of known substance (g pr. mol)
$mass_{unknown}$	Mass of unknown substance (g pr. mol)
n	Number of time steps
N_{sz}	Vertical flux of DEHP in sediment (g pr. ($m^2 \cdot$ sec))
N_{wx}	Horizontal flux of DEHP in water (g pr. ($m^2 \cdot$ sec))

N_x	Horizontal flux (g pr. ($m^2 \cdot$ sec))
N_z	Vertical flux (g pr. ($m^2 \cdot$ sec))
$q_{f,narr}$	Freshwater flow to narrow passage (m^3 pr. (m · sec))
$q_{p,narr}$	Point source flow to narrow passage (m^3 pr. (m · sec))
Q_1	Water exchange from narrow passage to sea (m^3 pr. sec)
Q_2	Water exchange from bredning to narrow passage (m^3 pr. sec)
Q_3	Water exchange from vig to bredning (m^3 pr. sec)
$Q_{bred\text{-}vig}$	Water exchange from bredning to vig (m^3 pr. sec)
$Q_{f,bred}$	Freshwater flow to Roskilde Bredning (m^3 pr. sec)
$Q_{f,vig}$	Freshwater flow to Roskilde vig (m^3 pr. sec)
Q_{narr}	Water flow in narrow passage (m^3 pr. sec)
$Q_{narr\text{-}bred}$	Water exchange from narrow passage to bredning (m^3 pr. sec)
$Q_{p,bred}$	Point source flow to bredning (m^3 pr. sec)
$Q_{p,vig}$	Point source flow to vig (m^3 pr. sec)
$Q_{sea\text{-}narr}$	Water exchange from sea to narrow passage (m^3 pr. sec)
Q_{WWTP}	Water flow from WWTP discharge (m^3 pr. hour)
R	Retention factor
R_s	Retention factor for sediment
R_w	Retention factor for water
R_{WWTP}	Retention factor for WWTP discharge
S	Sediment accumulation rate (mm pr. year)
v_{ext}	Extraction velocity (m pr. day)
v_{sed}	Sedimentation velocity (m pr. day)
v_p	Advective pore water velocity (m pr. sec)
x	Distance from WWTP discharge (m)
X_s	Concentration of dry matter in sediment (kg pr. litre)
X_w	Concentration of dry matter in water (kg pr. litre)

P	Product from bio-degradation
t	Time (sec, years)
t_{sed}	Time for increasing the sediment with depth dz with a sedimentation rate S (years)
z	Depth in sediment (m)
α	Longitudinal dispersivity (m)
θ_s	Water content in sediment (litre water pr. litre total)

11 Acknowledgements

The authors wish to thank the following persons and institutions for their important contributions to the investigation:

Monthly fjordwater samples: Bruno Hansen, Roskilde County.

Stream hydraulics information: Ivar Hansen, Roskilde County.

Sampling equipment: Iver Hansen, NERI Technical Division

WWTP samples: Gunnar Clausen and Ove Petersen, Bjergmarken wastewater treatment plant, Roskilde.

Salinity and temperature of fjord water: Søren Hedal, Roskilde County and Martin M. Larsen, NERI, Department of Marine Environment .

Meteorological data: Kim Pilegaard, Risø National Laboratory.

Critical review of manuscript: Henrik Søren Larsen, DEPA.

12 Appendix A.
Analytical performance test

12.1 Detection limits

The detection limits are derived from the performance experiment, described in the analytical chapter. They are essentially the standard deviation at the low concentration level, given in Table 9. However, since the blank is subtracted, the detection limit depends on the standard deviation of the difference between measurement and blank. The corresponding variance is equal to the sum of variances of the sample and blank. Hence, the detection limit is calculated according to the formula

$$\mathrm{LD}=\sqrt{\mathrm{VarS}+\frac{\mathrm{VarB}}{n}} \qquad (30)$$

where:

LD = Limit of determination (single determination, 1 σ level)

VarS = Variance of sample (pooled level 0 and 100, disregarding 0-variances)

VarB = Variance of the blank

n = multiplicity of blank determination (3 in case of test experiment)

As can be seen from Table 9, the experimentally found detection limits ranged from 2 for the low-blank phthalates through about 30 ng/l for the high blank phthalates (DEHP and DBP) to about 40 ng/l for NPDE. The high LD for NPDE is due to a low MS-signal.

It is reported *(van der Velde et al. 1999, Remberg 1999)* that a limit of determination of about 20 ng/l for analysis of DEHP in sea water can be obtained routinely by means of a solid phase extraction (SPE) method. In principle lower DL can be reached by SPE than by a solvent extraction method, because larger samples may be drawn. Nevertheless, the detection limits of the solvent extraction method used in the present study come close to the reported detection limit.

During the actual measurements of the project, somewhat higher blank were encountered, especially for DEHP, leading to higher detection limits for this substance. Hence, the low concentrations found in the fjord water were in many cases close to the detection limit.

12.2 Figures, method for water

The results of the analytical test are shown in Figure 42 to Figure 49. The amount of substance added to the water in ng/l is shown on the x-axis, and the amount found on the y-axis. The mean and standard deviation for each level is shown as well as a regression line. The blank has not been subtracted. Hence, the y-intercepts in the figures can be interpreted as the sum of blank and the naturally occurring substance in the fjord water.

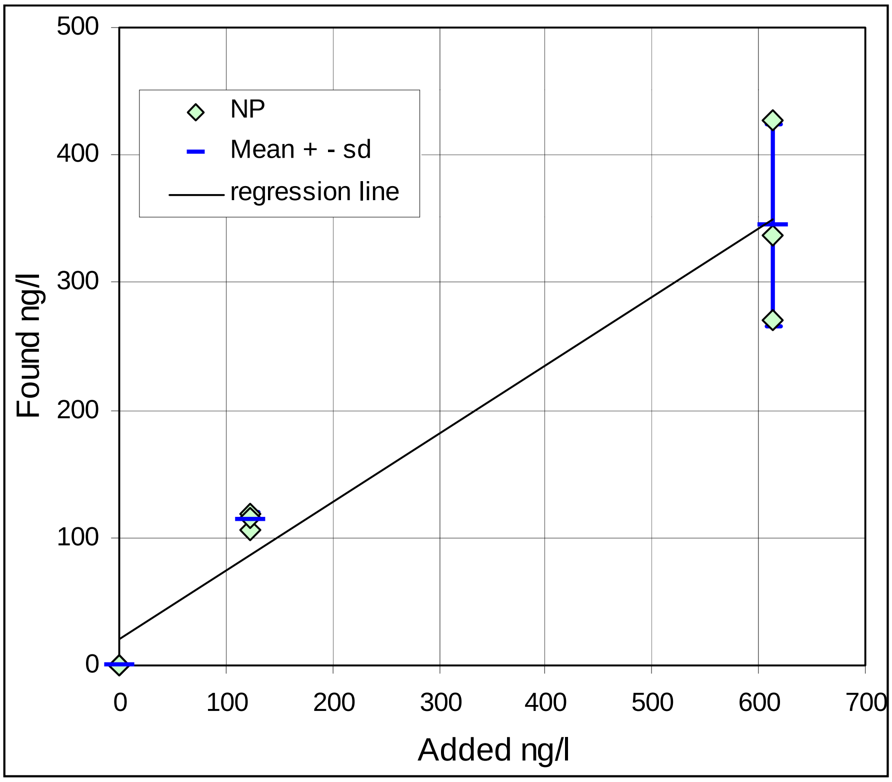

Figure 42 Linearity & precision test, NP in water.

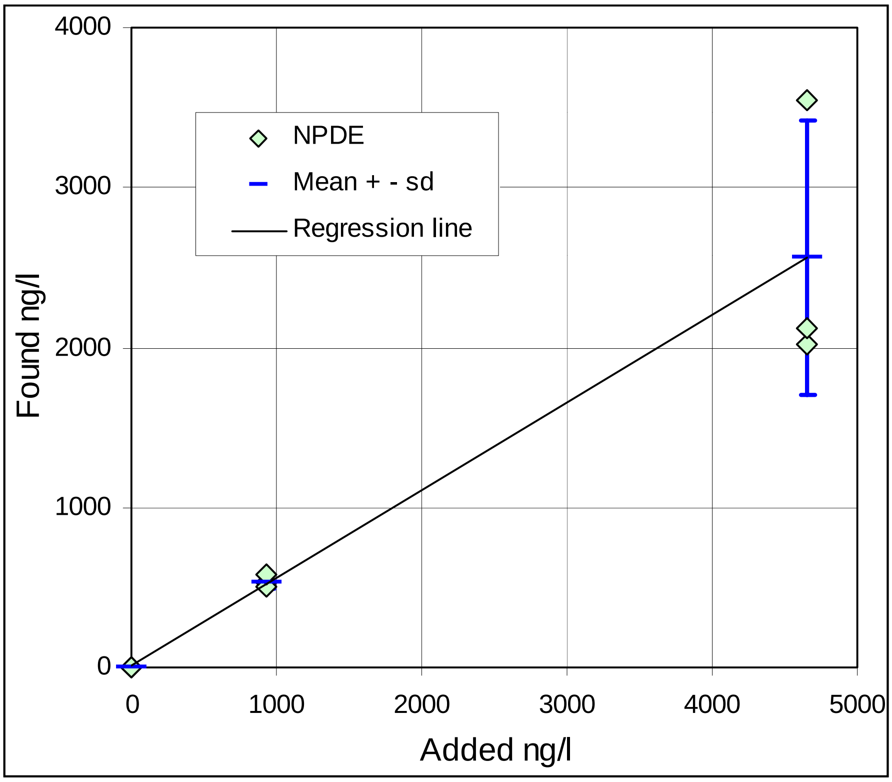

Figure 43 Linearity & precision test, NPDE in water.

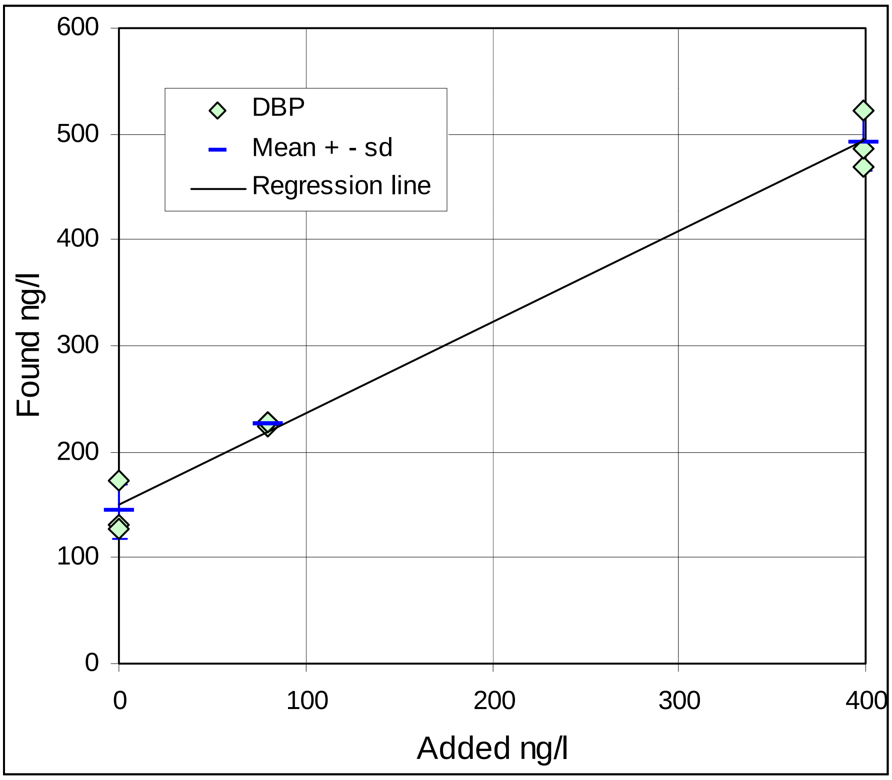

Figure 44 Linearity & precision test, DBP in water.

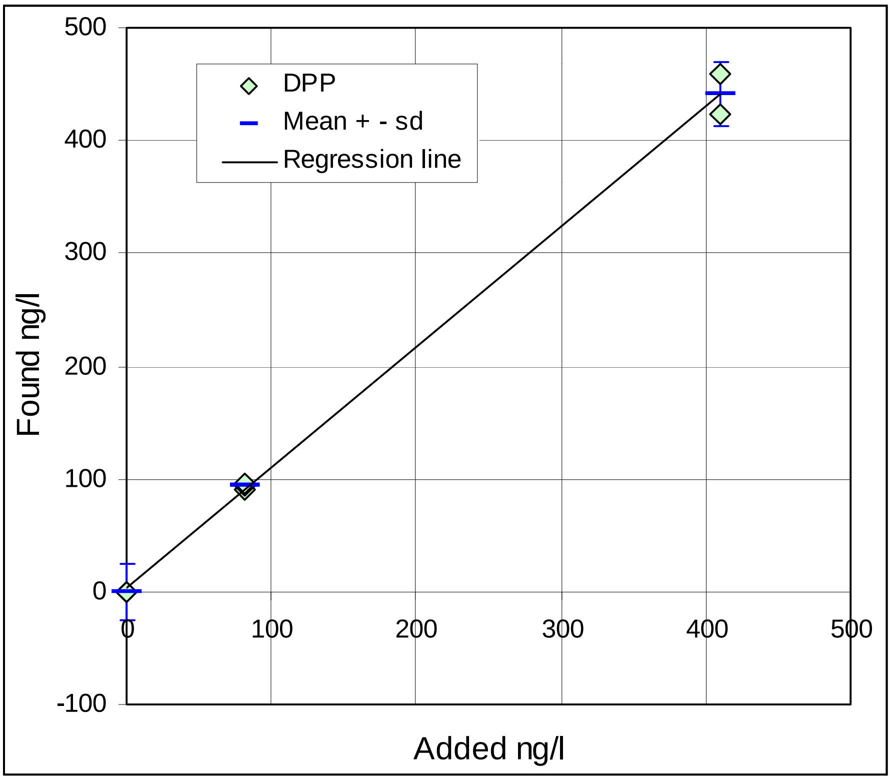

Figure 45 Linearity & precision test, DPP in water.

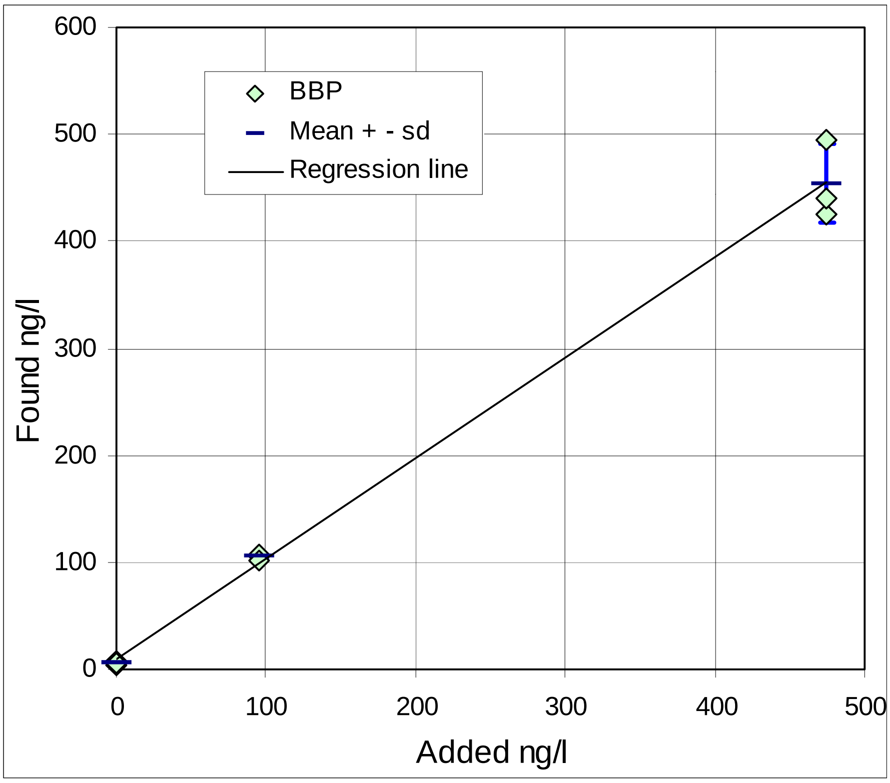

Figure 46 Linearity & precision test, BBP in water.

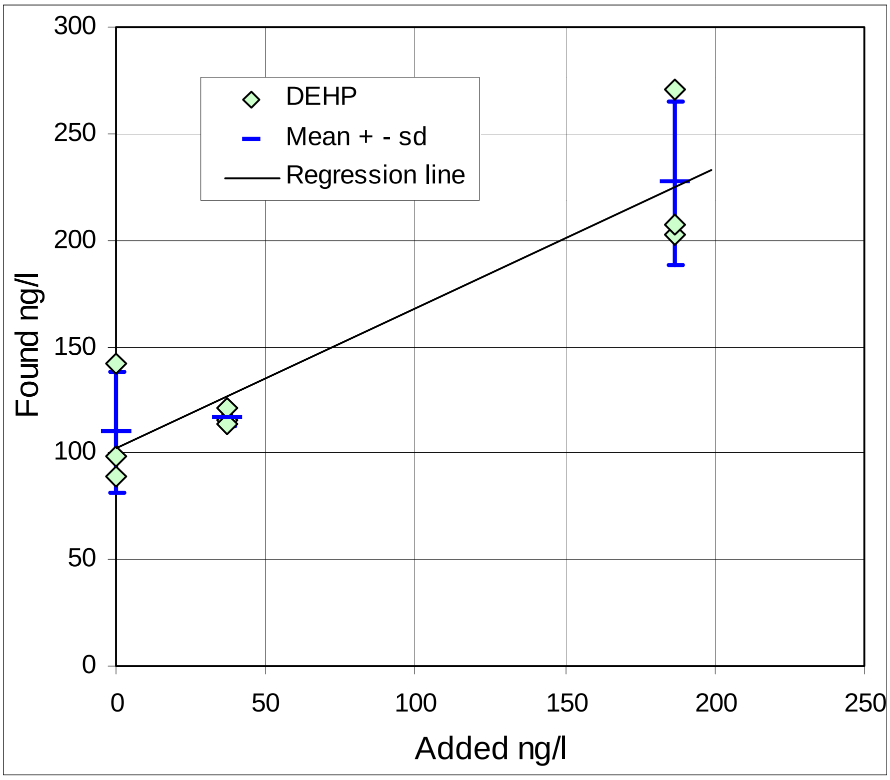

Figure 47 Linearity & precision test, DEHP in water.

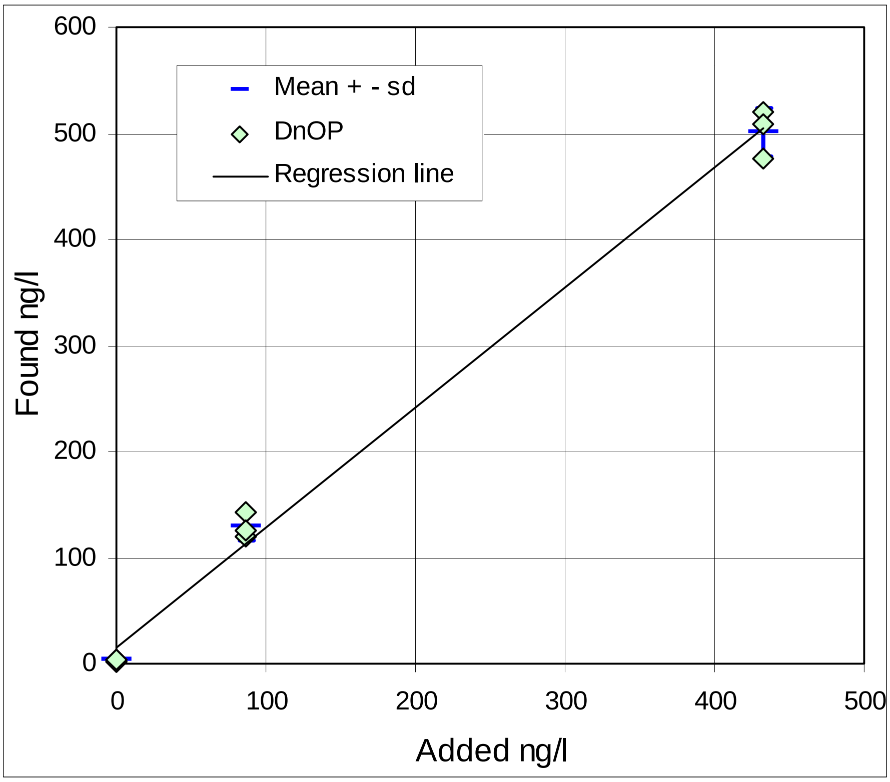

Figure 48 Linearity & precision test, DnOP in water.

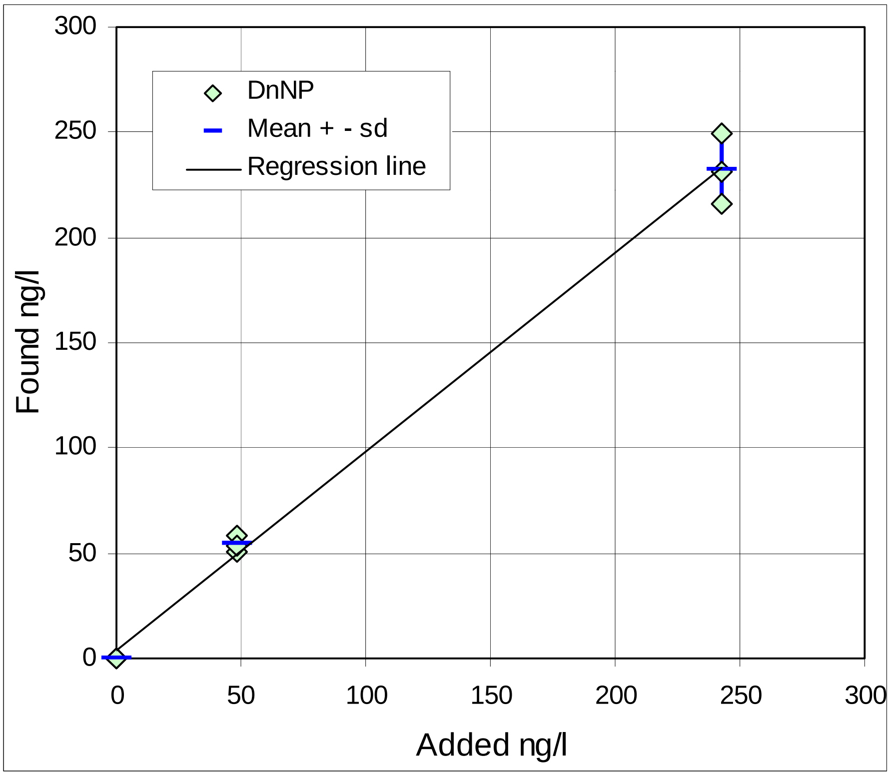

Figure 49 Linearity & precision test, DnNP in water.

As seen from the figures, the regression line is close to the mean and average indicating a good linearity within the range investigated, as tested statistically below. It is further seen that the standard deviation (shown as vertical bars) is considerably larger for BBP and DEHP, Figure42, than for the other phthalates, as noted above. It is also seen that the y-intercept is larger for DBP and DEHP.

12.2.1 Linearity of method for water

The linearity of the analytical method for water is tested by linear regression analysis, Table 26.

Table 26 Linear regression analysis of performance experiment for water method

Regression	**NP**	**NPDE**	**DBP**	**DPP**	**BBP**	**DEHP**	**DnOP**	**DnNP**
Slope	0.537	0.550	0.863	1.074	0.936	0.659	1.129	0.945
Intercept	21.3	10.9	149.5	2.5	10.1	101.8	15.9	3.6
Correlation coefficient	0.959	0.939	0.992	0.999	0.999	0.914	0.997	0.996
Residual sd	47.9	457.5	21.0	10.7	20.1	26.9	19.3	10.0
Within group sd	46.3	494.0	27.9	17.6	18.2	27.3	13.3	12.2
F residual/within	1.07	0.86	0.56	0.36	1.21	0.97	2.10	0.67
p	0.47	0.58	0.77	0.87	0.39	0.51	0.16	0.70

The slope of the regression line should theoretically be 1 in case of a perfect analysis. As can be seen from Table 26, the slopes are all reasonably close to 1, with the exception of NP and NPDE. The reason for this is without question that, unlike the phthalates, a “foreign” spike (D_4-DBP) is used for quantification for these substances, with other chemical and mass-spectrometrical characeristics. The intercept corresponds to the measured value without added substance, i.e. theoretically the sum of blank and naturally occurring substance. The residual standard deviation of is the deviation from the measurements to the regression line, and the within group standard deviation is the pooled group standard deviation from Table 9. As seen, these two standard deviations are of about the same magnitude for all phthalates. The linearity is tested by the F-test, which compares the corresponding variances, F > 1 indicating deviations from linearity. The level of significance p show no significant deviations from linearity (p<0.05).

12.3 Figures, method for sediment

The results of the analytical test are shown for the most abundant substances in fjordsediment in Figure 50 to Figure 55. The same remarks apply as for the figures of the water method experiment.

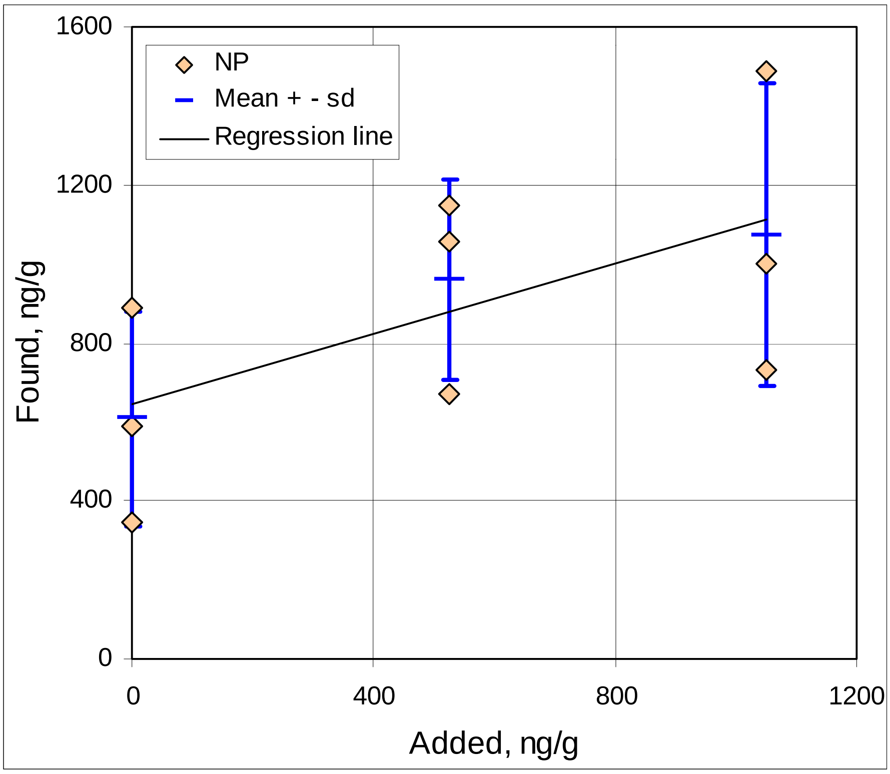

Figure 50 Linearity & precision test, NP in sediment.

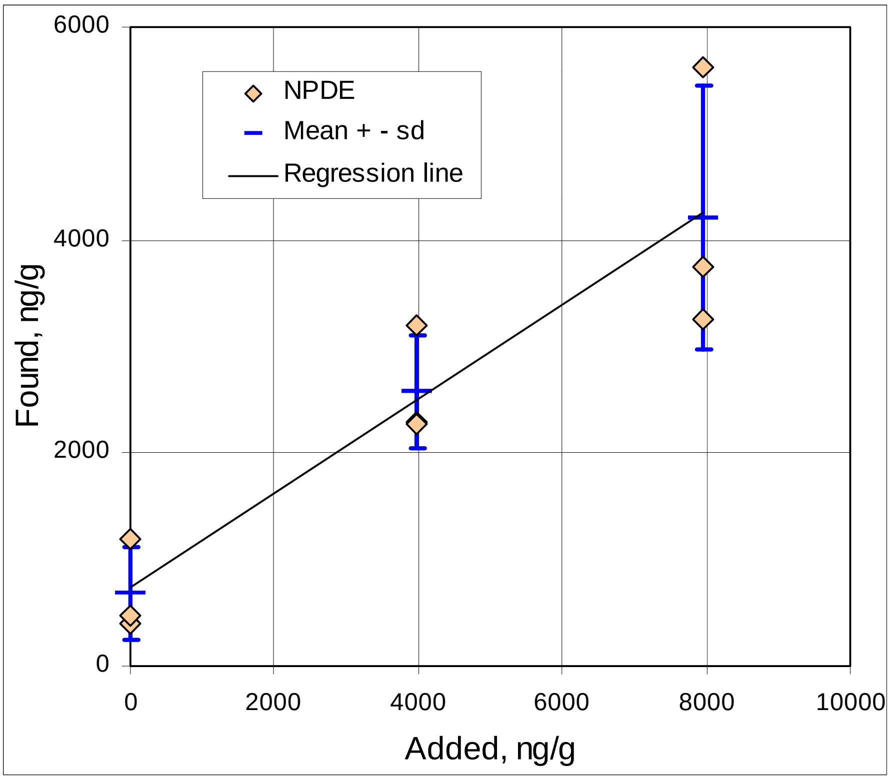

Figure 51 Linearity & precision test, NPDE in sediment.

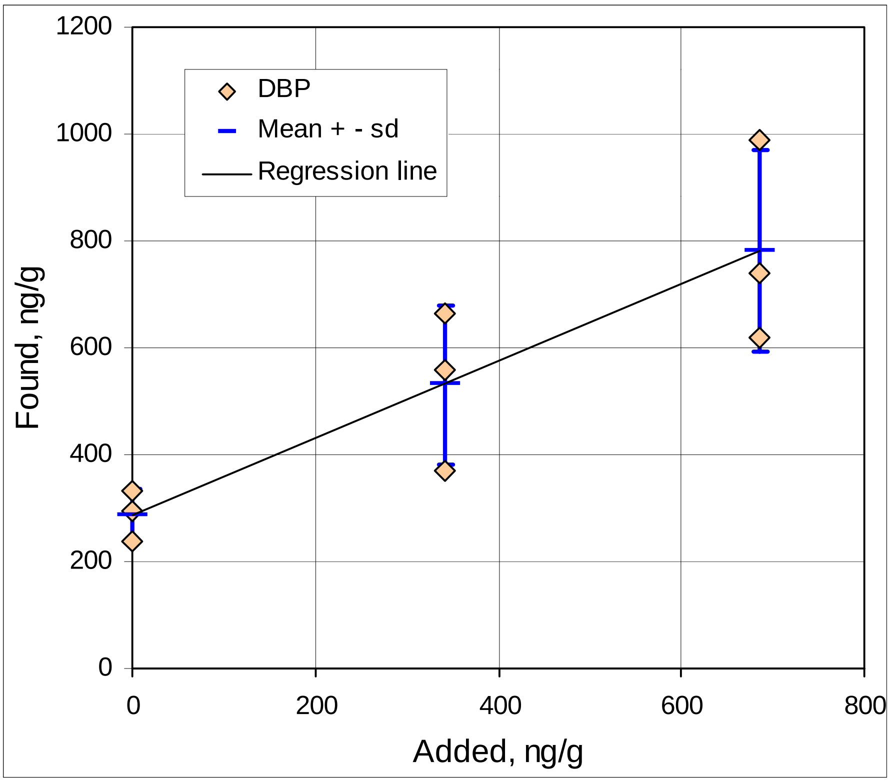

Figure 52 Linearity & precision test, DBP in sediment.

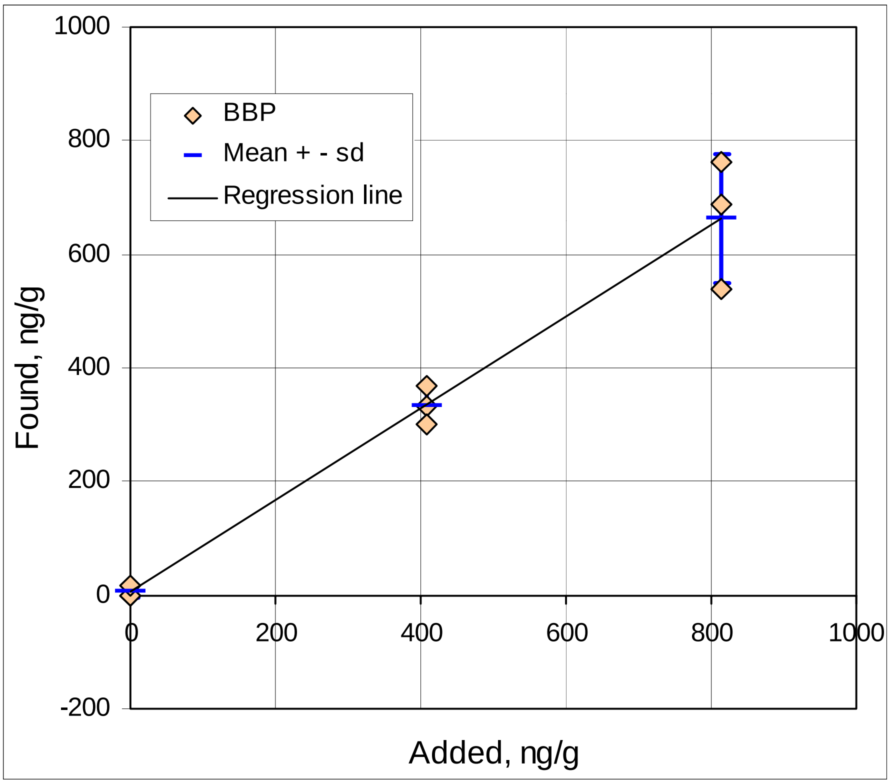

Figure 53 Linearity & precision test, BBP in sediment.

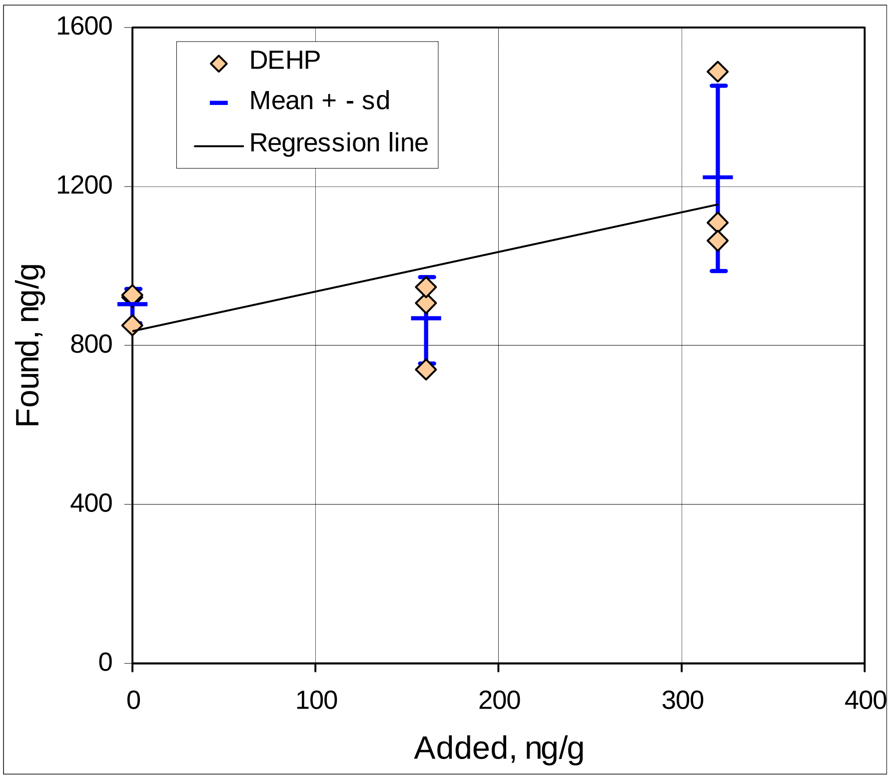

Figure 54 Linearity & precision test, DEHP in sediment.

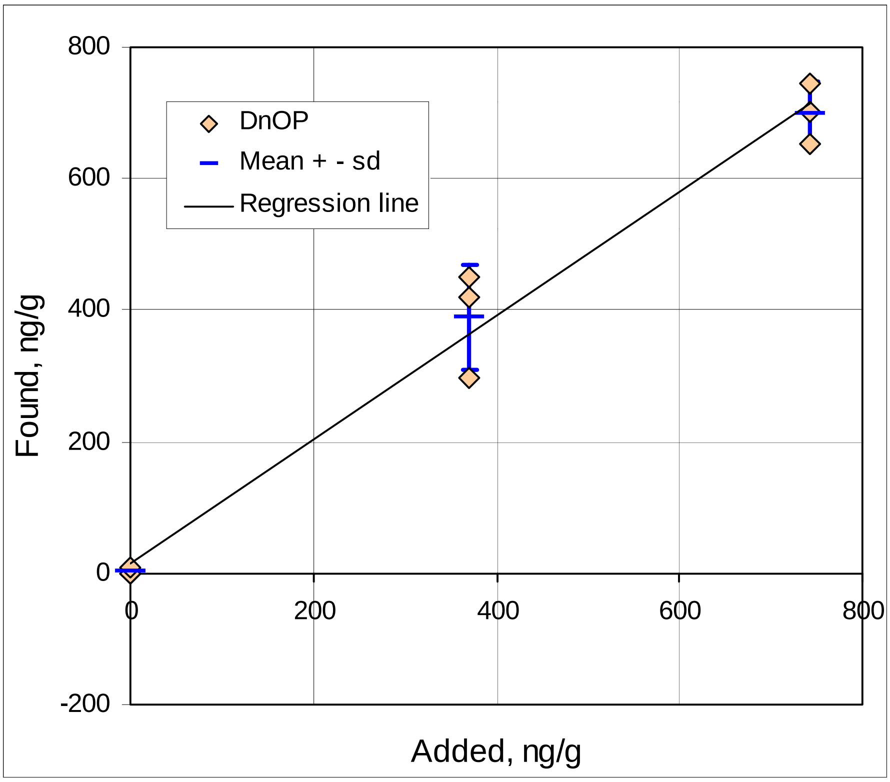

Figure 55 Linearity & precision test, DnOP in sediment.

12.3.1 Linearity of method for sediment

The linearity of the analytical method is tested by linear regression analysis, Table 27.

Table 27 Linear regression analysis of performance experiment for sediment method

Regression	**NP**	**NPDE**	**DBP**	**DPP**	**BBP**	**DEHP**	**DnOP**	**DnNP**
Slope	0.44	0.44	0.72	1.12	0.81	1.01	0.94	1.03
Intercept	647	733	286	10.1	5.78	834	15.1	31.7
Correlation coefficient	0.59	0.91	0.87	0.91	0.98	0.65	0.99	0.95
Residual sd	293	762	131	165	64	174	54	64
Within group sd	309	820	141	178	69	151	54	54
F residual/within	0.90	0.86	0.86	0.86	0.86	1.34	0.99	1.41
p	0.56	0.58	0.58	0.58	0.58	0.37	0.51	0.35

The slopes of the regression lines as seen from Table 27, are also for sediment all reasonably close to 1, with the exception of NP and NPDE, as was the case for the water, and no doubt for the same reason (spike used not chemical identical with substance measured). The intercept is theoretically the sum of blank and naturally occurring substance, but in case of sediment, the latter dominate. For the test of linearity, the same remarks as those for the water method apply. No significant deviations from linearity ($p<0.05$) were found.

National Environmental Research Institute

The National Environmental Research Institute, NERI, is a research institute of the Ministry of Environment and Energy. In Danish, NERI is called *Danmarks Miljøundersøgelser (DMU).*
NERI's tasks are primarily to conduct research, collect data, and give advice on problems related to the environment and nature.

Addresses:

URL: http://www.dmu.dk

National Environmental Research Institute
Frederiksborgvej 399
PO Box 358
DK-4000 Roskilde
Denmark
Tel: +45 46 30 12 00
Fax: +45 46 30 11 14

Management
Personnel and Economy Secretariat
Research and Development Section
Department of Atmospheric Environment
Department of Environmental Chemistry
Department of Policy Analysis
Department of Marine Ecology
Department of Microbial Ecology and Biotechnology
Department of Arctic Environment

National Environmental Research Institute
Vejlsøvej 25
PO Box 314
DK-8600 Silkeborg
Denmark
Tel: +45 89 20 14 00
Fax: +45 89 20 14 14

Environmental Monitoring Co-ordination Section
Department of Lake and Estuarine Ecology
Department of Terrestrial Ecology
Department of Streams and Riparian areas

National Environmental Research Institute
Grenåvej 12-14, Kalø
DK-8410 Rønde
Denmark
Tel: +45 89 20 17 00
Fax: +45 89 20 15 15

Department of Landscape Ecology
Department of Coastal Zone Ecology

Publications:
NERI publishes professional reports, technical instructions, and the annual report. A R&D projects' catalogue is available in an electronic version on the World Wide Web.
Included in the annual report is a list of the publications from the current year.

Faglige rapporter fra DMU/NERI Technical Reports

2000

Nr. 310: Hovedtræk af Danmarks Miljøforskning 1999. Nøgleindtryk fra Danmarks Miljøundersøgelsers jubilæumskonference Dansk Miljøforskning. Af Secher, K. & Bjørnsen, P.K. (i trykken)
Nr. 311: Miljø- og naturmæssige konsekvenser af en ændret svineproduktion. Af Andersen, J.M., Asman, W.A.H., Hald, A.B., Münier, B. & Bruun, H.G. (i trykken)
Nr. 312: Effekt af døgnregulering af jagt på gæs. Af Madsen, J., Jørgensen, H.E. & Hansen, F. 64 s., 80,00 kr.
Nr. 313: Tungmetalnedfald i Danmark 1998. Af Hovmand, M. & Kemp, K. (i trykken)
Nr. 314: Future Air Quality in Danish Cities. Impact Air Quality in Danish Cities. Impact Study of the New EU Vehicle Emission Standards. By Jensen, S.S. et al. (in press)
Nr. 315: Ecological Effects of Allelopathic Plants – a Review. By Kruse, M., Strandberg, M. & Strandberg, B. 64 pp., 75,00 DKK.
Nr. 316: Overvågning af trafikkens bidrag til lokal luftforurening (TOV). Målinger og analyser udført af DMU. Af Hertel, O., Berkowicz, R., Palmgren, F., Kemp, K. & Egeløv, A. (i trykken)
Nr. 317: Overvågning af bæver *Castor fiber* efter reintroduktion på Klosterheden Statsskovdistrikt 1999. Red. Berthelsen, J.P. (i trykken)
Nr. 318: Order Theoretical Tools in Environmental Sciences. Proceedings of the Second Workshop October 21st, 1999 in Roskilde, Denmark. By Sørensen, P.B. et al. (in press)
Nr. 319: Forbrug af økologiske fødevarer. Del 2: Modellering af efterspørgsel. Af Wier, M. & Smed, S. (i trykken)
Nr. 320: Transportvaner og kollektiv trafikforsyning. ALTRANS. Af Christensen, L. 154 s., 110,00 kr.
Nr. 321: The DMU-ATMI THOR Air Pollution Forecast System. System Description. By Brandt, J., Christensen, J.H., Frohn, L.M., Berkowicz, R., Kemp, K. & Palmgren, F. 60 pp., 80,00 DKK.
Nr. 322: Bevaringsstatus for naturtyper og arter omfattet af EF-habitatdirektivet. Af Pihl, S., Søgaard, B., Ejrnæs, R., Aude, E., Nielsen, K.E., Dahl, K. & Laursen, J.S. 219 s., 120,00 kr.
Nr. 323: Tests af metoder til marine vegetationsundersøgelser. Af Krause-Jensen, D., Laursen, J.S., Middelboe, A.L., Dahl, K., Hansen, J. Larsen, S.E. 120 s., 140,00 kr.
Nr. 324: Vingeindsamling fra jagtsæsonen 1999/2000 i Danmark. Wing Survey from the Huntig Season 1999/2000 in Denmark. Af Clausager, I. 50 s., 45,00 kr.
Nr. 325: Safety-Factors in Pesticide Risk Assessment. Differences in Species Sensitivity and Acute-Chronic Relations. By Elmegaard, N. & Jagers op Akkerhuis, G.A.J.M. 57 pp., 50,00 DKK.
Nr. 326: Integrering af landbrugsdata og pesticidmiljømodeller. Integrerede MiljøinformationsSystemer (IMIS). Af Schou, J.S., Andersen, J.M. & Sørensen, P.B. 61 s., 75,00 kr.
Nr. 327: Konsekvenser af ny beregningsmetode for skorstenshøjder ved lugtemission. Af Løfstrøm, L. (Findes kun i elektronisk udgave)
Nr. 328: Control of Pesticides 1999. Chemical Substances and Chemical Preparations. By Krongaard, T., Petersen, K.K. & Christoffersen, C. 28 pp., 50,00 DKK.
Nr. 329: Interkalibrering af metode til undersøgelser af bundvegetation i marine områder. Krause-Jensen, D., Laursen, J.S. & Larsen, S.E. (i trykken)
Nr. 330: Digitale kort og administrative registre. Integration mellem administrative registre og miljø-/naturdata. Energi- og Miljøministeriets Areal Informations System. Af Hansen, H.S. & Skov-Petersen, H. (i trykken)
Nr. 331: Tungmetalnedfald i Danmark 1999. Af Hovmand, M.F. Kemp, K. (i trykken)
Nr. 332: Atmosfærisk deposition 1999. NOVA 2003. Af Ellermann, T., Hertel, O. &Skjødt, C.A. (i trykken)
Nr. 333: Marine områder – Status over miljøtilstanden i 1999. NOVA 2003. Hansen, J.L.S. et al. (i trykken)
Nr. 334: Landovervågningsoplande 1999. NOVA 2003. Af Grant, R. et al. (i trykken)
Nr. 335: Søer 1999. NOVA 2003. Af Jensen, J.P. et al. (i trykken)
Nr. 336: Vandløb og kilder 1999. NOVA 2003. Af Bøgestrand J. (red.) (i trykken)
Nr. 337: Vandmiljø 2000. Tilstand og udvikling. Faglig sammenfatning. Af Svendsen, L.M. et al.(i trykken)
Nr. 338: NEXT I 1998-2003 Halogenerede Hydrocarboner. Samlet rapport over 3 præstationsprøvnings-runder . Af Nyeland, B. & Kvamm, B.L.
Nr. 339: Phthalates and Nonylphenols in Roskilde Fjord. A Field Study and Mathematical Modelling of Transport and Fate in Water and Sediment. The Aquatic Environment. By Vikelsøe, J., Fauser, P., Sørensen, P.B. & Carlsen, L. (in press)
Nr 340: Afstrømningsforhold i danske vandløb. Af Ovesen, N.B. et al. 238 s., 225,00 kr.
Nr. 341: The Background Air Quality in Denmark 1978-1997. By Heidam, N.Z. (in press)
Nr. 342: Methyl t-Buthylether (MTBE) i spildevand. Metodeafprøvning. Af Nyeland, B. & Kvamm, B.L.
Nr. 343: Vildtudbyttet i Danmark i jagtsæsonen 1999/2000. Af Asferg, T. (i trykken)

2001

Nr. 344: En model for godstransportens udvikling. Af Kveiborg, O. (i trykken)

The aim of the study has been to investigate the occurrence, sources, transport and fate of nonylphenols and phthalates in the aquatic environment of Roskilde Fjord. It was further intended to find the temporal as well as the spatial variation of these xenobiotics in the fjord and stream water. Further, to investigate nonylphenols and phthalates in sediment in the fjord including a sediment core in the southern part, expected to yield clues regarding the historical variation of the concentration of xenobiotics, as well as some streams and lakes. Finally, an important aim was to make a mass balance for the fjord system, including sources, transport and the mechanisms of elimination, and to make a mathematical model describing the fate of the substances in the fjord system.

Ministry of Environment and Energy
National Environmental Research Institute

ISBN 87-7772-585-9
ISSN 0905-815x
ISSN (electronic) 1600-0048